MENG LINGBO

MASTER OF SCIENCE

2025

MICROWAVE PYROLYSIS CONVERSION OF SHRIMP SHELL WASTE INTO BIOCHAR FOR LANDFILL WASTEWATER TREATMENT

MENG LINGBO

MASTER OF SCIENCE
UNIVERSITI MALAYSIA TERENGGANU
2025

MICROWAVE PYROLYSIS CONVERSION OF SHRIMP SHELL WASTE INTO BIOCHAR FOR LANDFILL WASTEWATER TREATMENT

MENG LINGBO

Thesis Submitted in Fulfilment of the Requirements for the Degree of Master of Science in the Institute of Tropical Aquaculture and Fisheries
Universiti Malaysia Terengganu

FEBRUARY 2025

Pusat Pengurusan Siswazah (PPS)

Borang Pengesahan Penyerahan Tesis / Disertasi/ Laporan Kertas Projek

Declaration Form for Submission of Theses/ Dissertation / Project Paper

Tajuk / *Title*: MICROWAVE PYROLYSIS CONVERSION OF SHRIMP SHELL WASTE INTO BIOCHAR FOR LANDFILL WASTEWATER TREATMENT

Nama Pelajar / *Student's Name*: Meng LingBo

No. Matrik / *Matric No.*: P4511

Saya dengan ini mengaku membenarkan Tesis/Dissertasi/Laporan Kertas Projek ini disimpan di Perpustakaan Sultanah Nur Zahirah, Universiti Malaysia Terengganu ("UMT") dan mengakui bahawa UMT mempunyai hak-hak seperti berikut:
I hereby declare that I have allowed this Theses/Dissertation/Project Paper to be kept by Perpustakaan Sultanah Nur Zahirah, Universiti Malaysia Terengganu ("UMT") and acknowledged that UMT reserves the rights as follows:

1. Hak cipta Tesis/Dissertasi/Laporan Kertas Projek ini adalah hak milik UMT.
   The copyright of this Theses/Dissertation/Project Paper belongs to UMT.

2. UMT berhak untuk membuat salinan Tesis/Dissertasi/ Laporan Kertas Projek ini untuk tujuan akademik.
   UMT shall has the right to make copies of this Theses/Dissertation/Project Paper for the academic purpose.

3. UMT berhak membuat salinan Tesis/Dissertasi/Laporan Kertas Projek ini sebagai bahan pertukaran antara institusi pengajian tinggi.
   UMT shall has the right to make copies for this Theses/Dissertation/Project Paper as an exchange between higher learning institutions.

4. Hak-hak UMT yang dinyatakan dalam perkara 2 dan 3 di atas adalah tertakluk kepada kategori Tesis/Dissertasi/Laporan Kertas Projek seperti yang dinyatakan di dalam ini.
   The rights of UMT stated in items 2 and 3 above are subject to the category of the Thesis/Dissertation/Project Paper Report as stated herein.

Sila tanda (/) bagi pilihan kategori di bawah:
Please tick (/) from the categories below:

(/)	Tidak Terhad / *Open Access*	
( )	Terhad / *Restricted*	Mengandungi maklumat terhad yang telah ditentukan oleh organisasi/badan di mana penyelidikan ini dijalankan. *Contains restricted information as specified by the organization/body where research was done.*
( )	Sulit / *Confidential*	Mengandungi maklumat yang dikategorikan di bawah keselamatan atau kepentingan Malaysia seperti yang termaktub dalam Akta Rahsia Rasmi 1972 *Contains information categorized under the security or interests of Malaysia as stipulated in the Official Secrets Act 1972.*

Meng LingBo

…….. ……..

Tandatangan Pelajar / *Student's Signature*

Tandatangan Penyelia / *Supervisor's Signature*
(Nama dan Cop Rasmi/ *Name & Official Stamp*)

Catatan: Jika Tesis/Dissertasi/Laporan Kertas Projek ini SULIT @ TERHAD, sila lampirkan surat dari pihak berkuasa/organisasi berkenaan dengan menyatakan sekali sebab dan tempoh Tesis/Dissertasi/Laporan Kertas Projek ini perlu dikelaskan sebagai SULIT atau TERHAD.

Note: If this Theses/Dissertation/Project Paper is CONFIDENTIAL @ RESTRICTED, please attach the letter from the relevant authority/organization stating its reason and duration of this Theses/Dissertation/Project Paper should be classified as CONFIDENTIAL or RESTRICTED.

Abstract of thesis presented to the Senate of Universiti Malaysia Terengganu in fulfilment of the requirements for the degree of Master of Science

MICROWAVE PYROLYSIS CONVERSION OF SHRIMP SHELL WASTE INTO BIOCHAR FOR LANDFILL WASTEWATER TREATMENT

MENG LINGBO

FEBRUARY 2025

Main Supervisor : **Professor Ts. Lam Su Shiung, PhD**

Co-supervisor : **Professor Peng Wanxi, PhD**

Peter Yek Nai Yuh, PhD

Faculty/Institute : **Institute of Tropical Aquaculture and Fisheries**

Shrimp shell waste (SSW) is a ubiquitous by-product of seafood processing whose improper disposal can disrupt terrestrial and aquatic ecosystems. Accordingly, objective 1 of this study is to examine the thermal behaviour and chemical composition of SSW to establish its suitability as a feedstock for thermochemical conversion. This is followed by objective 2 to convert SSW into biochar via a single-mode microwave pyrolysis reactor and to optimize processing parameters specifically irradiation powers of 500 W, 700 W and 900 W. Then, the resulting SSW-derived biochar in treating landfill leachate wastewater (LW) was evaluated in objective 3. For methodology, SSW was characterised by Thermogravimetric analysis (TGA) coupled with Fourier transform infrared spectroscopy (FTIR) and pyrolysis integrated with gas chromatography–mass spectrometry (PY–GCMS) to examine the suitability of SSW as pyrolysis feedstock. After that, single-mode microwave pyrolysis system was developed to convert SSW into biochar at different microwave power (500W, 700W and 900W). The biochar derived from SSW was further applied as adsorbent for landfill leachate treatment. TGA–FTIR revealed that primary devolatilization occurs between 400 °C and 700 °C, during which CO_2, CO and CH_4 are the dominant evolved gases. PY–GCMS conducted at 900 °C with a heating rate of 30 °C min^{-1} demonstrated that hydrocarbon species account for approximately 37.3 wt % of the gaseous products,

thereby confirming the feedstock's potential for high-value by-product recovery and informing the optimal pyrolysis conditions required to achieve Objective 1. Building on these findings, under 500 W irradiation, the process yielded the highest carbon retention (50 wt %), whereas treatment at 900 W produced biochar with a maximized Brunauer–Emmett–Teller (BET) surface area of 23 $m^2\ g^{-1}$. Batch adsorption trials demonstrated that the optimized biochar achieved biochemical oxygen demand (BOD) removal capacities of 15–64 mg g^{-1} and chemical oxygen demand (COD) uptakes of 177–210 mg g^{-1}. In summary, the study demonstrates that microwave pyrolysis can transform SSW into a cost-effective adsorbent for wastewater remediation.

Abstrak tesis yang dikemukakan kepada Senat Universiti Malaysia Terengganu sebagai memenuhi keperluan untuk Ijazah Sarjana Sains

PIROLISIS GELOMBANG MIKRO SISA KULIT UDANG KE DALAM BIOCHAR UNTUK RAWATAN AIR SISA TAPAK PELUPUSAN

MENG LINGBO

FEBRUARI 2025

Penyelia Utama : Profesor Ts. Lam Su Shiung, Ph.D

Penyelia Bersama : Profesor Peng Wanxi, Ph.D

Peter Yek Nai Yuh, Ph.D

Fakulti/Institut : Institut Akuakultur Tropika dan Perikanan

Sisa kulit udang (SSW) merupakan hasil sampingan yang meluas daripada pemprosesan makanan laut dan pelupusan yang tidak terkawal boleh mengganggu ekosistem darat dan akuatik. Sehubungan itu, Objektif 1 kajian ini adalah untuk mengkaji tingkah laku terma dan komposisi kimia SSW bagi menilai kesesuaiannya sebagai bahan asas untuk penukaran termokimia. Ini diikuti oleh objektif 2 adalah untuk menukarkan SSW kepada biochar menggunakan reaktor pirolisis gelombang mikro mod tunggal dan mengoptimumkan parameter pemprosesan, khususnya kuasa gelombang mikro pada tahap 500 W, 700 W dan 900 W. Oleh itu, kecekapan biochar terbitan SSW dalam rawatan air lindi pelupusan (LW) dinilai sebagai objektif 3. Bagi metodologi, Analisis Termogravimetri (TGA) dipadankan dengan Spektroskopi Inframerah Transformasi Fourier (FTIR) dan gabungan Pirolisis dengan Analisis Kromatografi Gas–Spektrometri Jisim (PY–GCMS) telah digunakan untuk menilai kesesuaiannya SSW sebagai bahan asas untuk penukaran termokimia. Selepas itu, sistem pirolisis gelombang mikro mod tunggal telah dibina untuk menukar SSW kepada biochar pada kuasa gelombang mikro yang berbeza (500 W, 700 W dan 900 W). Biochar yang dihasilkan daripada SSW telah digunakan sebagai penjerap untuk merawat air sisa. TGA–FTIR mendedahkan bahawa devolatilasi utama berlaku antara suhu 400 °C hingga 700 °C, di mana gas terbitan yang dominan adalah CO_2, CO dan

CH_4. PY–GCMS dijalankan pada 900 °C dengan kadar pemanasan 30 °C min^{-1} menunjukkan bahawa spesies hidrokarbon merangkumi kira-kira 37.3 wt % daripada produk gas, sekaligus mengesahkan potensi SSW untuk pemulihan produk tambahan bernilai tinggi dan membimbing penentuan syarat pirolisis optimal yang diperlukan untuk mencapai Objective 1. Berdasarkan pencarian ini, proses ini mencapai pulangan karbon tertinggi sebanyak 50 wt % di bawah penyinaran 500 W, manakala rawatan pada 900 W menghasilkan biochar dengan luas permukaan Brunauer–Emmett–Teller (BET) maksimum sebanyak 23 m^2 g^{-1}. Ujian penjerapan secara berkumpulan menunjukkan bahawa biochar teroptimum mencapai keupayaan pengurangan Biochemical Oxygen Demand (BOD) sebanyak 15–64 mg g^{-1} dan Chemical Oxygen Demand (COD) antara 177–210 mg g^{-1}. Kajian ini menunjukkan bahawa pirolisis gelombang mikro mampu mengubah SSW menjadi penjerap kos efektif untuk penambahbaikan air sisa.

ACKNOWLEDGEMENT

I would like to take this opportunity to express my sincerest gratitude and respect to all those who helped me and made this paper possible. First of all, I am very grateful to my supervisor Prof. Lam Su Shiung. Thank him for giving me this valuable opportunity to conduct this research. His guidance, opinions, suggestions, and his willingness to share his experiences helped me overcome most of my research hurdles. He gave me the greatest support in terms of experiments. He also helped me improve a lot in my thesis. For me, with his guidance and supervision, the research process of this project was an unforgettable, enjoyable and growing experience. In addition, I would like to sincerely thank my two other supervisors, Professor Peng Wanxi and Dr. Peter Yek Nai Yuh, for their help. Whether it was experimental processes or papers, they were willing to share their expertise and provide valuable suggestions to me. With the help of the above experts, this paper has certain value.

My sincere thanks to all the team members of the Pyrolysis Technology Research Group, especially Ms. Foong Shinying for their enthusiastic help, enthusiastic guidance, support and suggestions. And I am also very grateful to Ms. Elfina Azwar for her support and help in my experiments. My sincere thanks go to all those who took the time to assist me with laboratory skills, use of laboratory analytical instruments, and data interpretation.

Finally, I would like to thank my dear family for their patience, understanding, guidance and encouragement when I needed it most. Allow me to complete my experiments and papers firmly. Thanks again to everyone for their support and help in this research, which gave me such an unforgettable time.

APPROVALS

I certify that an Examination Committee has met on 21 February 2025 to conduct the final examination of Meng LingBo, on his Master of Science thesis entitled "Microwave pyrolysis of shrimp shell waste into biochar for landfill wastewater treatment" in accordance with the regulations approved by the Senate of Universiti Malaysia Terengganu. The Committee recommends that the candidate be awarded the relevant degree. The members of the Examination Committee are as follows:

Assoc. Prof. ChM. Ts. Nor Azman Kasan, Ph. D
Institute of Tropical Aquaculture and Fisheries
Universiti Malaysia Terengganu
(Chairperson)

Mok Wen Jye, Ph. D
Institute of Climate Adaptation and Marine Biotechnology
Universiti Malaysia Terengganu
(Internal Examiner)

Prof. Yang Sun, Ph. D
College of Life Science
Jilin Agricultural University
Changchun, China
(External Examiner)

_____

MUHAMMAD IKHWANUDDIN ABDULLAH, Ph.D
Professor/Director
Institute of Tropical Aquaculture and Fisheries
Universiti Malaysia Terengganu

Date:

APPROVALS

This thesis has been accepted by the Senate of Universiti Malaysia Terengganu in fulfilment of the requirement for the degree of Master of Science.

_____

MUHAMMAD IKHWANUDDIN ABDULLAH, Ph.D
Professor/Director
Institute of Tropical Aquaculture and Fisheries
Universiti Malaysia Terengganu

Date:

DECLARATION

I hereby declare that the thesis is based on my original work except for quotations and citations which have been duly acknowledged. I also declare that it has not been previously or concurrently submitted for any other degree at UMT or other institutions.

_____

MENG LINGBO

Date:

TABLE OF CONTENTS

LIST OF TABLES

Table **Page**

LIST OF FIGURES

Figure **Page**

LIST OF ABBREVIATIONS

BET	Brunauer-Emmett-Teller
BJH	Barrett-Joyner-Halenda
BOD	Biochemical oxygen demand
COD	Chemical oxygen demand
C	Carbon
H	Hydrogen
N	Nitrogen
S	Sulphur
O	Oxygen
SSW	Shrimp shell waste
SSB 500	Biochar from shrimp shell waste prepared by microwave pyrolysis at a power of 500 W
SSB 700	Biochar from shrimp shell waste prepared by microwave pyrolysis at a power of 700 W
SSB 900	Biochar from shrimp shell waste prepared by microwave pyrolysis at a power of 900 W
DTG	Derivative thermogravimetry
e.g.,	For example (exemplī grātiā, in Latin)
Eq.	Equations
et al.	And others (et alibi, in Latin)
FC	Fixed carbon
FR	Fuel ratio
FS	Fixed substance
HHV	Higher heating value
i.e.	It is (id est, in Latin)
LW	Landfill wastewater
MC	Moisture content
MF	Microfiltration
MP	Microwave pyrolysis
NF	Nanofiltration
Py-GC/MS	Pyrolyzer coupled with gas chromatography/mass spectrometry
Ref.	Reference
RO	Reverse osmosis
SEM	Scanning electron microscopy
SW	Shellfish waste
TGA	Thermogravimetric analysis
TG-FTIR	Thermogravimetric analyzer coupled with fourier-transform infrared spectrometer
UF	Ultrafiltration
VM	Volatile matter

CHAPTER 1

INTRODUCTION

This chapter introduces the background of shrimp shell waste and landfill effluent, current treatment methods and recovery of value-added products through pyrolysis method. In addition to the objective and scope of the study, the significance of the study is also introduced. Hypotheses are proposed for the findings of the study. Finally, the layout of this thesis is introduced.

1.1 Background of Study

Shrimp is tasty and rich in nutrients. The Food and Agriculture Organization (FAO) expects marine-farmed shrimp output to reach 6 million tons in 2024 (FAO, 2024). China brought in 251 000 tons in the first quarter of 2024. The United States imported 182 900 tons in the same period, up 1.2 % from last year. Ecuador shipped out 276 800 tons, the world's largest export volume. India sent 155 600 tons, ranking second and Vietnam's exports jumped 26.3 % in 2024 (FAO, 2024). Processing creates large amounts of shrimp-shell waste (SSW). About half of each processed shrimp becomes shells and tails. Some SSW becomes animal feed. Much still goes to landfills or the sea, causing pollution. The shrimp industry must adopt sustainable waste-management methods to cut its environmental impact (Kandra et al., 2012).

In recent years, significant progress has been made in developing more effective methods of adding value to SSW. Chitin extracted from shrimp shells is converted into high-value organic products such as chitosan beads. However, a significant challenge

is the generation of large amounts of wastewater during the treatment stage (Abadi, 2018). Several studies have explored the feasibility of using SSW for wastewater treatment, including using crushed shrimp shells to adsorb pollutants and carbonizing SSW into adsorbents (Núñez-Gómez et al., 2017). The surface area of the resulting products is relatively low, approximately 4-17 m^2/g, which limits their effectiveness and applications (Chao et al., 2020). Considering these challenges, there is a clear need to develop more efficient and environmentally friendly methods to exploit SSW. Pyrolysis technology emerges as a potentially viable option for SSW valorization, providing opportunities for efficient waste management and generation of value-added by-products. Pyrolysis is a thermochemical process that decomposes organic matter under an inert atmosphere into gaseous products, liquid bio-oil and biochar. Biochar has become an effective adsorbent for removing organic matter due to its high micropore volume, rich surface oxygen-containing functional groups, and high specific surface area applied as a wastewater treatment agent (Liu et al., 2019). Therefore, biochar can be used as an environmentally friendly, efficient and economical adsorption material in various aspects.

The increase in global population has led to a corresponding increase in the generation of solid waste (Ogunmakinde et al., 2019), and landfilling remains the main method of solid waste treatment, mainly due to its cost-effectiveness and simplicity (Ab Ghani et al., 2017; Luo et al., 2020). However, landfill wastewater (LW) containing suspended solids generated by rainwater infiltration into municipal waste in landfills can have negative impacts on the environment. Landfill wastewater (LW) may contaminate other water resources through soil and subsoil (Yong et al., 2018). Landfill wastewater (LW) has particularly high chemical oxygen demand (COD) and biochemical oxygen demand (BOD), and also contains large amounts of ammonia, nitrogen, and heavy metals such as copper, nickel, and zinc (Bilardi et al., 2018; Shadi et al., 2020). These characteristics make it a complex and variable wastewater that poses a significant risk to human health. Given the complexity and variability of LW traditional treatment technologies such as ozonation and photocatalysis are often challenged by high operating costs and complexity (Tugtas et al., 2013; Borba et al., 2019). In light of these challenges, simpler and more cost-effective treatment methods are urgently needed. Biochar as an economical adsorbent for wastewater treatment due

to its ease of production, availability of raw materials, and ability to remove soluble organic and inorganic compounds (Rambabu et al., 2019; Rambabu et al., 2020). Many studies have demonstrated the efficacy of biochar extracted from various raw materials in treating wastewater (Rajapaksha et al., 2016; You et al., 2017; Cho et al., 2019).

The above findings provide motivation and objectives for this study; thus, this study aims to produce shrimp shell biochar (SSB) through pyrolysis, a thermochemical technique, and then use it as an adsorbent for LW treatment. Studying the adsorption characteristics of LW treated with SSB contributes to a broader understanding of engineered biochar and promotes the use of microwave pyrolysis technology to treat SSW, thereby reducing its environmental impact. This study explores the potential of SSW used as a pyrolysis feedstock and convert it into biochar. Finally, study the feasibility of produced biochar as adsorbent treat LW.

1.2 Statement of the Problem

As living standards improve, people's requirements for the nutritional value of food are getting higher and higher. Shrimp is a super nutritious food with high protein, multiple amino acids, low fat, a certain amount of vitamin, and rich in minerals (Menon, 2018), which is deeply loved by consumers. As mentioned above, the production and consumption of shrimp are also increasing year by year. Shrimp is usually exported frozen with or without shells. Therefore, about 50-60% of the inedible parts are discarded as waste, such as shrimp heads, shrimp tails and shrimp shells (Nirmal et al., 2020). Due to the popularity of shrimp dishes, a large amount of SSW is generated. About 6 million to 8 million tons of SSW are discarded every year, causing urgent environmental problems (Suresh, 2012; Cheba et al., 2018). Most of the SSW generated by factories is sent to landfills or dumped into the sea (Evers and Carroll, 1998; Xu et al., 2013), while some SSW is sent to waste treatment plants for incineration (Kreag and Smith, 1973). These treatments cause damage to the environment. These wastes decompose quickly after landfill, causing flies and mosquitoes to breed, spread diseases, and affect people's health (Mathew et al., 2020). Thank you for your review, it has been corrected. In addition, due to the high nitrogen

content of solid waste, toxic gases such as nitrogen oxides are produced during incineration (Feng et al., 2013). Shrimp shell waste (SSW) contains about 30–40 wt% protein, 30-50 wt% calcium carbonate, 20–30 wt% chitin, and some esters and other compounds (Zhang et al., 2019). Therefore, exploring alternative treatment methods are needed to reduce the adverse effects of current disposal methods on human health and convert SSW into higher value products.

There are various treatment technologies that can be used to treat landfill wastewater; biological methods (aerobic and anaerobic), flotation, coagulation/flocculation, air stripping, ion exchange, etc. (Wiszniowski et al., 2006; Renou et al., 2008; Abbas et al., 2009). Although these treatment methods have certain effects, they also have obvious shortcomings, including low pollutant removal efficiency and high cost (Asaithambi et al., 2020). Therefore, there is an urgent need to develop more efficient and cost-effective treatment methods. Moreover, the conventional pyrolysis is limited by slow heating rate and limited heat distribution (Bundhoo, 2018; Yu et al., 2018b). A large amount of energy consumed to heat up the conventional furnace leads to the disadvantage of high energy consumption, release of volatiles and the purge of inert gas also lead to a large amount of heat and energy loss (Yunpu et al., 2016; Bundhoo, 2018). Therefore, efficient and energy-saving pyrolysis technology is needed to solve the limitations and problems.

1.3 Significance of Research

Microwave pyrolysis (MP) is an alternative pyrolysis method that uses microwaves as a heating method, achieved higher process efficiency and reduced energy consumption. Microwave pyrolysis uses microwaves to directly transfer energy to promote molecular or atomic interactions, thereby generating thermal energy within the heated material. This approach ensures a more uniform temperature distribution, thus mitigating product yield reduction due to adverse reactions (Lam and Chase, 2012). Microwave pyrolysis is performed in an enclosed space, using radiative indirect heating to enhance control of pyrolysis (Lam and Chase, 2012). During the microwave pyrolysis process gases are produced and discharged into a closed space and then

discharged into the air through filtration. In addition, single-mode microwave systems can be selected for experiments with specific cavity and waveguide designs that support only the required microwave propagation modes and minimize other modes to maintain the uniformity and directionality of microwave radiation. It is able to focus microwave energy into a single electromagnetic mode, thereby providing highly controllable and uniform heating for pyrolysis reactions (Putra et al., 2022). Therefore, MP is a potentially effective technology for converting SSW into biochar compared with conventional pyrolysis (Zhao et al., 2011; Yin, 2012).

Biochar produced from single-mode microwave pyrolysis of shrimp-shell waste offers a dual benefit for solid-waste reduction and wastewater treatment. The rapid, highly uniform heating inherent to single-mode systems generates a carbon matrix with extensive porosity and well-developed micro-mesopore architecture. Microwave energy couples directly with the char, spent adsorbent can be regenerated in situ, reducing the need for frequent replacement. The overall energy demand of the single-mode microwave process remains lower than that of conventional resistive or rotary-kiln pyrolysis, contributing to cost savings and smaller carbon footprints. Deployment of this biochar as a polishing step in existing leachate-treatment trains can help sites achieve stricter discharge limits without major infrastructure changes. Adoption of such circular-economy strategies transforms seafood-processing residues from an environmental burden into a valuable resource, which simultaneously mitigates landfill pollution, conserves finite activated-carbon supplies, and supports sustainable landfill-management practices. By integrating waste valorization with wastewater remediation, this technology aligns with broader objectives for resource efficiency and environmental stewardship (Qin et al., 2023).

1.4 Hypothesis of the Study

Shrimp shell waste (SSW) as a by-product of the seafood industry, is available in increasing quantities and holds potential as a renewable pyrolysis feedstock. This study hypothesizes that SSW can be efficiently converted into value-added products through

microwave pyrolysis. Unlike conventional pyrolysis, microwave pyrolysis able offers rapid and uniform heating, leading to the effective decomposition of SSW and the production of porous biochar. Shrimp shell waste (SSW) is expected to absorb microwave energy effectively and convert into biochar (Lam et al., 2015). The resultant biochar able to show unique porosity as a promising candidate for the adsorption and treatment of LW. Thus, the study aims to demonstrate that microwave pyrolysis of SSW can yield valuable products and provide an effective solution for LW treatment.

1.5 Aim and Objectives

This study aims to convert SSW into value-added products by microwave pyrolysis technology and apply it to the adsorption treatment of LW. The steps of this experiment were carefully planned and implemented to ensure that the following objectives could be achieved.

The objectives of this study are as follows:

1. To examine the thermal behaviour and chemical properties of SSW to determine its suitability as a pyrolysis feedstock.
2. To obtain and characterize SSB from microwave pyrolysis of SSW at different microwave powers.
3. To evaluate the effectiveness of SSB in the adsorption treatment of LW.

1.6 Scope of Study

The scope of this study included the analysis of SSW, biochar produced by microwave pyrolysis at different microwave powers, analysis of SSB, and the effect of SSB on LW treatment. Shrimp shell waste (SSW) was characterized by thermogravimetric analysis and CHNS elemental analysis to determine its thermal stability and elemental composition. Thermogravimetric analysis coupled with Fourier transform infrared spectrometer (TG-FTIR) and Pyrolyzer coupled with gas

chromatography/mass spectrometry (Py-GC/MS) were used to determine the gaseous composition of SSW pyrolysis emissions. Furthermore, biochar produced by microwave pyrolysis at different microwave powers. Then, the surface morphology and porosity of produced biochars were characterized, using scanning electron microscopy (SEM), and Brunauer-Emmett-Teller (BET) surface area analysis, respectively. Finally, the biochar was applied to the treatment of LW to explore its adsorption treatment effect on LW.

1.7 Organization of Thesis

This paper is divided into five chapters to explain this experiment. Chapter 1 introduces the growing SSW and its effects to the environment. Traditional treatment methods cannot properly handle it and caused more environmental problems. For this reason, this study proposes microwave pyrolysis as an alternative treatment method to be applied to the treatment of SSW, and the objectives, scope and hypothesis of the study are proposed. Chapter 2 reviews and discusses the possibility of SSW as a pyrolysis feedstock, the current thermal conversion pathways, and a detailed introduction to pyrolysis, then more advanced pyrolysis technology is introduced. The current traditional LW treatment methods and the application of biochar in LW are also reviewed. In Chapter 3, the design of this experiment is introduced, and the analytical techniques used in the experiment are explained. Chapter 4 summarizes the research results of this experiment, including the characterization of SSW, the characterization of SSB produced at different microwave powers, and the performance of SSB as an adsorbent in LW. In Chapter 5, the results of this experiment are summarized, the experimental objectives are answered one by one, and the limitations and future directions of the current research are provided.

CHAPTER 2

LITERATURE REVIEW

This chapter discuss the characteristics of SSW and limitation of current thermal treatment methods such as combustion and gasification. Microwave pyrolysis approach has been introduced as a better technology for the conversion of SSW. Compared with traditional pyrolysis, advanced pyrolysis technologies such as solar, vacuum and microwave pyrolysis have outperformed traditional pyrolysis technologies in terms of energy efficiency, product yield and quality, and production costs. The composition and application of pyrolysis products in gaseous, liquid, and solid states are also reviewed.

2.1 Shrimp shell waste as pyrolysis feedstock

The shell of shrimp is composed into a variety of substances, including protein, mineral salts, chitin, and other compounds. Protein accounts for about 30-40wt%, while mineral salts account for about 30-50wt%, and chitin and other compounds (such as pigments and lipids) account for about 20-30wt% (Cho et al., 1998) . These components may be recovered during the pyrolysis process, so shrimp shells are potentially suitable as raw materials for pyrolysis.

As one of the most institutionally diverse biopolymers in nature, chitin is a homopolymer of β-1,4-linked N -acetylglucosamine (NAG)(Halder et al., 2012) . Chitin mainly comes from fishery by-products and is extremely abundant in the natural environment. Chitin contains a large amount of carbon and a variety of functional

groups (Ahmadi et al., 2017; Vakilabadi et al., 2017). Among these fishery by-products, SSW has the highest chitin content and is well suited for the preparation of porous carbon due to its role as a nitrogen-rich carbon material (Yang et al., 2018).

Shrimp shells also contain mineral salts, calcium carbonate is abundant able improve the efficiency of the pyrolysis process (Qu et al., 2016). This is due to the high surface area and porosity of calcium carbonate, which allows the adsorption of organic compounds and can accelerate the thermal decomposition of these compounds (Ishimura et al., 2021; Zhang et al., 2021). In addition, due to its high surface area, chitin can effectively promote the decomposition of organic materials during pyrolysis and help shape the desired product, which is equivalent to acting as a catalyst in pyrolysis (Tsioptsias et al., 2009; Wang and Shen, 2022) .

Table 2.1 presents the characterization of SSW. Shrimp shell waste (SSW) contains more volatile substances, with a content of more than 60wt.%. A higher volatile content (VM) means that SSW contains a large amount of volatile organic matter make the degradation reaction easier to occur, thereby improving the efficiency of the pyrolysis process. In addition, High content of char (> 18 wt.%) has beneficial to adsorbent application. However, high ash content (>30wt.%) has a negative impact especially on combustion application that cause slagging and fouling within boilers (Sait et al., 2012) . The elemental analysis of SSW has shown that the oxygen content (>20wt.%) in SSW is high, which contains high carbonyl and hydroxyl functional groups in its structure (Mitu et al., 2019). In addition, high nitrogen content (>3wt.%), causes SSW emit nitrogen oxides during the combustion process, which is toxic and harmful to the human body (Telmo et al., 2010). However, SSW contains low sulphur content (Moreno and Font, 2015).

Table 2.1 Elemental and proximate analysis of shrimp shell waste (SSW) in different references.

Sample	Elemental content (wt.%)					Proximate content (wt.%)				Ref.
	C	H	N	O	S	VM	FC	Ash	MC	
Shrimp shell	26.85	5.10	5.96	21.98	0.65	60.42	0.12	39.46	-	(Zhang et al., 2019)
Shrimp shell	22.60	2.91	3.49	33.47	0.24	62.66	0.05	37.29	-	(Hisham et al., 2021)
Shrimp shell	27.82	4.01	4.61	30.87	0.26	67.44	0.13	32.43	-	(Zhang et al., 2019)
Shrimp shell	18.40	1.35	-	22.73	-	-	-	-	-	(Wang et al., 2021)
Shrimp shell	27.44	4.38	4.61	-	1.01	-	-	-	-	(Huang et al., 2021)
Shrimp shell	38.60	6.17	8.44	29.07	0.71	-	-	16.99	-	(Saha et al., 2023)
Shrimp shell	26.10	4.13	4.83	-	0.08					(del Carmen Borja-Urzola et al., 2020)

"-" refers to not detected,

"MC" refers to moisture content; "VM" refers to volatile matter; "FC" refers to fixed carbon

2.2 Current thermal conversion pathways

2.2.1 Combustion

Combustion is a highly exothermic thermochemical reaction, which is an oxidative heat process used in many energy-related industries. During the combustion process, biomass is converted into heat, gas and ash. Waste incineration power plants burn waste in an aerobic environment to generate heat and gas passed through a steam turbine to generate electricity (Nanda and Berruti, 2021). Combustion have been repeatedly highlighted in recent years, including global warming, fossil fuel consumption, and emissions of air pollutants (Kohse-Höinghaus, 2021).

The combustion of fossil fuels such as coal, oil and natural gas emits various toxic gases, such as carbon monoxide (CO), nitrogen oxides (NO_X), and sulphur dioxide (SO_2) (Chakravorty and Gong, 2015). These toxic gases cause air pollution, and air pollution affected people's health. The excessive mortality from cardiovascular, respiratory, and other diseases is mainly caused by air pollution (Lelieveld et al., 2019) . When biomass is used as fuel, its incomplete combustion also produces volatile compounds (VOC) and polycyclic aromatic hydrocarbons (PAH) (Moreno et al., 2017). The nitrogen content in SSW is high, and its combustion produce nitrogen oxides (NO_X), which pollute the environment. Therefore, burning treatment is not advisable for SSW because it produces toxic gases and pollutants that harm the environment.

2.2.2 Gasification

Gasification is a fuel processing technology in controls oxygen environment. The organic materials in biomass are oxidized by steam, air, carbon dioxide or other gasifying agents to produce synthesis gas (referring to H_2 and CO mixture) in a high temperature environment (>1600℃) (Lam et al., 2016). Syngas is a gaseous fuel that burns easily in furnaces or internal combustion engines and therefore can be used to generate electricity and heat (Mahari et al., 2021). In addition, the combustion of

gaseous fuel produced by gasification causes less air pollution and can reduce carbon dioxide emissions compared to incineration, thus protecting the environment and mitigating global warming (Kumar and Samadder, 2017). The raw materials for gasification such as plastics, biomass, municipal solid waste, etc can be used as raw materials for gasification to produce syngas (Mahari et al., 2021).

The gasification process is generally divided into drying, pyrolysis, combustion, and reduction. The first is drying. When drying is completed, the reactor reached 150°C and then enter the pyrolysis process, which is generally maintained at 250-700°C. The products of pyrolysis include carbon, gas, and oil. When the temperature reaches 700-1500°C, combustion begins to occur, which is an exothermic reaction due to the oxidation of the raw materials. The final reduction reaction occurs at 800-1100°C accompanied by an endothermic reaction. Although gasification has a good effect on treating waste, the gasification process produces carbonaceous residues, ash, and tar. These by-products reduce the efficiency of the gasifier and require frequent maintenance. This is undoubtedly posing many limitations to this technology (Madav et al., 2019). In addition, the high temperatures required for the gasification process also limit its development (Cheng et al., 2019).

2.2.3 Pyrolysis

Pyrolysis is an endothermic process in which feedstock is heated in an oxygen-free or limited oxygen environment to decompose it into porous carbon, pyrolysis oil, and synthesis gas (Lam et al., 2018). Pyrolysis divided into slow pyrolysis, fast pyrolysis and flash pyrolysis with different heating rates and steam retention times. The main product of slow pyrolysis is biochar (50 wt.%), while it is produced at lower heating rates (0.1−10°C/s) and longer steam retention (10−60 Minutes) pyrolysis process (Sekar et al., 2021). During this pyrolysis process, the decomposition temperature generally reaches about 400−500°C. Slow pyrolysis uses lower heating rate allows primary volatiles to be released, breaking weaker chemical bonds, thus leaving residues with stronger chemical bonds to produce higher carbon content of biochar (Aravind et al., 2020). Fast pyrolysis produced higher bio-oil content (60−75

wt.%) compared to slow pyrolysis at heating rate of rapid pyrolysis (10–200 ℃/s). Flash pyrolysis uses the highest heating rate (>1000°C) results in gaseous (Collard and Blin, 2014).

2.3 Advanced pyrolysis technology for waste recovery

To better process waste and convert it into value-added products, more advanced pyrolysis technologies need to be explored. Solar pyrolysis, vacuum pyrolysis, and microwave pyrolysis are some of the options (Foong et al., 2020).

2.3.1 Solar pyrolysis

Solar pyrolysis uses solar energy instead of electricity as the heat source for pyrolysis can greatly reduce the cost of pyrolysis, and solar energy is also more environmentally friendly selection (Giwa et al., 2019). In addition, compared with conventional pyrolysis, it has a lower heating rate and temperature, and can selectively control the pyrolysis process. The existence of these characteristics is very beneficial to the formation of pyrolysis products (Weldekidan et al., 2020). However, the selection of pyrolysis raw materials for solar pyrolysis is affected by solar radiation penetration, which undoubtedly limits the practical application of solar pyrolysis. The reaction kinetics and heat and mass transfer phenomena of solar pyrolysis is still limited (Sobek and Werle, 2020).

2.3.2 Vacuum pyrolysis

Vacuum pyrolysis is based on conventional pyrolysis and is performed in a vacuum environment. Vacuum pyrolysis removes the air from the reactor through a vacuum pump before the pyrolysis process starts to create a vacuum environment (i.e., an oxygen-free environment). By removing air from the reactor by the vacuum pump, hence continuous flow of carrier gas (i.e. nitrogen, argon, helium) to maintain an inert pyrolysis environment is not necessary. The products produced under vacuum pyrolysis are relatively pure as the primary pyrolysis during the pyrolysis process is

enhanced, thereby reducing the possibility of secondary reactions (Chen et al., 2018). In addition, under vacuum conditions, the boiling point of the feedstock is reduced, which makes the temperature required for vacuum pyrolysis lower than that for conventional pyrolysis (Lam et al., 2019). Vacuum pyrolysis is creating solid carbon and liquid oil because it can improve the porosity of solid carbon and bring the grade of the liquid oil near to that of diesel. However, vacuum pyrolysis also has certain limitations. The bio-oil produced by vacuum pyrolysis needs to be further processed (such as cracking), and the volatiles form a large number of polycyclic macromolecular compounds during the instantaneous condensation process, which lead to a decrease in the smaller fragment compounds decomposed by the volatiles. This result in very little generation of combustible gases (such as H_2, CO, CH_4) and light hydrocarbons (Lopez et al., 2009).

2.3.3 Microwave pyrolysis

Microwave pyrolysis technology is a relatively novel pyrolysis technology proposed in recent years. Compared with conventional pyrolysis, which uses electrical energy as the heat source, microwave pyrolysis uses microwaves radiation as the heat source in the pyrolysis process with better energy saving, rapidity, uniform heating, shorter processing time, and less cost (Lam et al., 2012; Zhang et al., 2018). Moreover, carbon-based materials have good absorption of microwaves, and microwaves do not heat the polar gases in the reactor, which allows microwaves to specifically unto raw materials, thereby reducing energy losses (Liew et al., 2019). The heating method of microwave pyrolysis is based on dielectric heating of the raw material, and then the microwave energy causes friction and collision between molecules to generate heat energy (Su et al., 2020). MP do not require heating of the reactor and transfer heat to feedstock like conventional pyrolysis. Therefore, it can greatly shorten the time required for pyrolysis and reduce unnecessary energy consumption. Table 2.2 shows the statistics of various products obtained by treating various wastes by microwave pyrolysis in previous microwave pyrolysis experiments.

Table 2.2 Yields of microwave pyrolysis of various wastes at different microwave powers and temperatures.

Feedstock	Microwave power (W)	Microwave pyrolysis temperature（℃）	Biochar (%)	Oil (%)	Gas (%)	Ref.
Baby diaper	700	-	40	37	23	(Lam, Su Shiung et al., 2019)
Olive pomace	400	-	25	-	-	(Kostas et al., 2020)
Palm kernel shell	-	500	55	20	25	(Shadi, A et al., 2020)
Horse manure	-	-	12	-	-	(Mong et al., 2020)
Wood sawdust	750	-	-	65	-	(Borges et al., 2014)
Polystyrene	700	-	-	80	-	(Zhang et al., 2022)
Oil palm shell	900	-	40	-	-	(Kong et al., 2019)
Shrub willow	1000	-	19	40	21	(Tarves et al., 2017)

"-" refers to not detected.

Compared with conventional pyrolysis, microwave pyrolysis has the advantages of energy saving and rapidity. In addition, the content of polycyclic aromatic hydrocarbons and harmful compounds (such as NO_X, SO_2) produced by microwave pyrolysis is reduced. (Dominguez et al., 2007). Therefore, microwave pyrolysis has the potential as an efficient and environmentally friendly pyrolysis method for converting waste into value-added products.

2.4 Current status of landfill wastewater treatment

2.4.1 Composition and hazards of LW

Landfill wastewater (LW) is a mixed liquid formed by the infiltration of rainwater from landfill waste, the inherent moisture of the waste, and the water produced by biodegradation of the waste (Teng et al., 2021). It is usually composed of high concentrations of biodegradable and recalcitrant organic pollutants (organic carbon, fatty acids), heavy metals (e.g., copper, zinc, lead, mercury), ammonia nitrogen, salts (chlorinated organic salts and inorganic salts), and humus and other recalcitrant compounds (Chávez et al., 2019; Anqi et al., 2020). Moreover, it has the characteristics of high BOD and COD (Mojiri et al., 2021). In addition, the characteristics of LW are also affected by many factors, including climate, hydrological conditions, age of landfill, type and mixture of wastes and the content of these wastes, temperature, etc. (Bhalla et al., 2013; Adhikari et al., 2014; Vithanage et al., 2014; Somani et al., 2019; Abdel-Shafy et al., 2024).

Landfill wastewater (LW) can be divided into three stages according to its age: young (0-5 years), middle (5-10 years), and old (>10 years) (Tejera et al., 2019). The characteristics presented by these three stages are also different. In the young stage, the pH value of LW is low, the liquid is acidic, and its BOD and COD are the highest among the three stages (Mojiri et al., 2021). When LW reaches the middle stage, its pH value gradually tends to be neutral, and humus and humus components are the main components of organic matter (Mojiri et al., 2021). In the old stage, the pH value of

LW increases, its liquid is alkaline, and BOD and COD gradually decrease (Mojiri et al., 2021). The existence of these characteristics also makes it a complex and changeable wastewater, which has caused great challenges in the treatment process of traditional technologies. With the rapid increase in population in recent years, solid waste has also increased, and landfills have brought more and more LW due to their low operating costs (Gotvajn and Pavko, 2015). The hazards caused by LW are also increasing. For example, wastewater may contaminate nearby groundwater, surface water and soil (Zamri et al., 2017). These hazards are usually related to insufficient LW treatment (Mojiri et al., 2016).

2.4.2 Current Treatment of LW

At present, the treatment methods for LW include leachate transfer (i.e. recycling LW and mixing it with ordinary domestic sewage for treatment) (Renou et al., 2008), biological treatment (i.e. biodegradation of LW, which can be divided into aerobic treatment and anaerobic treatment) (Kamaruddin et al., 2017), chemical and physical treatment (i.e. a series of treatment methods such as chemical oxidation, adsorption, chemical precipitation, coagulation/flocculation, sedimentation/flotation and air stripping) (Mojiri et al., 2021), and membrane technology (Abdel-Shafy and Abdel-Shafy, 2017).

The most traditional method for treating LW is recycling, which has been widely used in LW treatment in the past due to its convenience and low operating cost. The key factors affecting the operation effect of the recycling system are the number of cycles and the system volume (Teng et al., 2021). However, when the number of cycles is too high, some difficult-to-treat substances in LW may accumulate in the circulation system and make the subsequent treatment of LW more difficult (Chugh et al., 1998). Furthermore, the recycling of LW may inhibit the formation of methane, thereby causing organic acids to reach a higher level, which lead to the production of methanogens (Ghosh et al., 2017; He et al., 2019). The mixing of LW with domestic sewage for treatment is not widely accepted by the public and has been questioned (Carvajal-Flórez and Cardona-Gallo, 2019). This is due to the low biodegradability of

organic inhibitory compounds and heavy metals in LW, which can lead to low treatment efficiency and the risk of increased effluent concentrations (Baun and Christensen, 2004; Abdel-Shafy, 2015). In order to reduce the presence of nitrogen and phosphorus in LW and domestic sewage, some people have proposed optimizing the volume share of the two in the total wastewater and provided a sequential batch reactor (SBR) composed of filling, anoxic, oxygenated and sedimentation to treat the mixture of the two (Contrera et al., 2014). This method adjusted the ratio of domestic sewage to LW to 9/1, thereby achieving the goal of further reducing COD and NH_4+-N (Contrera et al., 2014).

Biological treatment is a promising wastewater treatment method with the advantages of simple operation, low economic cost and low environmental impact (Teng et al., 2021). These advantages have attracted widespread attention. Biological treatment is usually used in wastewater with high BOD content (Anqi et al., 2020). Biological treatment is the process of biodegradation of organic matter by microorganisms under aerobic or anaerobic conditions. Under aerobic conditions, microorganisms can degrade organic matter into carbon dioxide and sludge, while in anaerobic environments, they can degrade it into biogas (Abdel-Shafy and Mansour, 2014). Biogas is a compound mainly composed of CO_2 and CH_4, which has considerable recycling value (Bajpai, 2017). However, since activated sludge may be inhibited by components such as organic matter, inorganic salts and heavy metals (Gotvajn et al., 2009), many difficult-to-degrade components remain in LW after biological treatment. In addition, biological treatment is more effective for wastewater with a high BOD/COD ratio and can effectively treat organic matter and nitrogen-containing substances in wastewater (Maia et al., 2015). However, the difficult-to-degrade substances (i.e. humic acid and fulvic acid) present in LW limit the entire treatment process over time (Abdel-Shafy et al., 2024). This shows that the effect of biological treatment is largely affected by the type, age and composition of LW.

Chemical and physical treatment are generally used in pretreatment or final purification process, and it can also be used to remove certain specific pollutants (Renou et al., 2008). This method treats wastewater through chemical oxidation,

adsorption, chemical precipitation, coagulation/flocculation, and flotation to reduce suspended solids, toxic compounds, colloidal particles and floating objects. Each step in the physical and chemical treatment method has its own procedures and functions (Abbas et al., 2009). Chemical oxidation is a method for treating wastewater containing refractory compounds that has attracted increasing attention and research. It is suitable for old or well-stabilized wastewater and can make the oxidized organic matter in these wastewaters the most stable oxidation state (water and CO_2), or in other words, completely mineralized. In addition, it can also improve the biodegradability of refractory organic pollutants and enable subsequent biological treatment to achieve greater economic benefits (Wang et al., 2003). Generally, this process uses ozone (O_3), strong oxidants (such as H_2O_2), radiation (such as ultraviolet rays, ultrasound, etc.) and catalysts (such as photocatalysts, etc.) as strong oxidants in the chemical oxidation process (Aftab et al., 2018; Aftab and Hur, 2019; de Brito et al., 2019). Among them, the use of photocatalysts can effectively degrade stubborn compounds such as humus (Abdel-Shafy and Mansour, 2017). However, the high cost and the fact that intermediate oxidation products may increase the toxicity of the treated wastewater limit the application of this technology (Lopez et al., 2004; Aftab et al., 2018).

Chemical precipitation is a method of removing or co-precipitating pollutants in wastewater by using chemical coagulants and coagulant additives. The pH value, temperature and ionic strength of the wastewater are factors that affect its effectiveness (Abdel-Shafy, 2015). Common precipitants in this process include sodium hydroxide (used to precipitate metal hydroxides), sodium sulfide (used to precipitate heavy metal sulfides), barium chloride (used to precipitate sulfates), etc. This process is generally used in the pretreatment stage to remove high-intensity pollutants (Abdel-Shafy, 2015). Coagulation/flocculation is often used to treat aged and stabilized wastewater, and it can achieve the purpose of removing non-biodegradable organic materials (Assou et al., 2016; Abdel-Shafy and Mansour, 2020). Ferrous sulfate, ferric chloride, ferric chloride, lime and aluminum sulfate are commonly used as coagulants in this process (Ghafari et al., 2009). In previous studies, traditional inorganic flocculants have the possibility of being replaced by biological flocculants in this process. Zouboulis et al. used 20 mg/L biological flocculants to achieve a removal efficiency of more than 85% for humic acid (Zouboulis et al., 2004). However, the concentration of aluminum or

iron in the liquid was observed to increase simultaneously and the process produced a consistent sludge volume, which became its disadvantage (Silva et al., 2004).

Flotation is to add flotation agents and introduce tiny bubbles into the wastewater. The flotation agents reduce the surface hydrophilicity of suspended matter, so that suspended matter or mineral particles can adhere to the surface of bubbles, thereby forming a foam layer to float up and achieve the purpose of solid-liquid separation. This process can act on the reduction of ions, colloids, macromolecules, bacteria and fibers (Adlan et al., 2011; Dabaghian et al., 2018). According to the study conducted by Bashir et al. in 2015 (Bashir et al., 2015), the flotation method was used to treat LW, which had an effective treatment effect on COD, turbidity, color and NH_3-N in LW, with treatment efficiencies of 75%, 50%, 93% and 41% respectively. Moreover, in a recent study on the flotation method, the use of flotation columns for subsequent treatment of LW achieved significant results for non-biodegradable compounds (humic acid) in LW. After optimizing the experimental conditions, the removal rate of this compound reached about 60% (Zouboulis et al., 2003).

Adsorption has been widely concerned as an effective and promising wastewater treatment method. Moreover, in current LW treatment methods, adsorbents have been widely used due to their large surface area, thermal stability, surface reactivity, and microporous structure (Teng et al., 2021). Compared with chemical treatment methods, adsorption has a more significant effect on COD treatment in LW, and this effect is not affected by the initial concentration of organic matter (Aziz et al., 2011; Da Silva et al., 2014). Among adsorbent choices, activated carbon is the most commonly used option (Teng et al., 2021). In the past, activated carbon was used as an adsorbent in LW, which could improve the biodegradability of old LW to a certain extent, achieve a COD removal rate of 40%, and increase its BOD/COD ratio by 0.38 (Gotvajn et al., 2009). In another study, Rodriguez et al. (Rodrıguez et al., 2004) used activated carbon and different resins to treat LW in 2004. The treatment results of activated carbon were the most significant, with a removal rate of COD as high as 85%.

The combination of adsorption treatment and other physical and chemical treatment methods can achieve better treatment effects on wastewater. For example, Kargi and Pamukogul 2004 (Kargi and Pamukoglu, 2004) used wastewater pretreated by air stripping and ammonia coagulation-flocculation. After adding powdered activated carbon and powdered zeolite (the concentration of which was $2g/L^{-1}$) to the wastewater, respectively, biological treatment is carried out (i.e. its mixture is placed in an aeration tank in a repeated batch mode). Research results show that these two adsorbents reduced COD in wastewater by about 87% and 77% respectively. In addition, the combination of ozone-ac and adsorption treatment can effectively remove COD and ammonia nitrogen (NH_4+-N), with removal rates as high as 86% and 92% (Kurniawan et al., 2006). However, the main disadvantage of this process is the high consumption of activated carbon, which leads to high economic costs. In recent years, in order to solve this problem, biochar has come into people's view as a new adsorbent, which has the potential to become a good substitute for activated carbon. For example, Luo et al. in 2019 used phosphoric acid-activated biochar prepared from rice husk to achieve excellent results in the adsorption treatment of LW, which can remove approximately 80% of COD in LW (Luo et al., 2019).

The air stripping method uses an air stripping tower to reversely flow air and wastewater in the air stripping tower, thereby increasing the contact time and contact area between wastewater and air, thereby improving the mass transfer efficiency of pollutants and volatilizing wastewater. transfer of organic compounds into the air. This process has a significant removal effect on high-concentration ammonia nitrogen in LW (De et al., 2019). The pH value is the main influencing factor in this process. This method is more effective at treating ammonia at higher pH values. For example, in the study of this process, martininen et al. achieved a removal rate of ammonia in wastewater of as much as 89%. At this time, the pH value of the wastewater was 11 (Marttinen et al., 2002). However, this process reduce the emission of NH_3. Causes air pollution, so it is important to use H_2SO_4 or HCl to treat the gas phase contaminated by wastewater (Marttinen et al., 2002). In addition, the adjustment of pH value is also one of the difficulties in this process.

Membrane technology is a process that uses a semipermeable membrane to remove pollutants from wastewater through the selective permeability of the membrane. It can be divided into microfiltration (MF), ultrafiltration (UF), nanofiltration (NF) and reverse osmosis (RO) (Renou et al., 2008). Outstanding features of membrane technology are its enormous volume load, powerful disinfection ability, minimal footprint, and good effluent quality (Teng et al., 2021). MF has excellent removal effects on suspended solids, materials and colloids, and its pore size is 0.1-10 microns. Therefore, in general, the pretreatment step of LW is completed by MF. However, due to its low removal efficiency for other pollutants, it is not suitable for use alone (Piatkiewicz et al., 2001). UF has a certain treatment effect on large molecules and particles in LW, and its pore size is in the range of 0.01-0.1 microns (de Almeida et al., 2020). It is usually used in the pretreatment of RO because UF can be used to remove components with larger molecular weight in LW. These components are easy to cause contamination to reverse osmosis membranes. Using UF to pretreat LW can effectively avoid this problem (Syzdek and Ahlert, 1984). NF has a smaller pore size than the previous two. It is usually made of polymer membrane with a pore size of only 0.001-0.01 microns. This membrane technology can remove inorganic, organic and microbial pollutants (Amaral et al., 2016). Although the membrane material and geometry may be different, the removal efficiency of NF for COD and ammonia is not affected. It can reduce COD by 60-70% and ammonia by 50% at an average velocity of 3 ms-1 and a transmembrane pressure of 6-30 bar (Renou et al., 2008). In order to improve the removal efficiency of COD in wastewater, physical treatment methods and NF can be used in combination, which can increase the COD removal rate to 70-80% (Trebouet et al., 2001).

Compared with other membrane technologies, RO is considered to be one of the most promising technologies for treating LW. This is because compared with other membrane technologies, RO has a stronger interception ability and can intercept suspended solids, dissolved matter, heavy metals, organic matter and dissolved inorganic matter, thereby achieving the purpose of removing pollutants (Wang et al., 2018). The treatment mechanism of RO is to apply pressure on both sides of the semipermeable membrane to pass LW through the membrane, thereby separating the pollutants and wastewater in it (Chen et al., 2020). Although membrane technology

can effectively treat many wastewaters, there are still some limitations. First, membrane technology cannot degrade pollutants in wastewater, but can only filter wastewater to separate pollutants, so some concentrates containing pollutants produced, which still need to be further degraded (Tałałaj et al., 2019). Second, the process of filtering wastewater with membrane technology pollute the semipermeable membrane (pollutants accumulate on the surface and in the membrane pores), and the semipermeable membrane needs to be replaced frequently, resulting in increased operating costs (Chen et al., 2016).

In order to prevent the harm and environmental impact caused by improper treatment of SSW, appropriate methods must be used to treat it. Since SSW is abundant and easy to obtain and has the characteristics of high C and high VM, it can be used as a pyrolysis material for microwave pyrolysis. As a promising waste treatment method, pyrolysis can convert SSW into value-added products, namely biochar, bio-oil and gaseous products, which can be used in daily life. However, conventional pyrolysis has certain limitations. The efficiency of pyrolysis and the yield of pyrolysis products can be improved by changing the heating source (solar energy, microwave) and pyrolysis environment (vacuum). Although solar pyrolysis is more environmentally friendly than conventional pyrolysis, it requires higher costs and is therefore not suitable as a pyrolysis heat source for SSW. Vacuum pyrolysis also has many limitations and requires more optimization and improvement. However, compared with other pyrolysis methods, microwave pyrolysis has the advantages of energy saving, rapidity, and uniform heating, and is more suitable for treating SSW. This chapter also summarizes and explains the previous LW treatment methods. Although these methods have certain treatment effects, they also have some limitations, such as high operating costs, the generation of new pollutants, and low treatment effects. Therefore, biochar adsorption is expected to be an excellent adsorbent for the adsorption treatment of LW due to its high efficiency, convenience and low production cost. To the best of the authors' knowledge, there are limited detailed studies on the production of biochar from SSW by microwave pyrolysis for the treatment of LW. In summary, the above findings provide motivation and objectives for exploring the

potential of using microwave pyrolysis as an efficient and environmentally friendly method to treat SSW and convert it into value-added products.

.

CHAPTER 3

RESEARCH METHODOLOGY

This chapter provides a detailed description of the experimental methodology as shown in Figure 3.1. The process begins with the collection of shrimp-shell waste, thereby anchoring the investigation in a locally abundant biomass residue and aligning the work with regional waste-valorisation priorities. After manual inspection to remove extraneous matter, the shells are oven-dried to eliminate free moisture, a prerequisite for reproducible thermal processing and accurate mass-balance calculations. The dried shells are then subjected to single-mode microwave pyrolysis at three discrete power settings to generate a suite of biochars. This power-graded approach permits a systematic exploration of how microwave energy density influences devolatilizations kinetics, carbon yield, and pore development. Prior to pyrolysis, the raw feedstock is characterised by Thermogravimetric analysis (TGA) to establish baseline devolatilizations behaviour; CHNS elemental analysis to quantify carbon, hydrogen, nitrogen, and sulphur contents; integration of Thermogravimetric and Fourier-transform infrared spectroscopy (TG-FTIR) to monitor evolved-gas speciation as a function of temperature; and Pyrolysis gas chromatography (Py-GCMS) to map volatile-product distributions. Following microwave conversion, the resulting biochars undergo a second tier of characterisation. CHNS analysis, FTIR, SEM, Brunauer–Emmett–Teller (BET) surface-area were carried out to quantify the properties most

relevant to adsorption efficiency. The practical efficacy of each biochar is then evaluated in a batch-adsorption targeting BOD, COD, and phosphate removal. By correlating removal performance with the structural attributes captured in earlier characterisation stages, the study establishes a structure–function relationship that guides optimisation of microwave parameters strategies.

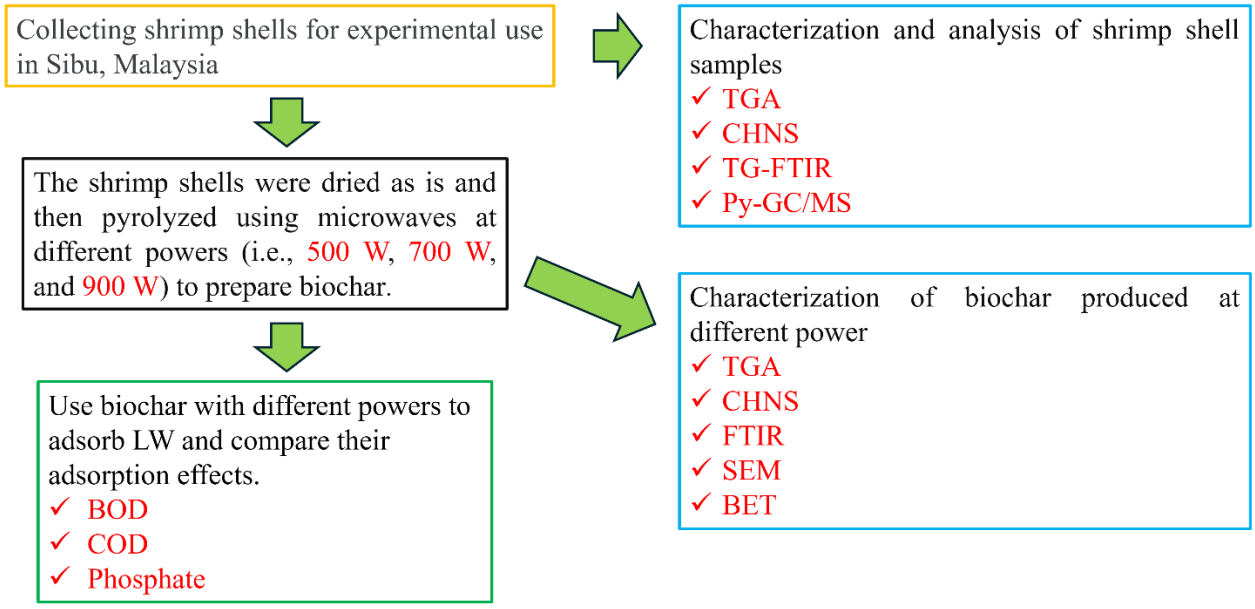

Figure 3.1 Experimental flow chart of shrimp shell waste (SSW) analysis and shrimp shell biochar (SSB) preparation processes.

3.1 Characterization of shrimp shell waste

3.1.1 Collection of shrimp shell waste

The SSW used in this experiment was collected from a breakfast shop in Sarawak, Malaysia. The SSW this time was obtained from fresh shrimp. Subsequently, the shrimp shells were placed in an oven and dried at 100°C for 24 h to remove moisture from the

shrimp shells (Figure 3.2a). Then, part of the shrimp shells was crushed to facilitate use in some experiments. Finally, the shrimp shells were processed into fine particles by a crusher (model: 2500Y) and packed into sealed bags for later use (Figure 3.2b).

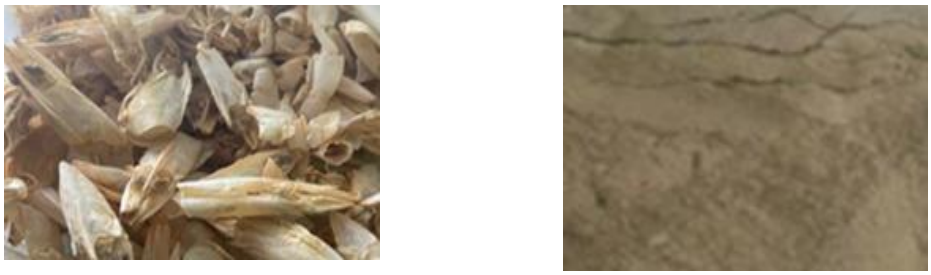

(a) (b)

Figure 3.2 a: Dried shrimp shell waste b: Shrimp shell powder

3.1.2 Chemical properties of shrimp shell waste

To determine the content of carbon (C), hydrogen (H), nitrogen (N) and sulfur (S) in SSW, it was decided to use a CHNS elemental analyzer (FlashHEA 1112, Thermo Electron Corporation, USA). First, the SSW that has been completely dehydrated is encapsulated in tin capsules, and 3 mg of SSW powder is enough, and then analyzed by the automatic sampler of the elemental analyzer. Second, the powder sample was heated and incinerated at 1000 °C to produce gaseous products including water, sulfur dioxide, and carbon dioxide to identify C, H, and S by infrared absorption. Detectors of thermal conductivity were then utilized to quantify the nitrogen content. The mass differences were then utilized to calculate the oxygen (O) content using the following formula: O (Oxygen) = 100 wt.%-C(carbon)-H(hydrogen)-N(nitrogen)-S(sulphur).

3.1.3 Energy properties of SSW

The energy properties of SSBs were determined by calculating high heating value (HHV), fuel ratio (FR), and the molar ratios of O/C and H/C. The term "HHV" stands for the maximum heat produced when a material totally burns(Perea-Moreno et al., 2016) . The bond energy among H, C, and O in SSW can be obtained by calculating the molar ratios of O/C and H/C (Hidayat et al., 2018) . The fuel characteristics of solid fuels are determined by FR. If the FR value of the sample is too low, increased the combustion speed, which is not suitable for direct use as fuel (Hidayat et al., 2018) . The following equations are the calculation methods of HHV, FR, H/C, and O/C (Eq1-4).

$$FR = \text{Fixed carbon SSW} / \text{Volatile matter SSW} \quad \text{(Eq.1)}$$

$$HHV(MJ/kg) = -1.3675 + 0.3137C + 0.7009H + 0.0318O \quad \text{(Eq.2)}$$

$$H/C = (H_{SSW} / \text{MW of H}) \div (C_{SSW} / \text{MW of C}) \quad \text{(Eq.3)}$$

$$O/C = (O_{SSW} / \text{MW of O}) \div (C_{SSW} / \text{MW of C}) \quad \text{(Eq.4)}$$

3.1.4 Thermogravimetric analysis

Shrimp shell waste (SSW) was analyzed at a constant nitrogen flow rate of 50 ml/min using a thermogravimetric analyzer (STA-8000, PerkinElmer, USA) to determine the approximate analysis of volatile compounds, moisture content, and fixed carbon. From 30 to 900 °C, a 10 mg sample was heated at a constant rate of 25 °C/min. By weighing samples at 150 °C and 550 °C, respectively, weight loss was utilized to determine the sample's water content and volatiles. Equation 5 was utilized to calculate the amount of fixed carbon:

$$\text{Fixed carbon (wt.\%)} = 100 \text{ wt.\%} - \text{moisture} - \text{volatile matter} - \text{ash.} \quad \text{(Eq.5)}$$

3.2 TG-FTIR analysis

The pyrolysis behaviour and product distribution of SSW were investigated with the aid of a thermogravimetric analyser (TA Instruments, New Castle, United States, TGA Q500) and a Fourier transform infrared spectrometer (FTIR). During heating of the SSW, a heating rate of 25 °C/min was performed by the TG analyser. Using a 50 mL/min nitrogen flow rate, 10 mg of samples were heated from 30 to 900 °C. For dynamic process control and to accommodate potential sample temperature gradients, a sample weight of 15 mg per run was ensured. When the exiting gas enters the gearbox line, the FTIR needs to be maintained at 200 °C to prevent possible gas condensation and subsequent reactions(Gu et al., 2013). The infrared spectral recording resolution range was set to 400–4000 cm-1, the scanning frequency to 64 scans/min, and the recording resolution to 4 cm-1. Utilizing the spectral database, analyze the FTIR spectra of the SSW.

3.3 Py-GC/MS analysis

The pyrolysis apparatus (Frontier EGA/PY3030D, Frontier, Japan) in conjunction with gas chromatography (TRACE1310, Italy) and mass spectrometer (ISQ, USA) was used to analyze gases emitted from the pyrolysis of SSW. The influence of pyrolysis temperature on the composition of SSW gas was studied by selecting 300, 500, 700, and 900 degrees Celsius as the pyrolysis temperatures, 30 seconds as the pyrolysis duration, and 50 degrees Celsius per minute as the heating rate. The temperature of the pyrolysis product delivery line and sampling valve was set to 320 degrees Celsius to prevent gas condensation. On a polar quartz capillary column (30 m x 0.25 mm x 0.25 m), pyrolytic vapours were separated by gas chromatography. The shunting mode employs a 100:1 shunt ratio and 50 mL/min shunt rate. Starting at 50 degrees Celsius,

the GC/MS temperature was held for 1 minute before being raised to 300 degrees Celsius at a rate of 10 degrees Celsius per minute. The ion source temperature was 300 degrees Celsius; the mass spectrometer's scanning range was 40800 amu at 70 eV electron energy, and the transmission line temperature was 320 degrees Celsius. Utilizing the NIST mass spectrometry library, the gas composition was determined. At least three analyses were conducted to ensure that the experiment could be repeated and that the results could be averaged.

3.4 Single-mode microwave pyrolysis of shrimp shell waste

3.4.1 Experimental setup

The microwave pyrolysis process of SSW was carried out on a single-mode microwave pyrolysis equipment. As shown in Figure 3.3(a, b), the single mode includes: temperature controller, magnetron, metal cover, K-type thermocouple, quartz reactor and single mode cavity. First, 30 grams of SSW (with shrimp shells, shrimp tails, but no shrimp heads) were placed in a quartz pyrolysis reactor. Then the quartz reactor containing SSW was placed in a single mold cavity and then covered with a metal lid to prevent microwave diffusion. Microwaves are emitted through a magnetron with a selected frequency of 2.45 GHz and a maximum power of 1000 W (Foong et al., 2020). In this experiment, the microwave power was set in three different ranges: 500 W, 700 W, and 900 W, and biochar was produced under different powers (ie, SSB 500, SSB 700, SSB 900) to examine the impact of different microwave powers on biochar production and structure. During the experiment, it is necessary to connect the K-type thermocouple and ensure that the thermocouple is in direct contact with the pyrolysis raw material to observe the temperature changes during the pyrolysis process under different microwave powers. The pyrolysis experiments for each different microwave power were repeated three times to ensure the repeatability of the experiments. After

the biochar is prepared, it is stored in glass bottles for adsorption treatment of LW. The average yield of three replicate samples was recorded as the biochar yield, and the biochar yield was calculated according to the following formula:

$$\text{Yield (wt.\%)} = (W_f/W_{i)} \times 100 \quad \text{(Eq.6)}$$

where W_f is the weight of biochar produced (g) and W_i is the weight of the sample (g). Figure 3.4 shows the flow chart of this microwave pyrolysis experiment.

(a)

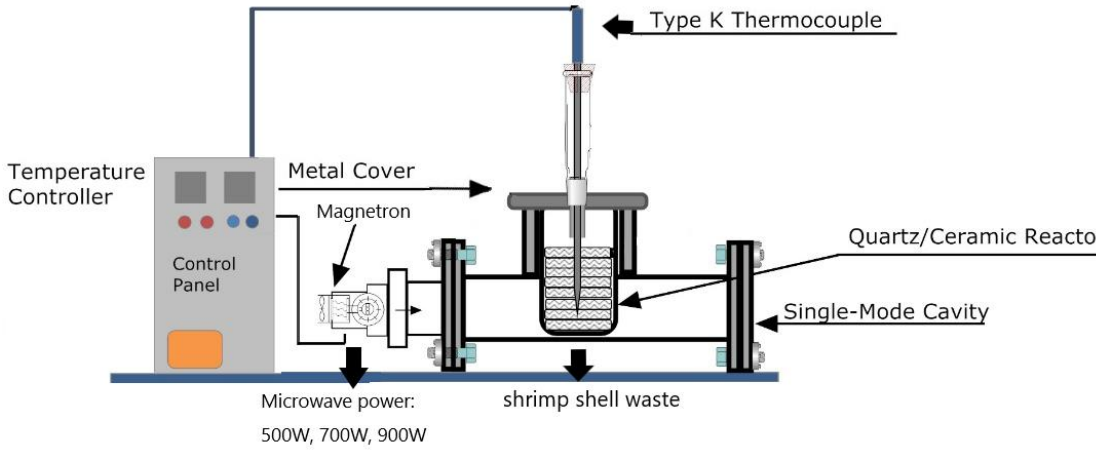

(b)

Figure 3.3 a: Physical setup of experimental equipment. b: Schematic diagram of experimental equipment.

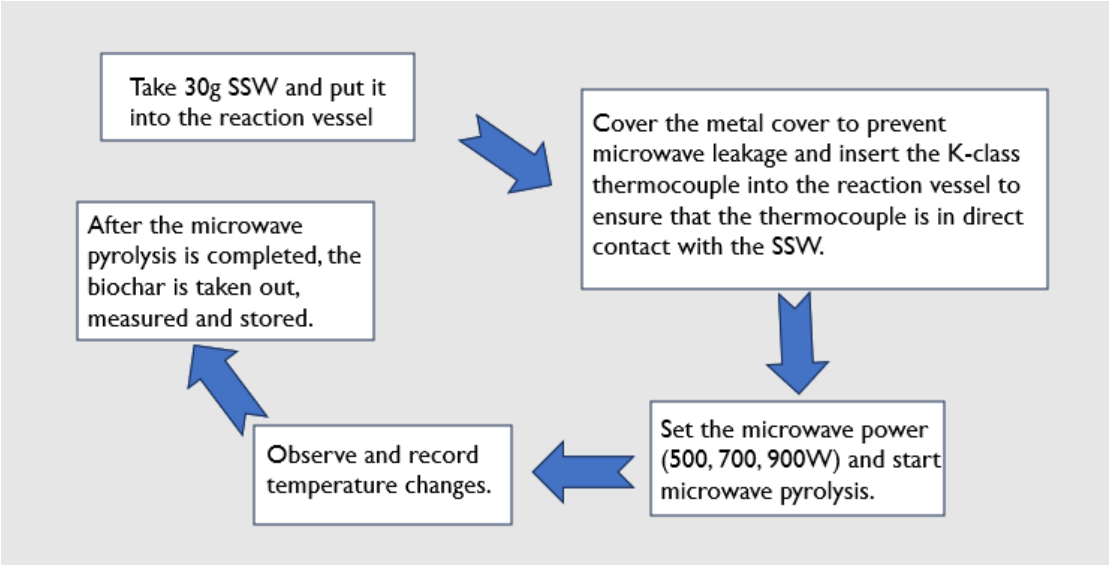

Figure 3.4 Microwave pyrolysis experimental flow chart.

3.4.2 Characterization of Biochar

Using a Perkin-Elmer Special Spectrum 100 FTIR spectrometer (Thermo Nicolet® IS10® FTIR spectrometer, Thermo Fisher Scientific, USA), the chemical functional groups in the biochar samples were determined. First, the biochar was put into the FTIR spectral measuring apparatus, which used the attenuated total reflectance (ATR) mode to scan the spectrum between 4000 cm^{-1} and 400 cm^{-1}. There were 64 scans and a resolution of 4 cm^{-1}. The data were then processed and examined. The experiment was conducted in triplicate to ensure the accuracy and validity of the data obtained. Both the Barrett-Joyner-Halenda (BJH) approach and the Brunauer-Emmett-Teller (BET) method were used to determine the biochar samples' specific surface area and pore properties. Prior to measurement, the sample was degassed (under vacuum) at a temperature of 90 °C for 10 h while heating at a rate of 10 °C per minute to eliminate any remaining moisture. The material was subsequently subjected to an extremely low temperature of –196 °C using liquid nitrogen. This produced N_2 adsorption-desorption isotherms allowed for the determination of the sample's total pore volume and BET surface area. Finally, the BJH desorption method was used to calculate the sample's characteristic porosity. The t-plot approach was employed to derive the micropore volume. A JEOL JSM-6360 LA scanning electron microscope (SEM) was used to analyze the biochar's surface morphology. The accelerating voltage used in this research was 10 kV. To improve the electrical conductivity, platinum was applied to the biochar samples. SSB underwent elemental analysis and industrial analysis. For detailed experimental procedures discussed in section 3.1.2, 3.1.3 and 3.1.4.

3.5 Adsorption of hazardous LW

For the application of biochar in LW treatment, LW samples were obtained from a landfill wastewater treatment plant in Sibu, Malaysia. After collection from the

sampling site, the LW samples were refrigerated at 4 °C to suppress microbial activity. The experiment utilized SSB produced at three different pyrolysis temperatures (SSB 500, SSB 700, and SSB 900) to assess their adsorption capabilities on LW. In the adsorption experiments, biochar was mixed with LW at a concentration of 20 g/L. This mixture was then stirred to ensure thorough mixing and prevent the biochar from settling, facilitating complete interaction between the biochar and contaminants in the wastewater. After 72 h, the mixture was filtered to separate the treated LW.

The main parameter of the investigations on treated LW was the phosphate content, chemical oxygen demand (COD), and biochemical oxygen demand (BOD). These investigations play a significant role in assessing the effectiveness of biochar in treating LW. The results aim to provide insights into biochar's pollutant removal efficiency and its potential application in wastewater treatment systems. BOD measures the oxygen consumed by microorganisms when decomposing organic matter in water. It is a key indicator of the organic pollutant load in wastewater. In BOD analysis, a wastewater sample was incubated for a standard period (5 days at 20 °C), and the decrease in oxygen concentration was measured. The greater the BOD, the higher the amount of degradable organic material in the water, indicating lower water quality.

The COD of the LW was determined by employing high-range COD digestion reagent vials (HACH) and utilizing both a DRB-200 reactor and a HACH-DR6000 UV-VIS spectrophotometer. Initially, the LW underwent filtration before being inserted into the HACH COD digestion reagent vial. The vial was subsequently heated in the DRB-200 reactor at 150 °C for 2 hours, followed by a controlled cooling to 120°C. After removing the sample from the reactor, it was allowed to cool to room temperature. The COD measurement was then conducted using the HACH-DR6000 UV-VIS spectrophotometer. Concurrently, phosphate levels in the water sample were assessed using the same spectrophotometer. The water sample was filtered and treated with a phosphate-specific standard, which induced the formation of a coloured complex. The

intensity of this colour, which develops after a designated reaction time, is indicative of the phosphate concentration in the sample.

CHAPTER 4

RESULTS AND DISCUSSION

This chapter first introduces and discusses the chemical properties, thermogravimetric analysis, and energy properties of SSW, confirming that SSW has high carbon content and high volatile content, and is suitable as a pyrolysis raw material. In addition, through its internal composition, it is concluded that SSW is not suitable for direct combustion and cause environmental pollution. At the same time, the volatilization time and temperature of light gases were explored through TG-FTIR data analysis, and the gas composition of SSW was further analyzed in combination with Py-GC/MS results to understand its thermal properties and solution behavior. Then, the SSB yield of microwave pyrolysis under different microwave powers was compared. When the microwave power was 500W, the SSB yield was the highest, about 50%. Subsequently, the chemical properties, thermogravimetric analysis, and energy properties of SSB were discussed and compared with the analytical data of SSW. The FTIR of SSB was also compared with the TG-FTIR data of SSW. In addition, this experiment explored the porous properties of biochar. Finally, biochar prepared with different microwave powers was applied as an adsorbent to LW, and the adsorption effect of biochar on BOD, COD, and phosphate in LW was studied, exploring the application potential of SSB in LW adsorption treatment. Some of the results of this chapter have been published in Energy & Environment.

4.1 Characteristics of shrimp shell waste

4.1.1 Chemical and physical properties of shrimp shell waste

The chemical properties of SSW are shown in Table 4.1. By analyzing its chemical properties, it can be seen that the main elements in SSW are oxygen (O) (46.7%) and carbon (C) (36.5%), followed by nitrogen (N) (10.9%) and hydrogen (H) (5.1%), and sulphur (S) is about 0.9%. The major composition of carbon and oxygen in SSW is critical for various applications, particularly in fields like biochar production and waste-to-energy conversion. The high levels of carbon and oxygen in SSW highlight its potential as a precursor for biochar and activated carbon, both of which are vital in environmental management and energy recovery processes. Carbon is the backbone element for many organic compounds and is crucial in the formation of biochar (Zhang et al., 2019). The high carbon content is advantageous because it ensures a stable, carbon-rich product that can sequester carbon dioxide, thereby reducing greenhouse gas emissions. In the context of biochar production through processes like pyrolysis, carbon acts as the primary element that contributes to the high surface area, porosity, and chemical stability of the final product. Oxygen in organic waste materials is typically bound in various oxygen-containing groups for the chemical reactivity of biochar. They are involved in reactions that can help to improve the adsorption of pollutants and the retention of nutrients in soil when used as a soil enhancer. Furthermore, the presence of oxygen influences the thermal degradation pathways during pyrolysis, affecting the yield, composition, and energy content of both the biochar and syngas produced.

In addition, SSW contains a certain amount of N and S. Therefore, SSW produce NO, NO_2, SO_2 and other harmful gases when burned; these toxic gases discharged into the air cause a certain degree of pollution to the environment and people's health, so direct incineration is not recommended (Lee et al., 2019). Compared with direct combustion, SSW can produce bio-oil through pyrolysis. Previous studies have found that bio-oil emits less polycyclic aromatic hydrocarbons and NO_X during the combustion process and has potential as a fuel (Sippula et al., 2019). Therefore, SSW should be used as pyrolysis raw material for pyrolysis treatment and is not suitable for direct combustion to avoid the emission of harmful gases.

The SSW contains 20.0% fixed carbon as detected from proximate analysis, which is essential for forming a stable biochar structure. Moisture content stands at 10.0%, which is relatively low and beneficial, as it reduces the energy required for drying before thermal processing. The volatile matter, at 50.0%, signifies a high potential for conversion into gaseous products during pyrolysis, beneficial for syngas production (Ofem et al., 2015; Wang et al., 2022). However, a 20.0% ash content could be problematic; high ash can hinder biochar quality and effectiveness (Marinković et al., 2016).

The oxygen to carbon (O/C) ratio is 1.0, indicating a balanced presence of carbon and oxygen, crucial for the thermal decomposition behavior and stability of the biochar produced. The hydrogen to carbon (H/C) ratio is 1.8, pointing towards a more aliphatic character of the organic matter, which typically results in a lower degree of aromaticity in the biochar. The high heating value is 15.11 MJ/kg, confirming that SSW is a promising candidate for energy generation, providing a substantial amount of energy per unit mass. The fuel ratio at 0.34 shows a dominance of volatile components over fixed carbon, which could influence the burning characteristics, making SSW more suitable for applications requiring rapid and complete combustion.

Table 4.1 The chemical properties of Shrimp shell waste (SSW)

Proximate analysis (wt%)	**Shrimp shell waste**
Fixed carbon (FC)	20.0±11.5
Moisture	10.0±3.2
Volatile matter (VM)	50.0±5.8
Ash	20.0±2.5
Elemental analysis (wt.%)	
Nitrogen (N)	10.9±0.1
Hydrogen (H)	5.1±0.1
Sulphur (S)	0.9±0.1
Oxygen (O)	46.7±3.7
Carbon (C)	36.5±3.4
O/C	1.8±0.3
H/C	1.0±0.2
Energy Properties	
High heating value (HHV)	15.11±11.8
Fuel ratio (FR)	0.34±0.1

4.1.2 Energy properties of shrimp shell waste

As shown in Table 4.1, the Fuel ratio (FR) value of SSW is 0.34. When the FR value is low, it indicates that combustion is ineffective and it increased the air pollutant emissions (Lee et al., 2019). In addition, according to the results, the High heating value (HHV) of SSW is 15.11 MJ/kg. The value of HHV can show the energy content of SSW when burned as fuel. The higher the value of HHV, the higher the energy content of the fuel when burned. Compared with traditional energy sources such as lignite (24.4-30.2 MJ/kg), SSW has a low HHV value, making it unsuitable as a fuel(Akhtar et al., 2017). Moreover, SSW has higher H/C (1.0) and O/C (1.8), while fuels with lower H/C and O/C contents release less smoke when burned and are therefore suitable for use as fuel (Wang et al., 2019). Therefore, SSW is not suitable for direct combustion.

4.1.3 Thermogravimetric analysis

Figure 4.1 depicts the TGA curve of SSW. In this experiment, the TGA curves of SSW at two different heating rates of 10 °C/min and 25 °C/min were observed. It can be seen from the TGA curve that the mass reduction of SSW can be divided into three stages.

The first stage is when the temperature is before 200 °C. The mass loss of SSW at this stage is 10%. The reason for the mass loss is due to water evaporation and lipid component decomposition(Zhang et al., 2019). The second stage of mass loss begins when the temperature reaches 200 °C and continues until 600 °C, during which the mass loss of SSW is approximately 50 %. The reason for this part of the mass loss may be due to the degradation of chitin and protein(Zhang et al., 2019), because chitin generally decomposes at around 220 °C-420 °C. It can be seen from the TGA curve that when the temperature reaches 450 °C, the downward trend of the SSW mass curve decreases significantly, which can also verify the impact of chitin decomposition on SSW mass loss. Due to the secondary decomposition of SSW, the shrimp shell loses approximately 20% of its weight in the third stage (>600°C). This is due to the fact that high temperatures destroy chemical bonds and macromolecular compounds in this section(Zhang et al., 2017; Yu et al., 2018a). The decomposition process of $CaCO_3$ begins after 700 °C, and the calcium carbonate content in SSW is also one of the reasons for the mass loss at this stage (Han et al., 2010). It was observed through TGA curves that the heating rate affects the pyrolysis process. This effect is evident at different heating rates. Accelerating the heating process can reduce pyrolysis time by overcoming heat and mass transfer limitations(Zhang et al., 2019).

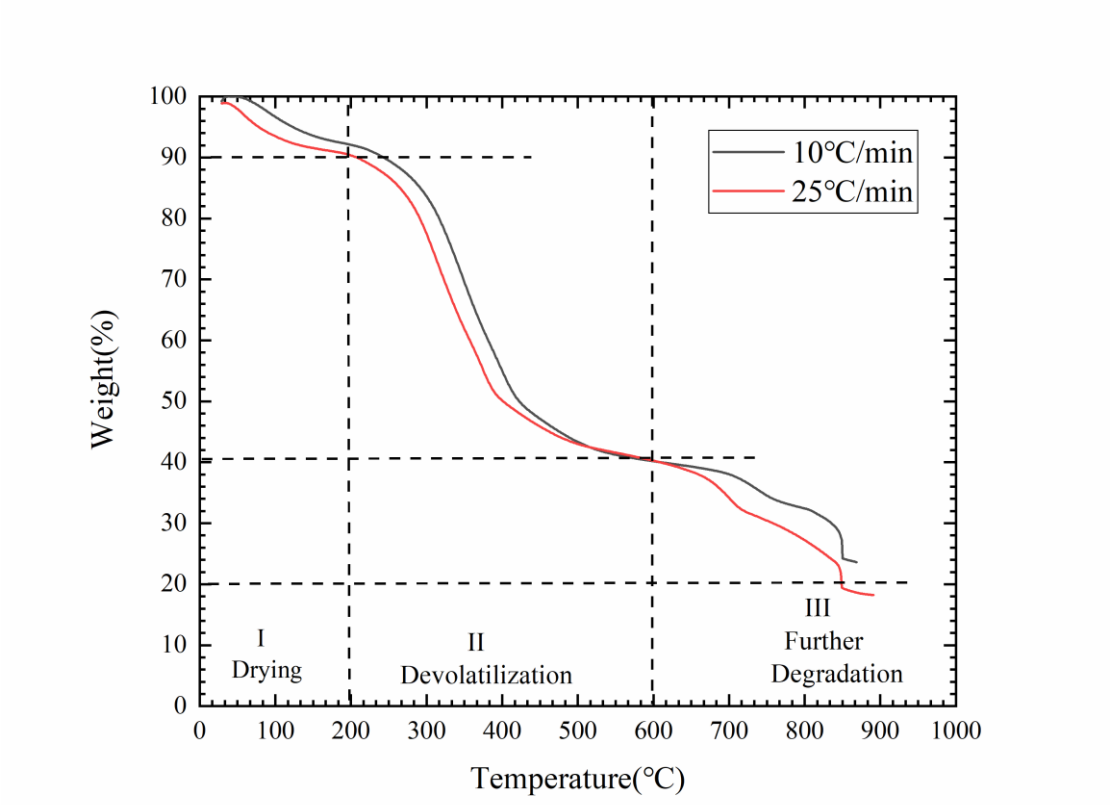

Figure 4.1 The Thermogravimetric Analysis (TGA) curves of shrimp shells at heating rates of 10 °C and 25 °C

4.2 TG-FTIR and Py-GC/MS

4.2.1 TG-FTIR analysis

The FTIR spectra of SSW at different temperatures are shown in Figure 4.2. Through the study of the FTIR spectrum of SSW, it was found that there are components such as CO_2, $CaCO_3$, phenols, alcohols, lipids, proteins, carbohydrates, nitrogen-containing functional groups and furan rings. At 90 °C, peaks detected at 3700~3600 cm^{-1} and 1700~1500 cm^{-1} were assigned to H_2O. This may be due to the evaporation of different forms of water during pyrolysis and the cleavage or reaction of oxygen functional groups(Lin et al., 2022). The peaks detected at 2400 and 600 cm^{-1} belonged to CO_2 (Ma et al., 2018). The release of CO_2 is primarily due to the decarboxylation of organic acids, sugar cleavage, and reforming (Ma et al., 2018). The FTIR spectra of SSW at 400, 600, and 800 °C do not show noticeable differences. The

stretching vibration of -OH was detected in the 3800–3500 cm^{-1} range, which inferred the existence of phenols and alcohols in SSW(Zhang et al., 2019). Stretching and bending at 3200 cm^{-1} and 3000 cm^{-1} inferred the presence of C-H due to the dehydrogenation of proteins, lipids and carbohydrates in the shrimp shell(Peng et al., 2015). In addition, C–H bonds can be generated in the pyrolysis of heterocyclic aromatic compounds such as pyridine, pyrrole, and indole(Li et al., 2020). At temperatures between 600-800 °C, the organic matter undergoes pyrolysis and becomes volatile, causing a fluctuation in the peak (Onay and Kockar, 2003; Tang et al., 2010; Yu et al., 2016).

Furthermore, N–H absorption peaks (bending vibrations in 1700–1600 cm^{-1}) were observed, possibly due to the presence of N-containing functional groups in proteins and chitin (Wei et al., 2017). The overlapping peaks among 1200 and 1000 cm^{-1} were ascribed to C-O-C functional groups, which mainly originate from the furan ring, and the elevated temperature promoted the decomposition of the furan ring, shortening the peak at higher temperatures, which can also be detected by GC /MS analysis to confirm (section 3.4) (Xiao and Yang, 2013; Shadangi and Mohanty, 2014; Pereira et al., 2016). The fluctuations at 2300 cm-1, 1600 cm-1 and 600 cm-1 are due to the gradual conversion of organic calcium to $CaCO_3$ during CO_3^{2-} pyrolysis(Zhang et al., 2019). It can be seen from TG-FTIR that the pyrolysis reaction of SSW is the most violent in the range of 400-600 °C. For example, at 600°C, glycosidic bonds and C-N bonds in chitin and C-R bonds in amino acids are more likely to occur. lysis. Therefore, 400-600 °C is the optimal pyrolysis temperature range for SSW (Zhang et al., 2019). From the spectra, it can be concluded that the volatiles released during the pyrolysis of SSW undergoes complex decomposition and reformation reactions, while more specific components released were identified via Py-GC/MS.

The optimal pyrolysis temperature range for SSW, as indicated by the FTIR spectra, appears to be between 400-600 °C. Within this range, key transformations occur, including the decarboxylation process, leading to significant CO_2 release. This suggests efficient degradation of complex organic materials. The spectra also highlight the production of high-value by-products like phenols and alcohols, as evidenced by -

OH stretching vibrations. Additionally, critical bio-components show signs of dehydrogenation, implying that bonds in these materials are breaking down into simpler, more volatile compounds. Nitrogen-containing functional groups are also being altered, as indicated by N–H absorption peaks, which is relevant for further biochemical applications. Therefore, the 400-600 °C range offers a balanced scenario for multiple objectives: breaking down complex molecules, releasing valuable compounds, and maintaining energy efficiency, making it the most advantageous temperature range for the pyrolysis of SSW.

The pyrolysis of SSW offers significant advantages over direct burning, particularly when high contents of nitrogen-containing chemicals are produced. Direct combustion of SSW with high nitrogen content risks would emit harmful nitrogen oxides, contributing to environmental and health issues such as air pollution and respiratory problems(Aryal et al., 2022). In contrast, pyrolysis allows for the controlled conversion of SSW into valuable nitrogen-containing chemicals and diverse pyrolysis oils. These products have a wide range of potential industrial applications, from fertilizers to chemical feedstocks, adding economic value to the waste-to-wealth process. Additionally, pyrolysis aligns with sustainable waste management strategies by fully utilizing the resource and minimizing environmental impact, thereby making it a more advantageous and responsible method for SSW treatment (Tan et al., 2023).

The TG-FTIR analysis of SSW revealed insights into its thermal decomposition behavior and the nature of the evolved gases. The analysis identified key temperature ranges where significant weight loss occurs, corresponding to the release of various gaseous products such as CO_2, CH_4, and CO. These findings underscore the suitability of SSW as a pyrolysis feedstock due to its high volatile content and the presence of functional groups conducive to gas formation. The data obtained from TG-FTIR analysis provide an understanding of the pyrolysis process, guiding the optimization of operational parameters to maximize biochar yield and quality. This knowledge is instrumental in advancing the application of microwave pyrolysis for efficient and sustainable conversion of SSW into value-added products.

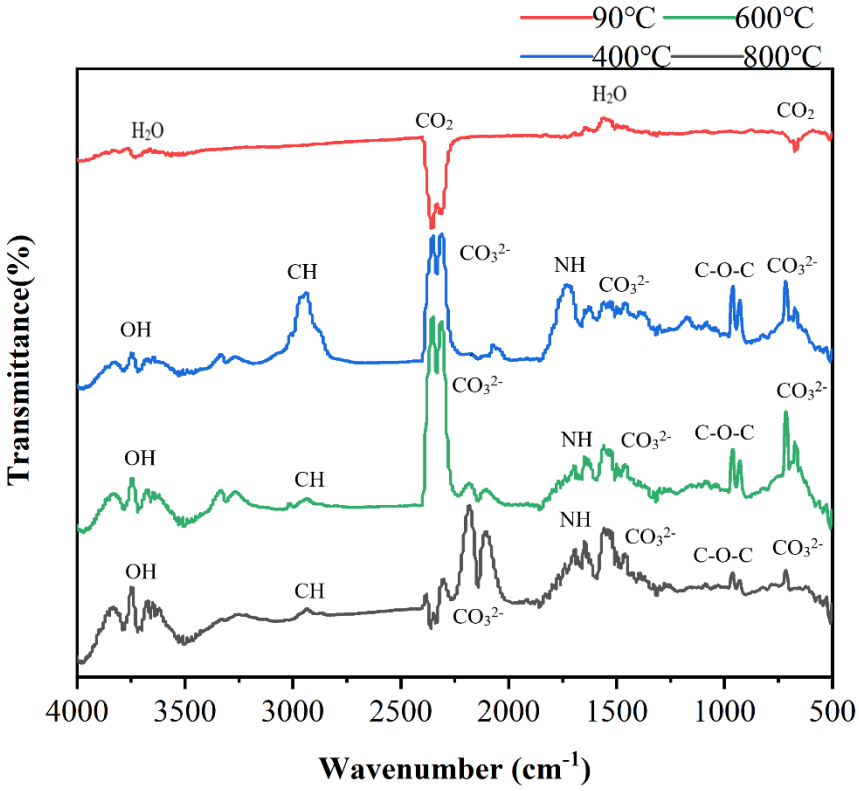

Figure 4.2 Fourier Transform Infrared Spectroscopy (FTIR) spectra of shrimp shell at different temperatures(i.e. 400°C, 600°C, 800°C, 900°C.).

4.2.2 Py-GC/MS analysis

Table 4.2 illustrates the chemical composition of SSW detected during pyrolysis. At different final temperatures, the detected chemical compositions are also different. These chemical components can be divided into carboxylic acids, hydrocarbons, nitrogen-containing compounds, ketones, esters, alcohols, phenols, sulfur-containing compounds, benzene, aldehydes and light gases. Among them, alkenes, aromatics and alkanes are classified as "hydrocarbons". The remaining oxygenates are classified as "other". The results showed carbon dioxide exists at 700 °C and is classified as a light gas. In addition to these classifications, this experiment also classifies the pyrolysis products based on the amount of carbon they contain. Due to the limitations of GC/MS in detecting light gases, lower molecular weight compounds cannot be detected.

Table 4.2 Classification of gaseous compounds in shrimp shell waste at different temperatures.

Gaseous compounds	**Area %**
Temperature: 500 ℃	
Carboxylic acid	28.73±0.45
N-containing	23.40±0.89
Ketone	14.43±0.55
Hydrocarbon	7.67±0.17
Alcohol	7.07±0.33
Ester	6.97±0.18
Phenol	5.44±0.32
Benzene	2.55±0.08
S-containing:	1.88±0.05
Other	1.89±0.04
Aldehyde	0.28±0.01
Light gas	0
Temperature: 700 ℃	
Carboxylic acid	7.19±0.31
N-containing	9.70±0.11
Ketone	4.37±0.12
Hydrocarbon	21.63±0.79
Alcohol	22.24±1.04
Ester	8.47±0.22

Phenol	2.94±0.11
Benzene	2.94±0.07
S-containing:	0
Other	2.18±0.11
Aldehyde	2.70±0.06
Light gas	15.36±0.63
Temperature: 900 ℃	
Hydrocarbon	51.11±4.16
Carboxylic acid	18.33±0.39
N-containing	15.86±0.69
Alcohol	5.01±0.19
Ester	3.53±0.12
Ketone	2.74±0.06
Phenol	1.95±0.06
S-containing:	0.02±0.00
Other	0.45±0.00
Benzene	0
Aldehyde	0
Light gas	0

According to the analysis of experimental results, it can be seen that the compounds produced by SSW pyrolysis change significantly with the pyrolysis temperature. The reduction in ketone concentrations observed in SSW pyrolysis as temperature increases from 500°C to 900°C can be attributed to several chemical and process dynamics as ketones formed during early decomposition stages, are relatively unstable at high temperatures and tend to undergo further reactions such as decarboxylation, transforming into hydrocarbons, or dehydration and dehydrogenation, which lead to the formation of alkenes and possibly aromatic compounds. As the temperature rises, the energy provided facilitates these transformations, shifting the dominant chemical pathways from the formation of functionalized oxygenates like ketones to more stable, energy-rich hydrocarbons. This process dynamic suggests a move towards complete decomposition and reformation of these molecules into simpler, less oxygenated forms as the temperature increases, thus explaining the observed decrease in ketones and increase in hydrocarbons at higher temperatures (He et al., 2020).

As the temperature increases, a gradual decrease in the amount of phenolic chemicals can be observed. The formation of phenolic chemicals usually occurs at temperatures below 450 °C(He et al., 2020). When the temperature increases, further demethoxylation and alkylation of phenolic compounds occured at higher temperatures, so the proportion of phenolic compounds decreased as the temperature increases (Kang et al., 2011, 2013). In contrast, the proportion of hydrocarbons gradually increases with the increase of temperature. Its content is 7.67% at 500 °C, and when the temperature rises to 700 °C, its content increases to 21.63%. When reaching 900 °C, the content increases to 51.11%. The reason why this happens is mainly due to the higher protein content in SSW. The decomposition of proteins and the cyclization of hydrocarbons promote the synthesis of cyclic hydrocarbons, thereby increasing the proportion of hydrocarbons (He et al., 2020).

In addition, the content of nitrogen-containing compounds changes as the temperature increases. The proportion of nitrogen-containing compounds is 23.40 % at 500°C, 9.70% at 700°C, and 15.86% at 900°C. The reason for this may be that proteins and chitin with nitrogen-containing functional groups start to decompose between 500 and 700°C, thus showing a downward trend. At 900°C, the Maillard reaction occurs, causing the amino acids decomposed from proteins to react with sugars to generate many N-heterocyclic compounds, thus increasing the content of nitrogen-containing compounds (He et al., 2020).

In addition to analyzing the types of pyrolysis products, this experiment also counted the carbon number of SSW pyrolysis products. Through the analysis of Tables S1, S2, and S3, it is found that among the pyrolysis products of SSW, the carbon number is mainly low carbon number, that is, C_1C_{10}. Regarding the formation of smaller molecular weight products, it is mainly due to the cleavage of chitin, such as CO_2, H_2O, etc. (Sebestyén et al., 2020). As the final temperature changes, it can be seen that the C_{11}-C_{15} content shows a clear downward trend. The reason for this is that the C-N bond between the polysaccharide chain and the chitin acetamide side group is broken to produce amides, amines and other nitrogen-containing compounds. , these compounds react more frequently with light hydrocarbons (compounds in the carbon

number range C_{11}-$C1_5$) to form complex carbon components (C_{20} and >C_{20})(Zhan et al., 2019), whereas from 700°C and 900°C C_{16}-C_{20}, The increase in C>20 content can also verify this.

In addition to the differences mentioned above, the types of compounds with the highest content are also different at different temperatures. The highest carboxylic acid content (28.73%) is at 500°C, the highest alcohol compound content (22.24 %) is at 700°C, and the highest hydrocarbon compound content (51.11%) is at 900°C. These high-content compounds have high utilization value. For example, carboxylic acids are used in polymers, solvents, and food additives. Alcohol can be used as fuel and as a raw material for scientific research or industry. A 50% volume ethylene glycol aqueous solution is widely used as an antifreeze product. Hydrocarbons are used in lubricants, asphalt and waterproofing materials. Therefore, through pyrolysis, SSW can be converted into useful by-products.

4.3 Microwave pyrolysis of shrimp shell waste

4.3.1 Temperature profiles of microwave pyrolysis

Conversion of SSW into biochar via MP at different microwave power levels provides an innovative method for processing SSW. This study carefully examined the temperature distribution corresponding to different microwave powers (Figure 4.3). The temperature profile comprises an initial drying phase followed by devolatilization and carbonization. A significant observation in this study is the rapid temperature increase to 900°C at 900 W. This phenomenon may be attributed to the inherent moisture in SSW, which effectively absorbs microwaves. As a result, the molecules and atoms gain energy from the microwaves, quickly generating kinetic energy and converting it into thermal energy. This phenomenon shows that increasing microwave power can significantly accelerate the drying stage, allowing the process to rapidly advance to the carbonisation stage. This finding highlights the critical correlation

between microwave power and pyrolysis efficiency, where higher power settings led to increased heating rates and thus enhanced carbonization of SSW.

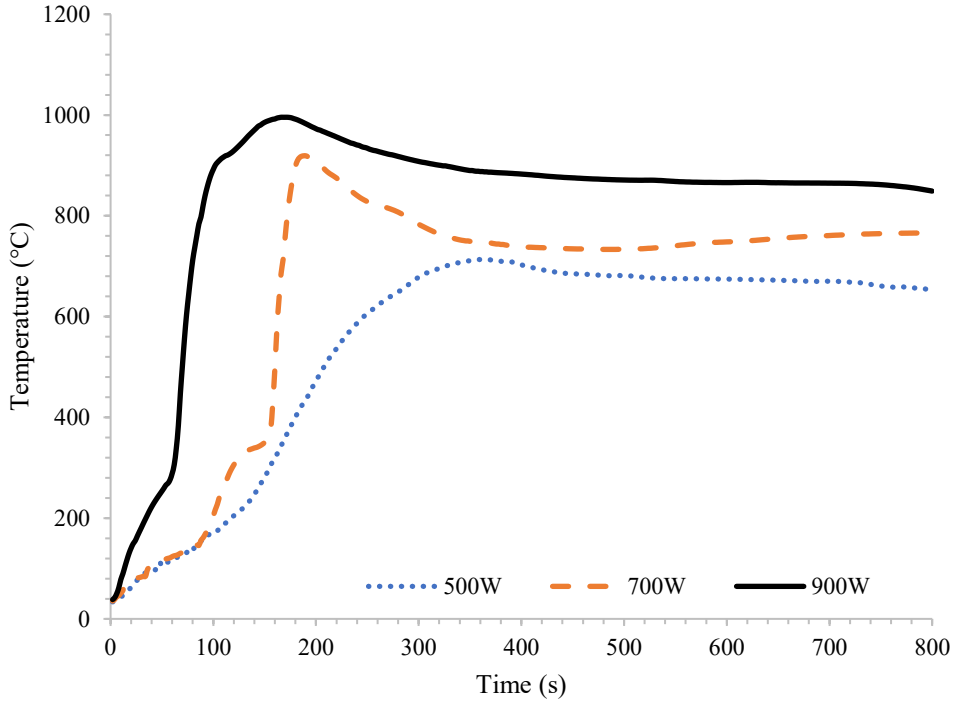

Figure 4.3 Temperature profile of Shrimp shell waste (SSW) microwave pyrolysis at different microwave powers (500 W, 700 W, 900 W).

The temperature curves for 500 W, 700 W, and 900 W exhibit a sharp ascent during the drying stage, indicating rapid moisture evaporation from the SSW. Specifically, the 900 W curve demonstrates a heating rate of 250 °C/min, reaching up to 250 °C, in contrast to the 80 °C/min observed at 500 W and 700 W. This suggests that higher microwave powers result in more rapid moisture evaporation (Intani et al., 2016). Each power setting exhibits different thermal behaviors as the heating and pyrolysis process proceed. The 500 W curve ascends more gradually, peaking at around 700 °C at a rate of 125 °C/min. In comparison, both 700 W and 900 W settings exhibit a more pronounced heating rate of 400 °C/min, reaching temperatures exceeding 900 °C. Notably, the 900 W curve displays the most aggressive temperature increase, peaking at approximately 1000 °C within 200 s. After that, the 900 W curve shows a slight decrease before stabilising, possibly signaling the culmination of the main reaction phase during pyrolysis. Concurrently, the pyrolysis temperature

stabilizes at 650 °C, 750 °C, and 850 °C for microwave powers of 500 W, 600 W, and 700 W, respectively.

The efficiency of SSW in absorbing microwaves significantly influences the pyrolysis process, as demonstrated by the varying temperature profiles observed at different microwave power levels. During pyrolysis, the release of volatile compounds can initiate exothermic reactions that elevate the temperature of the process (Duan et al., 2013), hence affecting the pyrolysis temperature and the resulting porosity and surface area of the biochar produced. To produce biochar with optimal porosity and extensive surface area as adsorbent, it is crucial to explore the peak temperatures and temperature profile of SSW during the microwave pyrolysis process.

The peak temperature could influence the decomposition of organic matter within the SSW as the chitin, proteins, and minerals decompose at various temperature ranges. At temperatures around 300-400 °C, chitin begins to decompose, releasing volatiles and starting the formation of pores within the biochar structure (Duan et al., 2013). However, to maximize porosity and surface area, temperatures need to be higher, typically around 600 °C (Zhang et al., 2019). At these elevated temperatures, proteins and minerals in the SSW also decompose and volatilize, further contributing to the pore formation and creating a more extensive and interconnected pore network.

The temperature profile, including the heating rate and holding time at peak temperature, significantly influences the overall SSB properties. The higher heating rate signified that SSW has better microwave absorbing properties and better temperature distribution within the SSW, promoting larger pore development (Lam et al., 2020). Conversely, a slower heating rate prompt to sub-optimal pore formation. This significant enhancement in biochar properties highlights the importance of optimizing the peak temperature and temperature profile during the microwave pyrolysis of SSW. By carefully controlling peak temperature and heating rate, this would enhance its efficiency as an adsorbent and contribute to sustainable waste management.

4.3.2 Elemental and porosity analysis

Table 4.3 shows the elemental analysis of SSW and the SSB produced under different microwave powers, revealing notable differences in carbon and oxygen content. The pyrolysis of SSW involves the thermal decomposition of its primary constituents of chitin, proteins, and minerals (Zhang et al., 2019). The thermal degradation of these materials can be understood in stages, and their chemical reactions can be complex due to the variety of bonds and the presence of multiple elements. The minerals in SSW are primarily composed of calcium carbonate ($CaCO_3$) (Zhang et al., 2019). The decomposition of $CaCO_3$ during pyrolysis is represented by the following Eq (7).

$$CaCO_3 \rightarrow CaO + CO_2 \qquad \text{(Eq. 7)}$$

When the temperature is increased, the breakdown of chitin is complete, leading to a higher release of nitrogenous compounds (NH_3) and carbon oxides (CO, CO_2). This results in a reduction in carbon content as well as a potential increase in oxygen content due to the formation of oxygen-containing surface groups on the biochar (Zhang et al., 2019). Hence, the rise in oxygen content and decreased carbon content at higher pyrolysis temperatures was noticed. The increased oxygen content in the biochar can be due to the retention of oxygen-containing functional groups or the incomplete combustion of the material. Simultaneously, the decrease in carbon content can result from the volatilization of carbon as gaseous compounds and the formation of a more oxidized char residue.

Table 4.3 Elemental composition and porosity analysis of Shrimp shell waste (SSW)

Analysis	**SSW**	**SSB 500**	**SSB 700**	**SSB 900**
Yield (wt.%)	-	50	45	35
Elemental composition (wt.%)				
Carbon (C)	36.5±3.4	43.6±2.2	28.9±5.4	27.8±3.2
Hydrogen (H)	5.1±0.1	4.3±0.1	1.9±0.2	2.0±0.1

Nitrogen (N)	10.9±0.1	6.9±0.2	3.9±0.1	3.3±0.2
Sulphur (S)	0.9±0.1	0.2±0.1	0.5±0.1	0.4±0.1
Oxygen (O)	46.7±3.7	45.0±2.6	64.7±5.8	66.5±3.6
Proximate content (wt.%)				
Moisture	10.0±3.5	5.8±2.2	3.5±1.2	2.0±0.5
Volatile matter (VM)	50.0±5.5	42.8±4.5	40.2±4.0	15.4±5.8
Ash	20.0±2.5	8.3±2.5	1.5±0.1	5.7±0.5
Fixed carbon (FC)	20.0±11.5	43.1±9.2	54.8±5.3	76.9±6.8
Porosity analysis				
BET surface area (m^2/g)	-	11.3±1.3	15.1±2.2	22.9±3.2
Total pore volume (cm^3/g)	-	0.9±0.3	0.9±0.2	0.9±0.1
Average pore size (nm)	-	6.6±0.1	6.5±0.1	5.6±0.1
Energy analysis				
High heating value (HHV)	15.1±11.8	16.7±5.1	11.2±11.5	10.8±7.1
Fuel ratio (FR)	0.3±0.1	0.2±0.1	0.1±0.1	0.4±0.1

When microwave power is increased from 500 W to 900 W, biochar production decreases from 50% to 35%. This reduction can be attributed to higher microwave power leading to higher heating rates and temperatures and a more extensive pyrolysis process. This in turn causes a higher production of volatiles and gases, leading to reduced biochar production. Additionally, it was observed that the carbon content peaked at 43.6% in SSB 500 and exhibited a declining trend with increasing microwave power. This pattern may be due to the more pronounced decomposition and gasification of carbonaceous components at higher temperatures. For instance, $CaCO_3$ undergoes a decomposition reaction to yield CaO and CO_2. The amount of carbon present in the SSB reduces proportionally to the amount of CO_2 released.

Therefore, the higher the microwave pyrolysis temperature, the lower the carbon content in the SSB.

As the power level of the microwave increases, the hydrogen and nitrogen content in the material decrease. Specifically, the content of hydrogen and nitrogen decreases from 4.3% and 6.9% for SSB 500 to 1.9% and 3.9% for SSB 700, and 2.0% and 3.3% for SSB 900. This indicates a higher degree of decomposition of organic compounds, resulting in the release of these elements in gaseous form at higher temperatures. The sulphur content follows an irregular pattern that fluctuates between 0.2–0.5 wt.%. The lower sulphur content observed in the final product (compared to the original 0.9%) is likely due to various processes during microwave pyrolysis of SSW. Firstly, high temperatures of microwave pyrolysis can induce sulphur-containing protein decomposition or breakdown. This decomposition releases sulphur in different forms, some of which may not be retained in the final product. Additionally, the intense heat can cause the volatilization of sulphur compounds, leading them to evaporate and escape as gases (e.g., SO_2) during pyrolysis. These observations indicate variations in the behaviour of elemental compositions, which warrants further investigation to understand the underlying mechanisms giving rise to these patterns.

Table 4.3 elucidates the porosity attributes of SSB, highlighting a clear correlation between the microwave power used during pyrolysis and the resulting properties of the biochar. As the microwave power increases, the heating rate during pyrolysis also increases, leading to a higher final pyrolysis temperature. This allows for a more thorough pyrolysis cracking of SSW, resulting in a significant increase in the BET surface area from 11.28 m^2/g for SSB 500 to 22.89 m^2/g for SSB 900. The primary factor driving this increase is the enhanced release of volatile components from SSW as the temperature rises, leading to the improved porosity (Zhang et al., 2020). The average pore diameter of SSB ranges from 5.63 nm to 6.61 nm, which belongs to the mesoporous category (Gao et al., 2021).

Moreover, the total pore volume of SSB remains relatively invariant, with values ranging from 0.9014 to 0.9036 cm^3/g, indicating a predominance of mesopore volume within the biochar structure. This invariance suggests that while the internal surface area and pore size are responsive to the microwave power, the overall volumetric capacity for containment within the pores of SSB is maintained across the different

power settings. Therefore, the porosity analysis demonstrates that increasing the microwave power refines the surface area of SSB yet inversely impacts its average pore size without significantly affecting the total pore volume.

Overall, the comparative analysis of SSW and SSB subjected to different microwave powers illustrates significant carbon and oxygen content variations. Pyrolysis generates intricate chemical reactions involving chitin, proteins, and minerals such as calcium carbonate. As the pyrolysis temperature increases, an obvious reduction in carbon content and a potential rise in oxygen content occur possibly due to the emission of nitrogenous and carbon oxides. Moreover, an increase in microwave power can result in a higher heating rate and microwave pyrolysis temperature, leading to a decrease in the biochar yield due to an increase in volatilization reactions within the SSW. This in turn could affect the composition of elements including hydrogen, nitrogen, and sulphur.

4.3.3 Proximate analysis

The proximate analysis shows a clear trend in which the moisture content within the biochar shows a clear decreasing trend with increasing microwave power. This phenomenon effectively elucidates the proficiency of microwave power in expediting moisture evaporation. Concurrently, a similar trend was observed for the volatile content, which decreased as the microwave power increased. This situation suggests that higher microwave power can promote a more pronounced devolatilization process.

Interestingly, the effect of different microwave powers on pyrolysis can be seen from the fixed carbon and ash content. The fixed carbon content dropped dramatically when the microwave power was increased from 500 W to 700 W. There was an abrupt decline of 1.5% from 8.3%, followed by a little gain at 900 W (5.7%). In contrast, the ash content increases with higher microwave power, implying that the non-combustible inorganic components progressively dominate the composition of the biochar when the volatile and combustible organic constituents are expelled (Zhang et al., 2019). The higher heating value (HHV) range recorded for SSB is 10.83–16.73 MJ/kg, indicating a relatively low energy content. In addition, the fuel ratio of SSB

falls within the range of 0.037–0.370, suggesting that it may not be suitable for direct combustion.

Figure 4.4 shows the thermogravimetric analysis (TGA) curves depicting the decomposition characteristics of SSB produced at different microwave powers. TGA serves as an important tool to quantify a material's weight loss upon heating, thereby offering insights into the composition of the material such as moisture, volatiles, and fixed carbon content, and its thermal stability. This analysis helps to understand the heating behavior of the material and its potential applications.

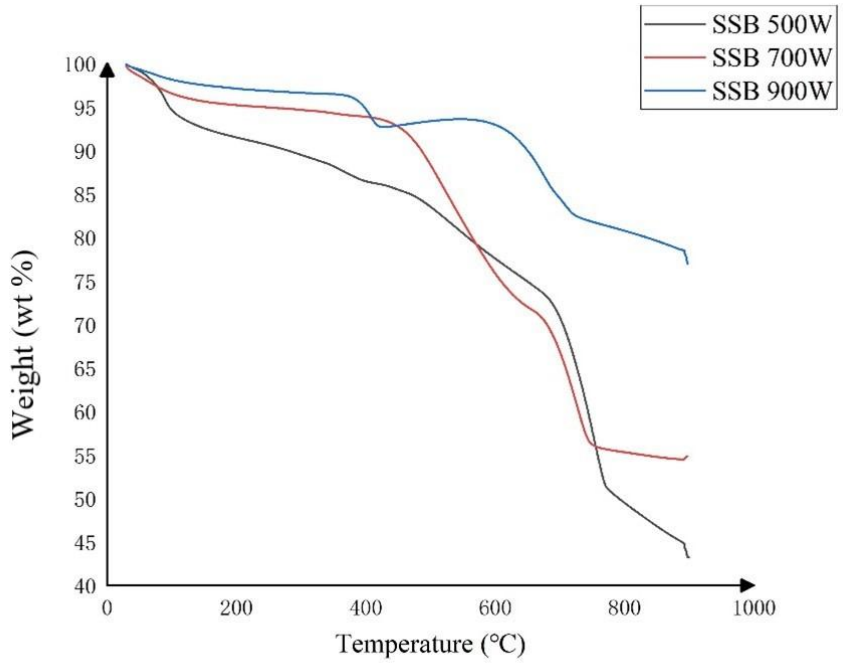

(a)

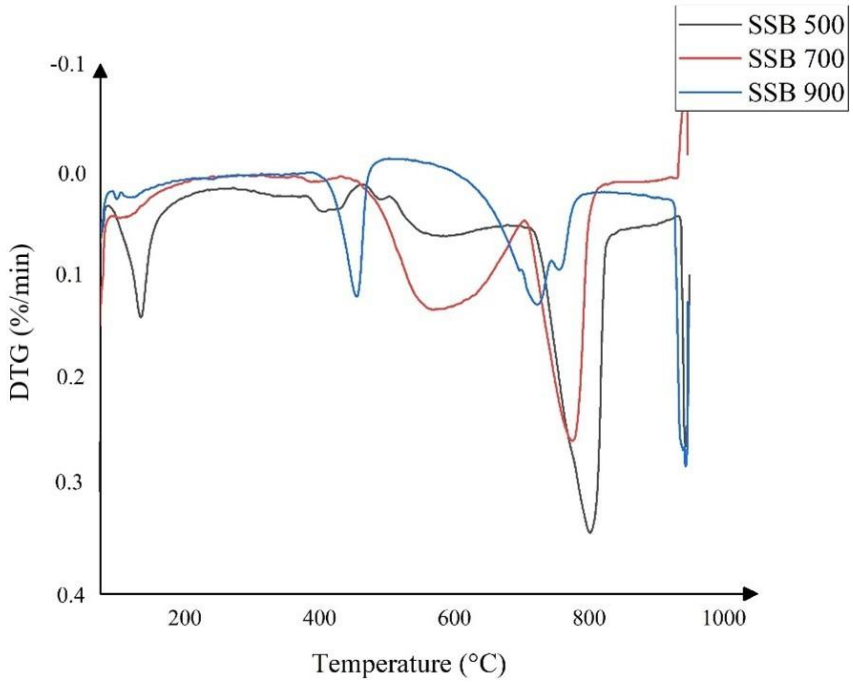

(b)

Figure 4.4 (a) Thermogravimetric Analysis (TGA) and (b) Derivative Thermogravimetry (DTG) Curves of Shrimp Shell Biochar (SSB) under Microwave Powers of 500 W, 700 W, and 900 W

The TGA and DTG curves for SSB produced at varying microwave powers offer an analysis of the thermal degradation properties of the biochar samples. From the TGA curve (a), it can be observed that all samples exhibit initial weight loss up to approximately 200 °C, which can be attributed to the release of moisture content.

As the temperature increases, the curves for SSB 500, SSB 700, and SSB 900 diverge significantly, indicating differences in their thermal degradation behaviours. The SSB 500 has significant weight loss at a lower temperature (150 °C) compared to SSB 700 and SSB 900, suggesting that it contains a higher amount of volatile matter expelled at lower temperatures. On the other hand, SSB 700 and SSB 900 maintained a higher weight percentage until reaching temperatures between 400 and 500 °C. This may be attributed to the higher microwave power settings of both, providing increased temperatures to more effectively shatter and volatilize the low-temperature volatile materials in SSW. There are multiple peaks observed in the DTG curves, which indicate that various decompositions occurred within the temperature range studied.

These peaks line up with the thermal breakdown of the various organic components of the biochar. Overall, the TGA and DTG curves analysis shows that SSBs generated at higher microwave powers (especially 900 W) are heated faster during pyrolysis than SSBs produced at lower powers. As the temperature increases, the proportion of fixed carbon increases and volatile substances decrease. The findings indicate that the microwave power used during production significantly impacts the yield, elemental composition, and thermal degradation properties of SSB.

4.3.4 Functional group analysis by FTIR

Figure 4.5 shows the FTIR spectrum analysis that reveals the variations in the chemical structure of SSB when subjected to different microwave pyrolysis powers. Spectral examination of SSB at 500 W, 700 W, and 900 W power levels shows the existence of certain functional groups that indicate the changes in chemical composition that take place during the pyrolysis process. For all three samples, SSB 500, SSB 700 and SSB 900, the presence of carbonate (CO_3^{2-}) groups is evident as shown by the peaks in the region corresponding to CO_3^{2-} (570 cm^{-1}, 871 cm^{-1} and 1034 cm^{-1}). The peaks observed in the analysis indicate the occurrence of calcination process, during which the organic calcium compounds present in the shrimp shells are transformed into CaO. The intensity of these peaks rose as microwave power increased, suggesting a more complete conversion at higher energies.

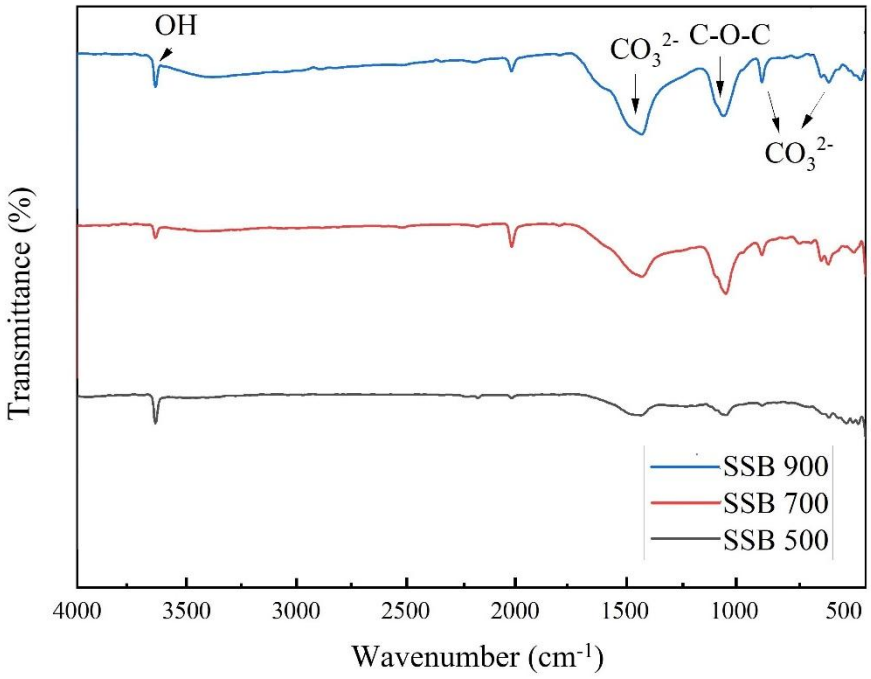

Figure 4.5 Fourier Transform Infrared Spectroscopy (FTIR) spectra of biochar prepared with different microwave powers:500 W,700 W and 900 W.

The C-O-C functional groups represented by their characteristic peaks (1049 cm^{-1}) are observed across all the biochar. These peaks suggest the presence of residual polysaccharides or the formation of ether or ester linkages (Kai et al., 2019). The C-O-C structures are essential as they contribute to the stability of the biochar and its potential chemical reactivity. Furthermore, the spectrum highlights the -OH (3640 cm^{-1}) functional groups, which indicate the presence of alcohols or phenols within the biochar (Xiao and Yang, 2013; Shadangi and Mohanty, 2014; Pereira et al., 2016).

The SSB 500 shows lower carbonate peak intensities at wavelengths of 570 cm^{-1}, 871 cm^{-1} and 1034 cm^{-1}, implying a less thorough conversion process at this energy level. The SSB 700 biochar shows a marked increase in these peaks, indicative of greater transformation due to the intermediate microwave power. The SSB 900 sample exhibits the most intense peaks, reflecting the highest conversion level of organic material to possibly inorganic carbonates at the highest power setting. Overall, the FTIR spectral analysis highlights the significant impact of microwave power on the composition and structure of SSB. By altering the power settings during pyrolysis, one

can tailor the properties of the biochar such as adsorptive capacity and pH buffering ability to suit specific environmental or agricultural applications. The variations in peak intensities and shapes provide insights into the degree of transformation and help to predict the behaviour and potential applications of biochar in various domains.

4.3.5 Surface morphology of biochar

Figure 4.6 provides the changes in surface morphology in SSB at various stages of microwave pyrolysis, as illustrated by SEM images. These images clearly demonstrate the transformations, deformation, shrinkage generation and pores formation occurring on the surface of the SSW due to the pyrolysis process. Figure 4.6(a) displays the raw SSW, which exhibits a smooth surface, highlighting its unprocessed state. In contrast, Figure 4.6(b) captures the formation of bubbles on the surface of SSB 500, indicative of volatile gases being released during the pyrolysis. Figure 4.6(c) illustrates the surface of SSB 700, showing noticeable shrinkage as a result of the higher temperature exposure. Lastly, Figure 4.6(d) shows the surface of SSB 900 which is extensively populated with pores, further evidencing the intense structural changes induced by varying microwave power intensities. These SEM images effectively depict the progressive morphological transformations of SSB under different conditions of microwave pyrolysis.

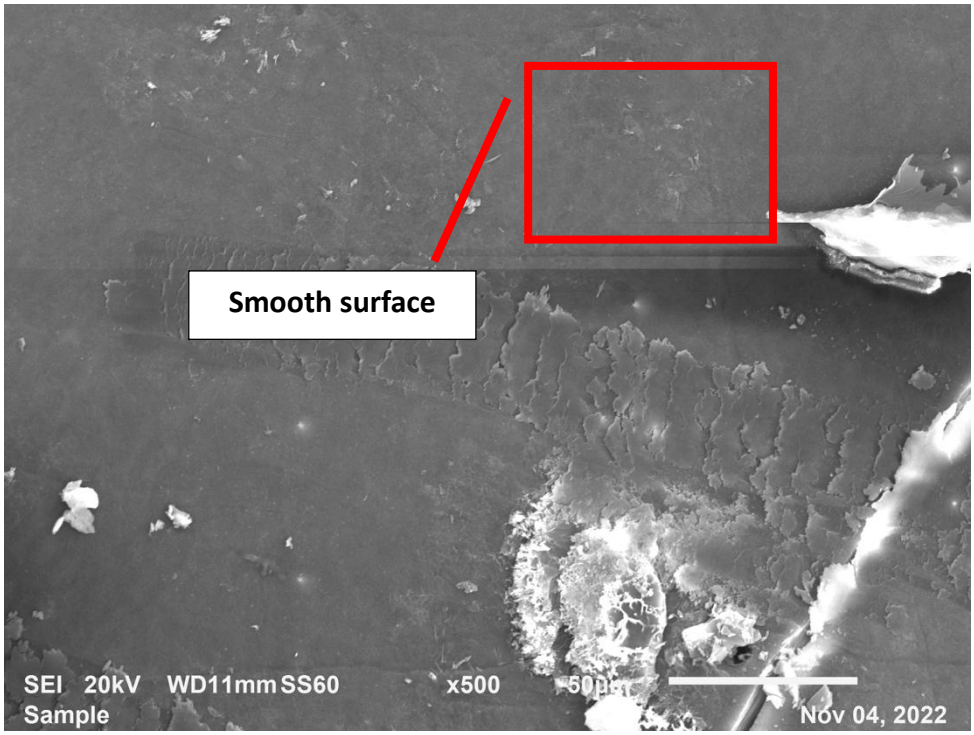
Smooth surface
SEI 20kV WD11mm SS60 x500 50µm
Sample
Nov 04, 2022

(a)

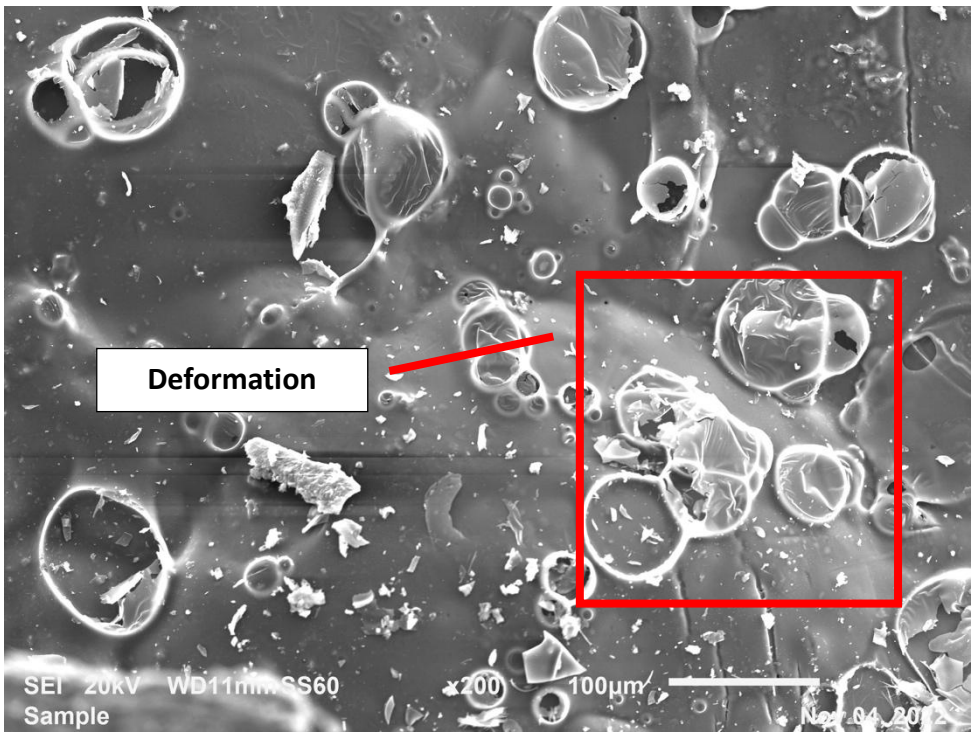
Deformation
SEI 20kV WD11mm SS60 x200 100µm
Sample

(b)

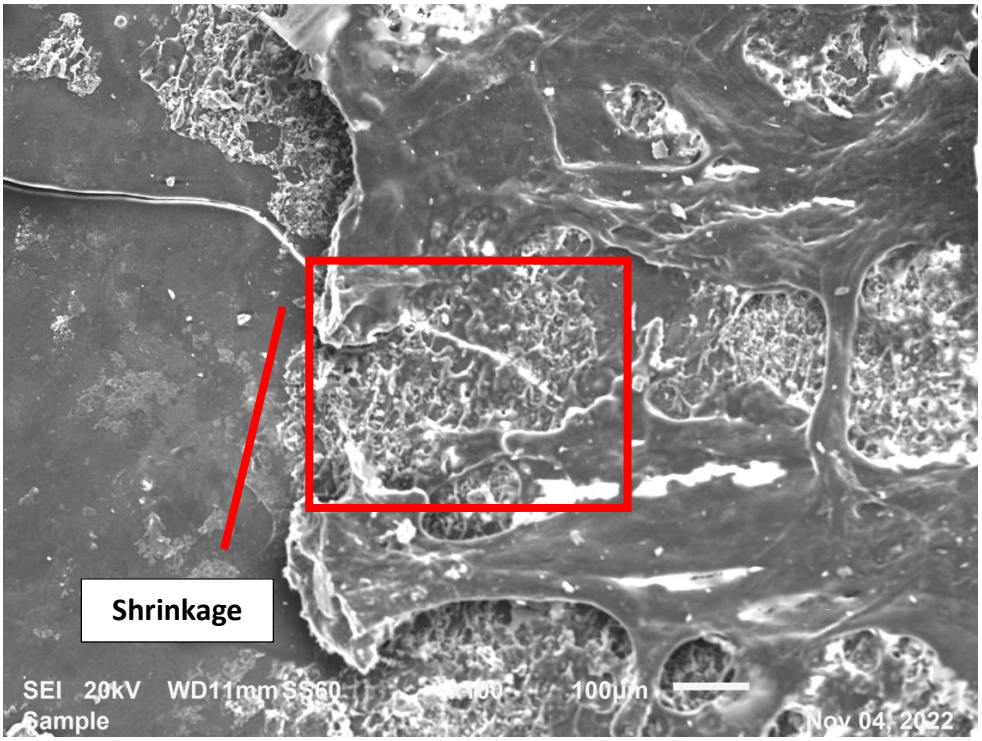

(c)

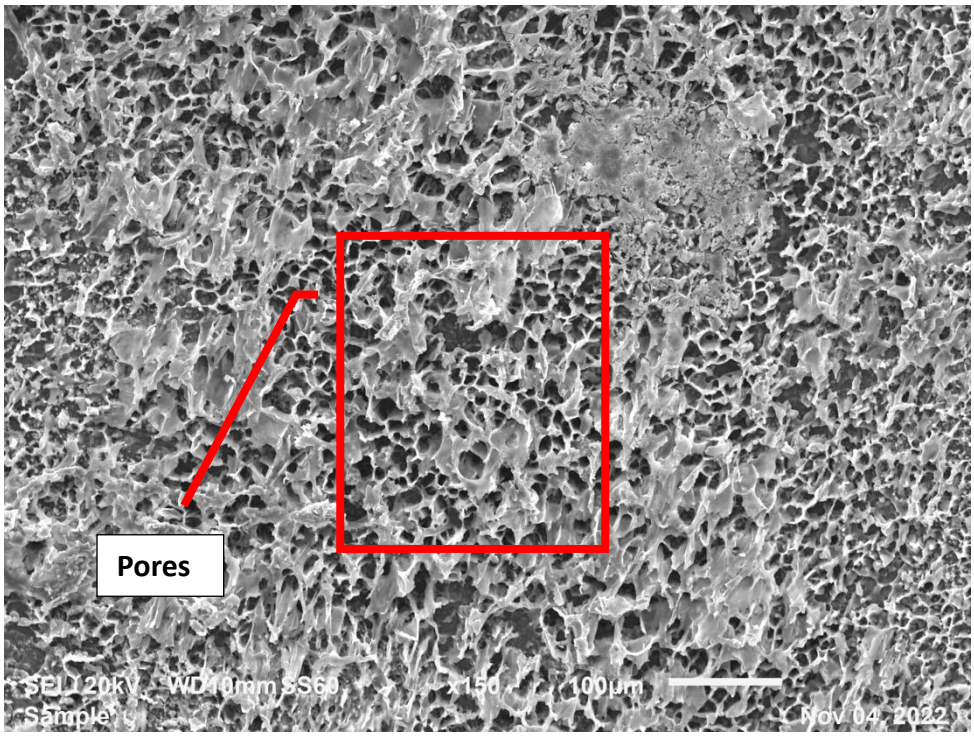

(d)

Figure 4.6 Scanning Electron Microscopy (SEM) Micrographs of Shrimp Shell Waste (SSW) and Shrimp Shell Biochar (SSB) Prepared at Different Microwave Powers: (a) Raw SSW, (b) SSB 500W, (c) SSB 700W, (d) SSB 900W

4.4 Production cost analysis

Table 4.4 estimated the SSW conversion to biochar under two microwave-heating regimes with small-scale batch processing and a modest continuous line at fixed at 900 W and a benchmark electricity tariff of RM 0.30 kWh^{-1}. The batch reactor handles only 9.6 kg/day of wet shells against 30 kg/day in the continuous system, the unit production costs converge at RM 15/kg of char for the batch route and RM 14.8/kg for the continuous route. The continuous design enabling quicker accumulation of saleable inventory, smoother staffing schedules, and easier integration with downstream activation or palletisation steps that can triple the product's selling price. The table implicitly highlights that capital-light batch reactors excel in flexibility but sacrifice scale economies, whereas continuous lines exchange higher capex for a more attractive cost-per-kilogram trajectory once feedstock logistics and off-take agreements are in place.

Table 4.4. Estimated production cost of Shrimp shell waste (SSW) biochar per day

Parameter	**Batch mode(200 g/batch; 10 min cycle; 48 batches/day)**	**Continuous mode 30 kg feed/day; 20 h operation)**
Feedstock collection	RM5/kg	RM5/kg
Capacity	200g/batch	30.0
Feedstock processed (kg/day)	9.6	30.0
Biochar produced, 35 % yield (kg/day)	3.36	10.50
Microwave energy demand (kWh/day)	8	20
Electricity cost (RM0.30/KWh)	2.4	6.00
Feedstock cost (RM/day)	48.00	150.00
Production cost (RM/kg char)	**15.00**	**14.80**

4.5 Application of biochar in landfill wastewater treatment

Table 4.5 shows the efficiency of LW adsorption by SSB produced at different microwave powers. The performance of each biochar was measured in terms of adsorption efficiency (mg/g) and removal percentage. The evaluation of the adsorption efficiency was based on the removal of BOD, COD, and phosphate. For BOD removal, SSB 900 shows the highest adsorption efficiency at 75 mg/g and a removal percentage of 70%, followed by SSB 700 at 69 mg/g and 65%, and SSB 500 at 64 mg/g and 60%. Because more adsorption sites for organic contaminants are available due to the increased BET surface area of the biochar generated, the adsorption efficiency and elimination percentage trend upward with higher microwave power. The COD removal trends indicate that SSB 900 has the highest adsorption efficiency at 210 mg/g, resulting in a 57% removal of complex organic molecules contributing to the COD of LW. In contrast, SSB 700 and SSB 500 exhibit lower efficiencies and removal percentages, which are likely due to their smaller surface areas.

Phosphate removal shows increased adsorption efficiencies of 4.5−8.3 mg/g and removal percentages of 10.1−20.9%. As the microwave power increases, the temperature rises and the capacity of the biochar to adsorb phosphate improves due to higher porosity. Overall, the results indicate a direct correlation between the microwave power used during biochar production and the adsorption capacities of the resultant biochar. Higher microwave powers lead to biochar with enhanced adsorption properties, as evidenced by the increased removal percentages of BOD, COD, and phosphate from LW.

Table 4.5. Adsorption Efficiency of Shrimp Shell Biochar Prepared at Microwave Powers (500 W, 700 W, 900 W) for Landfill Wastewater Treatment

LW (Dosage: 4 g/L)	**SSB 500**	**SSB 700**	**SSB 900**
pH	9.2±0.3	9.4±0.2	9.8±0.5
BOD (mg/L)			
Adsorption efficiency (mg/g)	64.0±3.5	69.0±3.2	75.0±4.0
Removal percentage (%)	60.3±2.2	65.0±3.2	70.0±3.8

COD (mg/L)			
Adsorption efficiency (mg/g)	177.0±0.5	190.0±0.3	210.0±0.2
Removal percentage (%)	48.3±1.3	51.9±1.5	57.3±1.7
Phosphate(mg/L)			
Adsorption efficiency (mg/g)	4.5±0.2	6.0±0.2	8.3±0.3
Removal percentage (%)	10.1±1.5	15.0±2.1	20.9±3.3

4.6 Summary

This study aims to convert SSW into value-added products through microwave pyrolysis technology and apply SSW in the adsorption treatment of LW. The results of this research show that microwave pyrolysis technology can achieve this goal. The research results show that SSW is suitable as a pyrolysis feedstock for biochar production due to its characteristics of high carbon and high volatile matter. The yield of SSB can reach up to 50%. In addition, the SSB produced under different microwave powers has excellent adsorption effect on LW. Among them, SSB 900 shows the best adsorption effect in the adsorption treatment of LW, with a phosphate removal rate of 20.9%, a COD removal rate of 57.3%, and the best BOD treatment effect, up to 70%.

CHAPTER 5

CONCLUSION AND RECOMMENDATION

5.1 Conclusion

The study's objectives were systematically fulfilled, and the results provide a robust foundation for future scale-up and commercialization. The thermogravimetric analysis coupled with Fourier-transform infrared spectroscopy established that devolatilization of shrimp-shell waste is most efficient between 400 °C and 600 °C. Complementary pyrolysis–gas chromatography/mass spectrometry further demonstrated that the volatile product spectrum is strongly temperature-dependent: carboxylic acids dominate at 500 °C, alcohols at 700 °C, and hydrocarbons at 900 °C. These findings confirm the suitability of SSW as a feedstock for targeted production of value-added intermediates, thereby satisfying the first research objective concerning feedstock appraisal and product mapping.

The second objective—generation and characterization of microwave-derived biochars was achieved through single-mode microwave pyrolysis at graded power levels, yielding three distinct materials SSB-500, SSB-700, and SSB-900 with 35 %, 45 %, and 50 % char yields, respectively. Detailed physicochemical profiling revealed systematic enhancements in specific surface area, pore-size hierarchy, and heteroatom functionality with increasing pyrolysis temperature, traits that directly influence adsorptive performance.

The third objective involved evaluating these biochars as adsorbents for landfill-leachate pollutants. Batch adsorption tests showed that SSB-900 delivered the highest removal efficiencies up to 70 % for biochemical oxygen demand, 57.3 % for chemical oxygen demand, and 20.9 % for phosphate, demonstrating its ability for leachate

polishing and underscoring the utility of high-temperature microwave biochar in wastewater remediation.

5.2 Limitations and the challenges

Although the single-mode MP can convert SSW into SSB capable of polishing LW, the technology still encounters notable obstacles across interrelated dimensions technical robustness, economic viability, and long-term sustainability. Technically, MP performance is highly sensitive to microwave frequency, power density, cavity geometry, feedstock moisture, and particle-size distribution; variations in any of these variables can alter heating uniformity, devolatilization kinetics, and ultimately the physicochemical properties of the resulting biochar. Achieving reproducible yields and consistent pore-structure development therefore demands tighter process control and standardised operating protocols that have yet to be fully established for heterogeneous seafood residues. In addition, scale-up from laboratory volumes to continuous, pilot-scale reactors must resolve challenges in wave penetration depth, standing-wave formation, and material handling to avoid cold spots and channel clogging.

From an economic standpoint, capital expenditure for industrial-grade magnetrons, single-mode cavities, and high-temperature off-gas treatment can exceed that of conventional resistive or rotary-kiln systems. Ongoing maintenance needed especially replacement of magnetron assemblies and shielding have adds to operating costs and may offset the energy savings derived from volumetric heating. Meanwhile, the market for SSB is still nascent; demand hinges on demonstrated adsorptive performance, regulatory acceptance, and cost competitiveness against incumbent activated carbon. Establishing reliable supply chains, quality standards, and regeneration services will be crucial for creating a durable revenue stream.

Sustainability concerns centre on the service life, regeneration potential, and ultimate fate of spent SSB. Repeated adsorption–desorption cycles can degrade surface functionality and reduce efficacy, dictating the frequency of media replacement and, by extension, the overall process footprint. Moreover, if regeneration relies on fossil-derived energy or yields secondary waste that is difficult to manage, the environmental advantages of MP may erode. Comprehensive life-cycle assessments incorporating

greenhouse-gas emissions, ecosystem impacts, and circular-economy metrics are therefore essential to verify net benefits.

MP provides a compelling route for valorising SSW and treating LW, yet its translation from laboratory proof-of-concept to industrial practice requires concerted efforts in process optimisation, reactor engineering, market development, and life-cycle analysis. Addressing these challenges through interdisciplinary research, pilot-scale demonstrations, and supportive policy instruments will be pivotal to realising the full environmental and economic potential of this technology.

5.3 Future development

The present study utilised shrimp-shell biochar to attenuate contaminants in landfill leachate, its comparatively modest specific surface area remains a central performance constraint. Future investigations should therefore examine ancillary process variables such as solution pH, sorbent dosage, and contact time to elucidate adsorption isotherms and kinetics under environmentally realistic conditions. Parallel work on reactor design and simulation are equally important including waveguide geometry, cavity coupling, and feedstock residence time in single-mode microwave pyrolyser may significantly influence char porosity, thereby affecting both product quality and energy consumption.

Surface modification offers an additional strategy for boosting adsorption capacity. Systematic comparisons of physical activation and chemical activation should be undertaken to generate hierarchical pore structures and heteroatom functionalities tailored to leachate constituents. Long-term service life and reusability also warrant detailed scrutiny. Continuous-flow or semi-batch pilot studies are needed to quantify breakthrough curves, fouling behaviour, and capacity decay across multiple adsorption–desorption cycles. Investigating mild thermal or chemical regeneration protocols could reveal cost-effective routes to restore adsorption efficacy and thus extend media longevity.

Finally, an integrated techno-economic assessment encompassing capital investment, operating expenditure, regeneration energy demand, and potential revenue from biochar sales are essential for determining commercial feasibility. By addressing these technical, operational, and economic knowledge gaps, forthcoming research can advance microwave-derived SSB toward scalable, sustainable applications in solid-waste valorisation and leachate remediation.

REFERENCES

Ab Ghani, Z., Yusoff, M. S., Zaman, N. Q., Zamri, M. F. M. A., and Andas, J. (2017). Optimization of preparation conditions for activated carbon from banana pseudo-stem using response surface methodology on removal of color and COD from landfill leachate. *Waste Management. 62*, 177-187.

Abadi, B. (2018). The determinants of cucumber farmers' pesticide use behavior in central Iran: Implications for the pesticide use management. *Journal of Cleaner Production. 205*, 1069-1081.

Abbas, A. A., Jingsong, G., Ping, L. Z., Ya, P. Y., and Al-Rekabi, W. S. (2009). Review on LandWll leachate treatments. *Journal of Applied Sciences Research. 5*(5), 534-545.

Abdel-Shafy, H. I. (2015). Chemical treatment for removal of heavy metals from industrial wastewater. *Egyptian Journal of Chemistry. 58*(1), 1-12.

Abdel-Shafy, H. I., and Abdel-Shafy, S. H. (2017). Membrane technology for water and wastewater management and application in Egypt. *Egyptian Journal of Chemistry. 60*(3), 347-360.

Abdel-Shafy, H. I., Ibrahim, A. M., Al-Sulaiman, A. M., and Okasha, R. A. (2024). Landfill leachate: Sources, nature, organic composition, and treatment: An environmental overview. *Ain Shams Engineering Journal. 15*(1), 102293.

Abdel-Shafy, H. I., and Mansour, M. S. (2014). Biogas production as affected by heavy metals in the anaerobic digestion of sludge. *Egyptian Journal of Petroleum. 23*(4), 409-417.

Abdel-Shafy, H. I., and Mansour, M. S. (2017). Treatment of pharmaceutical industrial wastewater via anaerobic/aerobic system for unrestricted reuse. *Journal of Scientific & Industrial Research. 76*, 119-127

Abdel-Shafy, H. I., and Mansour, M. S. (2020). Rehabilitation and upgrading wastewater treatment plant for safe irrigation reuse in remote area. *Water Practice & Technology. 15*(4), 1213-1227.

Adhikari, B., Dahal, K. R., and Khanal, S. N. (2014). A review of factors affecting the composition of municipal solid waste landfill leachate. *International Journal of Engineering Science and Innovative Technology. 3*(5), 273-281.

Adlan, M. N., Palaniandy, P., and Aziz, H. A. (2011). Optimization of coagulation and dissolved air flotation (DAF) treatment of semi-aerobic landfill leachate using response surface methodology (RSM). *Desalination. 277*(1-3), 74-82.

Aftab, B., and Hur, J. (2019). Unraveling complex removal behavior of landfill leachate upon the treatments of Fenton oxidation and MIEX® via two-dimensional correlation size exclusion chromatography (2D-CoSEC). *Journal of Hazardous Materials. 362*, 36-44.

Aftab, B., Shin, H.-S., and Hur, J. (2018). Exploring the fate and oxidation behaviors of different organic constituents in landfill leachate upon Fenton oxidation processes using EEM-PARAFAC and 2D-COS-FTIR. *Journal of Hazardous Materials. 354*, 33-41.

Ahmadi, M., Foladivanda, M., Jaafarzadeh, N., Ramezani, Z., Ramavandi, B., Jorfi, S., and Kakavandi, B. (2017). Synthesis of chitosan zero-valent iron nanoparticles-supported for cadmium removal: characterization, optimization and modeling approach. *Journal of Water Supply: Research and Technology—Aqua. 66*(2), 116-130.

Akhtar, J., Sheikh, N., and Munir, S. (2017). Linear regression-based correlations for estimation of high heating values of Pakistani lignite coals. *Energy Sources, Part A: Recovery, Utilization, and Environmental Effects. 39*(10), 1063-1070.

Amaral, M. C., Moravia, W. G., Lange, L. C., Zico, M. R., Magalhães, N. C., Ricci, B. C., and Reis, B. G. (2016). Pilot aerobic membrane bioreactor and nanofiltration for municipal landfill leachate treatment. *Journal of Environmental Science and Health. 51*(8), 640-649.

Anqi, T., Zhang, Z., Suhua, H., and Xia, L. (2020). *Review on landfill leachate treatment methods.* Paper presented at the IOP Conference Series: Earth and Environmental Science.

Aravind, S., Kumar, P. S., Kumar, N. S., and Siddarth, N. (2020). Conversion of green algal biomass into bioenergy by pyrolysis. A review. *Environmental Chemistry Letters. 18*, 829-849.

Aryal, B., Gurung, R., Camargo, A. F., Fongaro, G., Treichel, H., Mainali, B., . . . Puadel, S. R. (2022). Nitrous oxide emission in altered nitrogen cycle and implications for climate change. *Environmental Pollution. 314*, 120272.

Asaithambi, P., Govindarajan, R., Yesuf, M. B., and Alemayehu, E. (2020). Removal of color, COD and determination of power consumption from landfill leachate wastewater using an electrochemical advanced oxidation processes. *Separation and Purification Technology. 233*, 115935.

Assou, M., El Fels, L., El Asli, A., Fakidi, H., Souabi, S., and Hafidi, M. (2016). Landfill leachate treatment by a coagulation–flocculation process: effect of the introduction order of the reagents. *Desalination and Water Treatment. 57*(46), 21817-21826.

Aziz, S. Q., Aziz, H. A., Yusoff, M. S., and Bashir, M. J. (2011). Landfill leachate treatment using powdered activated carbon augmented sequencing batch reactor (SBR) process: Optimization by response surface methodology. *Journal of Hazardous Materials. 189*(1-2), 404-413.

Bajpai, P. (2017). Basics of anaerobic digestion process. In *Anaerobic Technology in Pulp and Paper Industry* (pp. 7-12).

Bashir, M. J., Aziz, H. A., Amr, S. S. A., Sethupathi, S. a. p., Ng, C. A., and Lim, J. W. (2015). The competency of various applied strategies in treating tropical municipal landfill leachate. *Desalination and Water Treatment. 54*(9), 2382-2395.

Baun, D. L., and Christensen, T. H. (2004). Speciation of heavy metals in landfill leachate: a review. *Waste Management & Research. 22*(1), 3-23.

Bhalla, B., Saini, M., and Jha, M. (2013). Effect of age and seasonal variations on leachate characteristics of municipal solid waste landfill. *International Journal of Research in Engineering and Technology. 2*(8), 223-232.

Bilardi, S., Calabrò, P. S., Greco, R., and Moraci, N. (2018). Selective removal of heavy metals from landfill leachate by reactive granular filters. *Science of The Total Environment. 644*, 335-341.

Borba, F. H., Leichtweis, J., Bueno, F., Pellenz, L., Inticher, J. J., and Seibert, D. (2019). Pollutant removal and acute toxicity assessment (Artemia salina) of landfill leachate treated by photo-Fenton process mediated by oxalic acid. *Journal of Water Process Engineering. 28*, 159-168.

Borges, F. C., Du, Z., Xie, Q., Trierweiler, J. O., Cheng, Y., Wan, Y., . . . Chen, P. (2014). Fast microwave assisted pyrolysis of biomass using microwave absorbent. *Bioresource Technology. 156*, 267-274.

Bundhoo, Z. M. (2018). Microwave-assisted conversion of biomass and waste materials to biofuels. *Renewable and Sustainable Energy Reviews. 82*, 1149-1177.

Carvajal-Flórez, E., and Cardona-Gallo, S.-A. (2019). Technologies applicable to the removal of heavy metals from landfill leachate. *Environmental Science and Pollution Research. 26*, 15725-15753.

Chakravorty, U., and Gong, Y. (2015). The Economics of Fossil Fuels and Pollution. *Sustainable Economic Development*, 67-75.

Chao, H., Lin, H., Dai, L., Qiu, R., Tang, Y., Wang, Y., . . . Ok, Y. S. (2020). Waste shrimp shell-derived hydrochar as an emergent material for methyl orange removal in aqueous solutions. *Environment International. 134*, 105340.

Chávez, R. P., Pizarro, E. C. C., and Galiano, Y. L. (2019). Tratamento de lixiviado de aterro sanitário com carvão ativado obtido de resíduos de café. *Engenharia Sanitaria e Ambiental. 24*, 833-842.

Cheba, B. A., Zaghloul, T. I., and EL-Mahdy, A. R. (2018). Demineralized crab and shrimp shell powder: Cost effective medium for bacillus Sp. R2 growth and chitinase production. *Procedia Manufacturing. 22*, 413-419.

Chen, W., Liu, X. Y., Huang, B. C., Wang, L. F., Yu, H. Q., and Mizaikoff, B. (2016). Probing membrane fouling via infrared attenuated total reflection mapping coupled with multivariate curve resolution. *ChemPhysChem. 17*(3), 358-363.

Chen, W., Zhuo, X., He, C., Shi, Q., and Li, Q. (2020). Molecular investigation into the transformation of dissolved organic matter in mature landfill leachate during treatment in a combined membrane bioreactor-reverse osmosis process. *Journal of Hazardous Materials. 397*, 122759.

Chen, Z., Niu, B., Zhang, L., and Xu, Z. (2018). Vacuum pyrolysis characteristics and parameter optimization of recycling organic materials from waste tantalum capacitors. *Journal of Hazardous Materials. 342*, 192-200.

Cheng, Y. W., Khan, M. R., Ng, K. H., Wongsakulphasatch, S., and Cheng, C. K. (2019). Harnessing renewable hydrogen-rich syngas from valorization of palm oil mill effluent (POME) using steam reforming technique. *Renewable Energy. 138*, 1114-1126.

Cho, D. W., Yoon, K., Ahn, Y., Sun, Y., Tsang, D. C. W., Hou, D., . . . Song, H. (2019). Fabrication and environmental applications of multifunctional mixed metal-biochar composites (MMBC) from red mud and lignin wastes. *J Hazard Mater. 374*, 412-419.

Cho, Y. I., No, H. K., and Meyers, S. P. (1998). Physicochemical characteristics and functional properties of various commercial chitin and chitosan products. *Journal of Agricultural and Food Chemistry. 46*(9), 3839-3843.

Chugh, S., Clarke, W., Pullammanappallil, P., and Rudolph, V. (1998). Effect of recirculated leachate volume on MSW degradation. *Waste Management & Research. 16*(6), 564-573.

Collard, F.-X., and Blin, J. (2014). A review on pyrolysis of biomass constituents: Mechanisms and composition of the products obtained from the conversion of cellulose, hemicelluloses and lignin. *Renewable and Sustainable Energy Reviews. 38*, 594-608.

Contrera, R. C., da Cruz Silva, K. C., Morita, D. M., Rodrigues, J. A. D., Zaiat, M., and Schalch, V. (2014). First-order kinetics of landfill leachate treatment in a pilot-scale anaerobic sequence batch biofilm reactor. *Journal of Environmental Management. 145*, 385-393.

Da Silva, A., Galvão, R., and Júnior, V. A. (2014). *Post-treatment of landfill leachate from Cianorte-PR by upward filtration in gravel followed by adsorption on granular activated carbon.* Paper presented at the Environmental Technology.

Dabaghian, Z., Peyravi, M., Jahanshahi, M., and Rad, A. S. (2018). Potential of advanced nano‐structured membranes for landfill leachate treatment: a review. *ChemBioEng Reviews. 5*(2), 119-138.

de Almeida, R., de Souza Couto, J. M., Gouvea, R. M., de Almeida Oroski, F., Bila, D. M., Quintaes, B. R., and Campos, J. C. (2020). Nanofiltration applied to the landfill leachate treatment and preliminary cost estimation. *Waste Management & Research. 38*(10), 1119-1128.

de Brito, R. A., Filho, H. l. J. I. r., Aguiar, L. G., de Alcântara, M. A. l. K., Siqueira, A. F., and Da Rós, P. C. M. (2019). Degradation kinetics of landfill leachate by continuous-flow catalytic ozonation. *Industrial & Engineering Chemistry Research. 58*(23), 9855-9863.

De, S., Hazra, T., and Dutta, A. (2019). Sustainable treatment of municipal landfill leachate by combined association of air stripping, Fenton oxidation, and enhanced coagulation. *Environmental Monitoring and Assessment. 191*(2), 49.

del Carmen Borja-Urzola, A., García-Gómez, R. S., Flores, R., and del Carmen Durán-Domínguez-de, M. (2020). Chitosan from shrimp residues with a saturated solution of calcium chloride in methanol and water. *Carbohydrate Research. 497*, 108116.

Dominguez, A., Menéndez, J., Fernandez, Y., Pis, J., Nabais, J. V., Carrott, P., and Carrott, M. R. (2007). Conventional and microwave induced pyrolysis of coffee hulls for the production of a hydrogen rich fuel gas. *Journal of Analytical and Applied Pyrolysis. 79*(1-2), 128-135.

Duan, B., Chang, C., Ding, B., Cai, J., Xu, M., Feng, S., . . . Zhang, L. (2013). High strength films with gas-barrier fabricated from chitin solution dissolved at low temperature. *Journal of Materials Chemistry A. 1*(5), 1867-1874.

Evers, D., and Carroll, D. (1998). Ensiling salt-preserved shrimp waste with grass straw and molasses. *Animal Feed Science and Technology. 71*(3-4), 241-249.

FAO. (2024). *International markets for fisheries and aquaculture products*. Retrieved from Rome, Italy: https://openknowledge.fao.org/server/api/core/bitstreams/7ccfb061-a98a-473a-9484-5cf475bdc8aa/content

Feng, D., Chyang, C., Wen, J., and Tso, J. (2013). Incineration of kitchen waste with high nitrogen in vortexing fluidized-bed incinerator and its NO emission characteristics. *Journal of Environmental Sciences. 25*(9), 1841-1846.

Foong, S. Y., Liew, R. K., Yang, Y., Cheng, Y. W., Yek, P. N. Y., Mahari, W. A. W., . . . Van Le, Q. (2020). Valorization of biomass waste to engineered activated biochar by microwave pyrolysis: Progress, challenges, and future directions. *Chemical Engineering Journal. 389*, 124401.

Gao, L., Li, Z., Yi, W., Li, Y., Zhang, P., Zhang, A., and Wang, L. (2021). Impacts of pyrolysis temperature on lead adsorption by cotton stalk-derived biochar and related mechanisms. *Journal of Environmental Chemical Engineering. 9*(4), 105602.

Ghafari, S., Aziz, H. A., Isa, M. H., and Zinatizadeh, A. A. (2009). Application of response surface methodology (RSM) to optimize coagulation–flocculation treatment of leachate using poly-aluminum chloride (PAC) and alum. *Journal of Hazardous Materials. 163*(2-3), 650-656.

Ghosh, P., Thakur, I. S., and Kaushik, A. (2017). Bioassays for toxicological risk assessment of landfill leachate: A review. *Ecotoxicology and Environmental Safety. 141*, 259-270.

Giwa, A., Yusuf, A., Ajumobi, O., and Dzidzienyo, P. (2019). Pyrolysis of date palm waste to biochar using concentrated solar thermal energy: Economic and sustainability implications. *Waste Management. 93*, 14-22.

Gotvajn, A., and Pavko, A. (2015). Perspectives on biological treatment of sanitary landfill leachate. *Wastewater Treatment Engineering. 13*, 31-39.

Gotvajn, A. Ž., Tišler, T., and Zagorc-Končan, J. (2009). Comparison of different treatment strategies for industrial landfill leachate. *Journal of Hazardous Materials. 162*(2-3), 1446-1456.

Gu, X., Ma, X., Li, L., Liu, C., Cheng, K., and Li, Z. (2013). Pyrolysis of poplar wood sawdust by TG-FTIR and Py–GC/MS. *Journal of Analytical and Applied Pyrolysis. 102*, 16-23.

Halder, S. K., Maity, C., Jana, A., Pati, B. R., and Mondal, K. C. (2012). Chitinolytic enzymes from the newly isolated Aeromonas hydrophila SBK1: study of the mosquitocidal activity. *BioControl. 57*, 441-449.

Han, L., Wang, Q., Ma, Q., Yu, C., Luo, Z., and Cen, K. (2010). Influence of CaO additives on wheat-straw pyrolysis as determined by TG-FTIR analysis. *Journal of Analytical and Applied Pyrolysis. 88*(2), 199-206.

He, P., Chen, L., Shao, L., Zhang, H., and Lü, F. (2019). Municipal solid waste (MSW) landfill: A source of microplastics?-Evidence of microplastics in landfill leachate. *Water Research. 159*, 38-45.

He, S., Cao, C., Wang, J., Yang, J., Cheng, Z., Yan, B., . . . Chen, G. (2020). Pyrolysis study on cattle manure: From conventional analytical method to online study of pyrolysis photoionization time-of-flight mass spectrometry. *Journal of Analytical Applied Pyrolysis. 151*, 104916.

Hidayat, S., Bakar, M. S. A., Yang, Y., Phusunti, N., and Bridgwater, A. (2018). Characterisation and Py-GC/MS analysis of Imperata Cylindrica as potential biomass for bio-oil production in Brunei Darussalam. *Journal of Analytical and Applied Pyrolysis. 134*, 510-519.

Hisham, F., Akmal, M. M., Ahmad, F., and Ahmad, K. (2021). Facile extraction of chitin and chitosan from shrimp shell. *Materials Today: Proceedings. 42*, 2369-2373.

Huang, S., Ding, Y., Li, Y., Han, X., Xing, B., and Wang, S. (2021). Nitrogen and sulfur co-doped hierarchical porous biochar derived from the pyrolysis of mantis shrimp shell for supercapacitor electrodes. *Energy & Fuels. 35*(2), 1557-1566.

Intani, K., Latif, S., Kabir, A. R., and Müller, J. (2016). Effect of self-purging pyrolysis on yield of biochar from maize cobs, husks and leaves. *Bioresource Technology. 218*, 541-551.

Ishimura, T., Iwai, I., Matsui, K., Mattonai, M., Watanabe, A., Robberson, W., . . . Teramae, N. (2021). Qualitative and quantitative analysis of mixtures of microplastics in the presence of calcium carbonate by pyrolysis-GC/MS. *Journal of Analytical and Applied Pyrolysis. 157*, 105188.

Kai, X., Yang, T., Shen, S., and Li, R. (2019). TG-FTIR-MS study of synergistic effects during co-pyrolysis of corn stalk and high-density polyethylene (HDPE). *Energy Conversion Management. 181*, 202-213.

Kamaruddin, M. A., Yusoff, M. S., Rui, L. M., Isa, A. M., Zawawi, M. H., and Alrozi, R. (2017). An overview of municipal solid waste management and landfill leachate treatment: Malaysia and Asian perspectives. *Environmental Science and Pollution Research. 24*, 26988-27020.

Kandra, P., Challa, M. M., and Kalangi Padma Jyothi, H. (2012). Efficient use of shrimp waste: present and future trends. *Applied Microbiology and Biotechnology. 93*, 17-29.

Kang, S., Li, X., Fan, J., and Chang, J. (2011). Classified separation of lignin hydrothermal liquefied products. *Industrial engineering chemistry research. 50*(19), 11288-11296.

Kang, S., Li, X., Fan, J., and Chang, J. (2013). Hydrothermal conversion of lignin: A review. *Renewable Sustainable Energy Reviews. 27*, 546-558.

Kargi, F., and Pamukoglu, M. Y. (2004). Repeated fed-batch biological treatment of pre-treated landfill leachate by powdered activated carbon addition. *Enzyme and Microbial Technology. 34*(5), 422-428.

Kohse-Höinghaus, K. (2021). Combustion in the future: The importance of chemistry. *Proceedings of the Combustion Institute. 38*(1), 1-56.

Kong, S. H., Lam, S. S., Yek, P. N. Y., Liew, R. K., Ma, N. L., Osman, M. S., and Wong, C. C. (2019). Self‐purging microwave pyrolysis: an innovative approach to convert oil palm shell into carbon‐rich biochar for methylene blue adsorption. *Journal of Chemical Technology & Biotechnology. 94*(5), 1397-1405.

Kostas, E. T., Durán-Jiménez, G., Shepherd, B. J., Meredith, W., Stevens, L. A., Williams, O. S., . . . Robinson, J. P. (2020). Microwave pyrolysis of olive pomace for bio-oil and bio-char production. *Chemical Engineering Journal. 387*, 123404.

Kreag, R. A., and Smith, F. J. (1973). *Seafood solid waste in Oregon: disposal or recovery?* Retrieved from https://ir.library.oregonstate.edu/concern/administrative_report_or_publications/cr56n202g

Kumar, A., and Samadder, S. R. (2017). A review on technological options of waste to energy for effective management of municipal solid waste. *Waste Management. 69*, 407-422.

Kurniawan, T. A., Lo, W.-H., and Chan, G. Y. (2006). Degradation of recalcitrant compounds from stabilized landfill leachate using a combination of ozone-GAC adsorption treatment. *Journal of Hazardous Materials. 137*(1), 443-455.

Lam, Mahari, W. A. W., Sik, Y., Peng, W., Chong, C. T., Ma, N. L., . . . Kwon, E. E. (2019). Microwave vacuum pyrolysis of waste plastic and used cooking oil for simultaneous waste reduction and sustainable energy conversion: Recovery of cleaner liquid fuel and techno-economic analysis. *Renewable and Sustainable Energy Reviews. 115*, 109359.

Lam, S. S., and Chase, H. A. (2012). A review on waste to energy processes using microwave pyrolysis. *Energies. 5*(10), 4209-4232.

Lam, S. S., Liew, R. K., Cheng, C. K., and Chase, H. A. (2015). Catalytic microwave pyrolysis of waste engine oil using metallic pyrolysis char. *Applied Catalysis B: Environmental. 176*, 601-617.

Lam, S. S., Liew, R. K., Jusoh, A., Chong, C. T., Ani, F. N., and Chase, H. A. (2016). Progress in waste oil to sustainable energy, with emphasis on pyrolysis techniques. *Renewable and Sustainable Energy Reviews. 53*, 741-753.

Lam, S. S., Mahari, W. A. W., Ma, N. L., Azwar, E., Kwon, E. E., Peng, W., . . . Park, Y.-K. (2019). Microwave pyrolysis valorization of used baby diaper. *Chemosphere. 230*, 294-302.

Lam, S. S., Russell, A. D., Lee, C. L., and Chase, H. A. (2012). Microwave-heated pyrolysis of waste automotive engine oil: Influence of operation parameters on the yield, composition, and fuel properties of pyrolysis oil. *Fuel. 92*(1), 327-339.

Lam, S. S., Su, M. H., Nam, W. L., Thoo, D. S., Ng, C. M., Liew, R. K., . . . Nguyen Vo, D. V. (2018). Microwave pyrolysis with steam activation in producing activated carbon for removal of herbicides in agricultural surface water. *Industrial & Engineering Chemistry Research. 58*(2), 695-703.

Lam, S. S., Yek, P. N. Y., Ok, Y. S., Chong, C. C., Liew, R. K., Tsang, D. C., . . . Peng, W. (2020). Engineering pyrolysis biochar via single-step microwave steam activation for hazardous landfill leachate treatment. *Journal of Hazardous Materials. 390*, 121649.

Lee, J., Hong, J., Jang, D., and Park, K. Y. (2019). Hydrothermal carbonization of waste from leather processing and feasibility of produced hydrochar as an alternative solid fuel. *Journal of Environmental Management. 247*, 115-120.

Lelieveld, J., Klingmüller, K., Pozzer, A., Burnett, R., Haines, A., and Ramanathan, V. (2019). Effects of fossil fuel and total anthropogenic emission removal on public health and climate. *Proceedings of the National Academy of Sciences. 116*(15), 7192-7197.

Li, J., Tian, Y., Zong, P., Qiao, Y., and Qin, S. (2020). Thermal cracking behavior, products distribution and char/steam gasification kinetics of seawater Spirulina by TG-FTIR and Py-GC/MS. *Renewable Energy. 145*, 1761-1771.

Liew, R. K., Chai, C., Yek, P. N. Y., Phang, X. Y., Chong, M. Y., Nam, W. L., . . . Lam, S. S. (2019). Innovative production of highly porous carbon for industrial effluent remediation via microwave vacuum pyrolysis plus sodium-potassium hydroxide mixture activation. *Journal of Cleaner Production. 208*, 1436-1445.

Lin, K., Tian, L., Zhao, Y., Zhao, C., Zhang, M., and Zhou, T. (2022). Pyrolytic characteristics of fine materials from municipal solid waste using TG-FTIR, Py-GC/MS, and deep learning approach: Kinetics, thermodynamics, and gaseous products distribution. *Chemosphere. 293*, 133533.

Liu, G., Sheng, H., Fu, Y., Song, Y., Redmile-Gordon, M., Qiao, Y., . . . Wang, F. (2019). Extracellular polymeric substances (EPS) modulate adsorption isotherms between biochar and 2, 2′ , 4, 4′ -tetrabromodiphenyl ether. *Chemosphere. 214*, 176-183.

Lopez, A., Pagano, M., Volpe, A., and Di Pinto, A. C. (2004). Fenton's pre-treatment of mature landfill leachate. *Chemosphere. 54*(7), 1005-1010.

Lopez, G., Aguado, R., Olazar, M., Arabiourrutia, M., and Bilbao, J. (2009). Kinetics of scrap tyre pyrolysis under vacuum conditions. *Waste Management. 29*(10), 2649-2655.

Luo, H., Zeng, Y., Cheng, Y., He, D., and Pan, X. (2020). Recent advances in municipal landfill leachate: A review focusing on its characteristics, treatment, and toxicity assessment. *Science of The Total Environment. 703*, 135468.

Luo, Y., Li, R., Sun, X., Liu, X., and Li, D. (2019). The roles of phosphorus species formed in activated biochar from rice husk in the treatment of landfill leachate. *Bioresource Technology. 288*, 121533.

Ma, Y., Wang, J., Zhang, Y. J. B. C., and Biorefinery. (2018). Analysis of pyrolysis characteristics and kinetics of Euphausia superba shell waste using TG-FTIR and distributed activation energy model. *Biomass Conversion Biorefinery. 8*, 329-337.

Madav, V., Das, D., Kumar, M., Surwade, M., Parikh, P., and Sethi, V. (2019). Studies for removal of tar from producer gas in small scale biomass gasifiers using biodiesel. *Biomass and Bioenergy. 123*, 123-133.

Mahari, W. A. W., Azwar, E., Foong, S. Y., Ahmed, A., Peng, W., Tabatabaei, M., . . . Lam, S. S. (2021). Valorization of municipal wastes using co-pyrolysis for green energy production, energy security, and environmental sustainability: A review. *Chemical Engineering Journal. 421*, 129749.

Maia, S., Restrepo, J., Junior, A. C., and Franco, D. (2015). Evaluation of the biological treatment of landfill leachate on a real scale in the Southern Region of Brazil. *International Journal of Environmental Research and Public Health. 20*, 665-675.

Marinković, D. M., Stanković, M. V., Veličković, A. V., Avramović, J. M., Miladinović, M. R., Stamenković, O. O., . . . Jovanović, D. M. (2016). Calcium oxide as a promising heterogeneous catalyst for biodiesel production: Current state and perspectives. *Renewable and Sustainable Energy Reviews. 56*, 1387-1408.

Marttinen, S., Kettunen, R., Sormunen, K., Soimasuo, R., and Rintala, J. (2002). Screening of physical–chemical methods for removal of organic material, nitrogen and toxicity from low strength landfill leachates. *Chemosphere. 46*(6), 851-858.

Mathew, G. M., Mathew, D. C., Sukumaran, R. K., Sindhu, R., Huang, C.-C., Binod, P., . . . Pandey, A. (2020). Sustainable and eco-friendly strategies for shrimp shell valorization. *Environmental Pollution. 267*, 115656.

Menon, V. V. (2018). Nutrients and nutraceuticals from seafood. *Bioactive Molecules in Food*, 1-45.

Mitu, M., Islam, M. A., Rahman, M. S., Feroz, S., Mollick, A. S., and Kabir, M. E. (2019). Pyrolysis kinetic study on waste particle residue from particle board industry. *Journal of the Indian Academy of Wood Science. 16*, 58-66.

Mojiri, A., Aziz, H. A., Zaman, N. Q., Aziz, S. Q., and Zahed, M. A. (2016). Metals removal from municipal landfill leachate and wastewater using adsorbents combined with biological method. *Desalination and Water Treatment 57*(6), 2819-2833.

Mojiri, A., Zhou, J. L., Ratnaweera, H., Ohashi, A., Ozaki, N., Kindaichi, T., and Asakura, H. (2021). Treatment of landfill leachate with different techniques: an overview. *Water Reuse. 11*(1), 66-96.

Mong, G. R., Chong, C. T., Ng, J.-H., Chong, W. W. F., Lam, S. S., Ong, H. C., and Ani, F. N. (2020). Microwave pyrolysis for valorisation of horse manure biowaste. *Energy Conversion and Management. 220*, 113074.

Moreno, A. I., and Font, R. (2015). Pyrolysis of furniture wood waste: Decomposition and gases evolved. *Journal of Analytical and Applied Pyrolysis. 113*, 464-473.

Moreno, A. I., Font, R., and Conesa, J. A. (2017). Combustion of furniture wood waste and solid wood: Kinetic study and evolution of pollutants. *Fuel. 192*, 169-177.

Nanda, S., and Berruti, F. (2021). Municipal solid waste management and landfilling technologies: a review. *Environmental Chemistry Letters. 19*, 1433-1456.

Nirmal, N. P., Santivarangkna, C., Rajput, M. S., and Benjakul, S. (2020). Trends in shrimp processing waste utilization: An industrial prospective. *Trends in Food Science & Technology. 103*, 20-35.

Núñez-Gómez, D., de Almeida Alves, A. A., Lapolli, F. R., and Lobo-Recio, M. A. (2017). Aplication of the statistical experimental design to optimize mine-impacted water (MIW) remediation using shrimp-shell. *Chemosphere. 167*, 322-329.

Ofem, M. I., Umar, M., and Muhammed, M. (2015). Mechanical properties of calcium carbonate crystallization of chitin reinforced polymer. *International Journal of Scientific & Technology Research. 4*(9), 272-280.

Ogunmakinde, O. E., Sher, W., and Maund, K. (2019). An assessment of material waste disposal methods in the Nigerian construction industry. *Recycling. 4*(1), 13.

Onay, O., and Kockar, O. M. (2003). Slow, fast and flash pyrolysis of rapeseed. *Renewable Energy. 28*(15), 2417-2433.

Peng, X., Ma, X., Lin, Y., Guo, Z., Hu, S., Ning, X., . . . Zhang, Y. (2015). Co-pyrolysis between microalgae and textile dyeing sludge by TG–FTIR: kinetics and products. *Energy Conversion Management. 100*, 391-402.

Perea-Moreno, A.-J., Aguilera-Ureña, M.-J., and Manzano-Agugliaro, F. (2016). Fuel properties of avocado stone. *Fuel. 186*, 358-364.

Pereira, S. C., Maehara, L., Machado, C. M., and Farinas, C. S. (2016). Physical–chemical–morphological characterization of the whole sugarcane lignocellulosic biomass used for 2G ethanol production by spectroscopy and microscopy techniques. *Renewable Energy. 87*, 607-617.

Piatkiewicz, W., Biemacka, E., and Suchecka, T. (2001). A polish study: treating landfill leachate with membranes. *Filtration & Separation. 38*(6), 22-26.

Putra, P. H. M., Rozali, S., Patah, M. F. A., and Idris, A. (2022). A review of microwave pyrolysis as a sustainable plastic waste management technique. *Journal of Environmental Management. 303*, 114240.

Qin, X., Cheng, S., Xing, B., Qu, X., Shi, C., Meng, W., . . . Xia, H. (2023). Preparation of pyrolysis products by catalytic pyrolysis of poplar: Application of biochar in antibiotic wastewater treatment. *Chemosphere. 338*, 139519.

Qu, J., Lv, S., Peng, X., Tian, S., Wang, J., and Gao, F. (2016). Nitrogen-doped porous "green carbon" derived from shrimp shell: Combined effects of pore sizes and nitrogen doping on the performance of lithium sulfur battery. *Journal of Alloys and Compounds. 671*, 17-23.

Rajapaksha, A. U., Chen, S. S., Tsang, D. C., Zhang, M., Vithanage, M., Mandal, S., . . . Ok, Y. S. (2016). Engineered/designer biochar for contaminant

removal/immobilization from soil and water: potential and implication of biochar modification. *Chemosphere. 148*, 276-291.

Rambabu, K., Banat, F., Pham, Q. M., Ho, S.-H., Ren, N.-Q., and Show, P. L. (2020). Biological remediation of acid mine drainage: Review of past trends and current outlook. *Environmental Science Ecotechnology. 2*, 100024.

Rambabu, K., Bharath, G., Monash, P., Velu, S., Banat, F., Naushad, M., . . . Show, P. L. (2019). Effective treatment of dye polluted wastewater using nanoporous CaCl2 modified polyethersulfone membrane. *Process Safety Environmental Protection. 124*, 266-278.

Renou, S., Givaudan, J., Poulain, S., Dirassouyan, F., and Moulin, P. (2008). Landfill leachate treatment: Review and opportunity. *Journal of Hazardous Materials. 150*(3), 468-493.

Rodrıguez, J., Castrillon, L., Maranon, E., Sastre, H., and Fernandez, E. (2004). Removal of non-biodegradable organic matter from landfill leachates by adsorption. *Water Research. 38*(14-15), 3297-3303.

Saha, S., Islam, M. T., Calhoun, J., and Reza, T. (2023). Effect of hydrothermal carbonization on fuel and combustion properties of shrimp shell waste. *Energies. 16*(14), 5534.

Sait, H. H., Hussain, A., Salema, A. A., and Ani, F. N. (2012). Pyrolysis and combustion kinetics of date palm biomass using thermogravimetric analysis. *Bioresource Technology. 118*, 382-389.

Sebestyén, Z., Jakab, E., Domán, A., Bokrossy, P., Bertóti, I., Madarász, J., and László, K. (2020). Thermal degradation of crab shell biomass, a nitrogen-containing carbon precursor. *Journal of Thermal Analysis and Calorimetry. 142*, 301-308.

Sekar, M., Mathimani, T., Alagumalai, A., Chi, N. T. L., Duc, P. A., Bhatia, S. K., . . . Pugazhendhi, A. (2021). A review on the pyrolysis of algal biomass for biochar and bio-oil–Bottlenecks and scope. *Fuel. 283*, 119190.

Shadangi, K. P., and Mohanty, K. (2014). Kinetic study and thermal analysis of the pyrolysis of non-edible oilseed powders by thermogravimetric and differential scanning calorimetric analysis. *Renewable Energy. 63*, 337-344.

Shadi, Kamaruddin, M. A., Niza, N. M., Emmanuela, M. I., Shaah, M. A., Yusoff, M. S., and Allafi, F. A. (2020). Characterization of stabilized leachate and evaluation of LPI from sanitary landfill in Penang, Malaysia. *Desalination and Water Treatment. 189*, 152-164.

Shadi, A., Niza, N., and Ijanu, M. (2020). Characterization of stabilized leachate and evaluation of LPI from sanitary landfill in Penang, Malaysia. *Desalination Water Treat. 189*, 152-164.

Silva, A., Dezotti, M., and Sant'Anna Jr, G. (2004). Treatment and detoxification of a sanitary landfill leachate. *Chemosphere. 55*(2), 207-214.

Sippula, O., Huttunen, K., Hokkinen, J., Kärki, S., Suhonen, H., Kajolinna, T., . . . Uski, O. (2019). Emissions from a fast-pyrolysis bio-oil fired boiler: Comparison of health-related characteristics of emissions from bio-oil, fossil oil and wood. *Environmental Pollution. 248*, 888-897.

Sobek, S., and Werle, S. (2020). Kinetic modelling of waste wood devolatilization during pyrolysis based on thermogravimetric data and solar pyrolysis reactor performance. *Fuel. 261*, 116459.

Somani, M., Datta, M., Gupta, S., Sreekrishnan, T., and Ramana, G. (2019). Comprehensive assessment of the leachate quality and its pollution potential from six municipal waste dumpsites of India. *Bioresource Technology Reports. 6*, 198-206.

Su, M. H., Azwar, E., Yang, Y., Sonne, C., Yek, P. N. Y., Liew, R. K., . . . Lam, S. S. (2020). Simultaneous removal of toxic ammonia and lettuce cultivation in aquaponic system using microwave pyrolysis biochar. *Journal of Hazardous Materials. 396*, 122610.

Suresh, P. (2012). Biodegradation of shrimp processing bio-waste and concomitant production of chitinase enzyme and N-acetyl-D-glucosamine by marine

bacteria: production and process optimization. *World Journal of Microbiology and Biotechnology. 28*, 2945-2962.

Syzdek, A. C., and Ahlert, R. C. (1984). Separation of landfill leachate with polymeric ultrafiltration membranes. *Journal of Hazardous Materials. 9*(2), 209-220.

Tałałaj, I. A., Biedka, P., and Bartkowska, I. (2019). Treatment of landfill leachates with biological pretreatments and reverse osmosis. *Environmental Chemistry Letters. 17*, 1177-1193.

Tan, S., Zhou, G., Yang, Q., Ge, S., Liu, J., Cheng, Y. W., . . . Chang, J.-S. (2023). Utilization of current pyrolysis technology to convert biomass and manure waste into biochar for soil remediation: A review. *Science of The Total Environment. 864*, 160990.

Tang, S.-R., Zong, Z.-M., Zhou, L., Zhao, W., Li, X.-B., Peng, Y.-L., . . . Wei, X.-Y. (2010). Molecular composition of soluble fraction from depolymerized cornstalk powder in supercritical methanol and ethanol. *Renewable Energy. 35*(5), 946-951.

Tarves, P. C., Serapiglia, M. J., Mullen, C. A., Boateng, A. A., and Volk, T. A. (2017). Effects of hot water extraction pretreatment on pyrolysis of shrub willow. *Biomass and Bioenergy. 107*, 299-304.

Tejera, J., Miranda, R., Hermosilla, D., Urra, I., Negro, C., and Blanco, Á. (2019). Treatment of a mature landfill leachate: comparison between homogeneous and heterogeneous photo-Fenton with different pretreatments. *Water. 11*(9), 1849.

Telmo, C., Lousada, J., and Moreira, N. (2010). Proximate analysis, backwards stepwise regression between gross calorific value, ultimate and chemical analysis of wood. *Bioresource Technology. 101*(11), 3808-3815.

Teng, C., Zhou, K., Peng, C., and Chen, W. (2021). Characterization and treatment of landfill leachate: A review. *Water Research. 203*, 117525.

Trebouet, D., Schlumpf, J., Jaouen, P., and Quemeneur, F. (2001). Stabilized landfill leachate treatment by combined physicochemical–nanofiltration processes. *Water Research. 35*(12), 2935-2942.

Tsioptsias, C., Michailof, C., Stauropoulos, G., and Panayiotou, C. (2009). Chitin and carbon aerogels from chitin alcogels. *Carbohydrate Polymers. 76*(4), 535-540.

Tugtas, A. E., Cavdar, P., and Calli, B. (2013). Bio-electrochemical post-treatment of anaerobically treated landfill leachate. *Bioresource Technology. 128*, 266-272.

Vakilabadi, D. R., Hassani, A. H., Omrani, G., and Ramavandi, B. (2017). Catalytic potential of Cu/Mg/Al-chitosan for ozonation of real landfill leachate. *Process Safety and Environmental Protection. 107*, 227-237.

Vithanage, M., Wijesekara, S., Siriwardana, A., Mayakaduwa, S. S., and Ok, Y. S. (2014). Management of municipal solid waste landfill leachate: a global environmental issue. *Environmental Deterioration and Human Health*, 263-288.

Wang, F., Smith, D. W., and El-Din, M. G. (2003). Application of advanced oxidation methods for landfill leachate treatment–A review. *Journal of Environmental Engineering and Science. 2*(6), 413-427.

Wang, K., Wu, D., Peng, Y., and Wang, S. (2018). Critical review of landfill leachate treatment technologies. *Journal of Beijing University of Technology. 23*, 59.

Wang, P., and Shen, Y. (2022). Catalytic pyrolysis of cellulose and chitin with calcined dolomite–Pyrolysis kinetics and products analysis. *Fuel. 312*, 122875.

Wang, S., Bian, S., Liu, J., Li, J., Xu, S., and Liang, Z. (2021). Highly adsorptive pristine and magnetic biochars prepared from crayfish shell for removal of Cu (II) and Pb (II). *Journal of the Taiwan Institute of Chemical Engineers. 127*, 175-185.

Wang, T., Li, Y., Zhi, D., Lin, Y., He, K., Liu, B., and Mao, H. (2019). Assessment of combustion and emission behavior of corn straw biochar briquette fuels under different temperatures. *Journal of Environmental Management. 250*, 109399.

Wang, Y., Yang, Y., Wang, R., Zhu, Y., Yang, P., Lin, Z., . . . Cong, W. (2022). Effectively inhibiting the degradation of chitin during extraction from crustacean waste via a novel deep eutectic solvent aqueous solution. *Process Biochemistry. 121*, 142-151.

Wei, F., Cao, J.-P., Zhao, X.-Y., Ren, J., Wang, J.-X., Fan, X., and Wei, X.-Y. (2017). Nitrogen evolution during fast pyrolysis of sewage sludge under inert and reductive atmospheres. *Energy & Fuels. 31*(7), 7191-7196.

Weldekidan, H., Strezov, V., Li, R., Kan, T., Town, G., Kumar, R., . . . Flamant, G. (2020). Distribution of solar pyrolysis products and product gas composition produced from agricultural residues and animal wastes at different operating parameters. *Renewable Energy. 151*, 1102-1109.

Wiszniowski, J., Robert, D., Surmacz-Gorska, J., Miksch, K., and Weber, J. (2006). Landfill leachate treatment methods: A review. *Environmental Chemistry Letters. 4*, 51-61.

Xiao, R., and Yang, W. (2013). Influence of temperature on organic structure of biomass pyrolysis products. *Renewable Energy. 50*, 136-141.

Xu, Y., Bajaj, M., Schneider, R., Grage, S. L., Ulrich, A. S., Winter, J., and Gallert, C. (2013). Transformation of the matrix structure of shrimp shells during bacterial deproteination and demineralization. *Microbial Cell Factories. 12*, 1-12.

Yang, F., Wang, J., Liu, L., Zhang, P., Yu, W., Deng, Q., . . . Deng, S. (2018). Synthesis of porous carbons with high N-content from shrimp shells for efficient CO_2-capture and gas separation. *ACS Sustainable Chemistry & Engineering. 6*(11), 15550-15559.

Yin, C. (2012). Microwave-assisted pyrolysis of biomass for liquid biofuels production. *Bioresource Technology. 120*, 273-284.

Yong, Z. J., Bashir, M. J., Ng, C. A., Sethupathi, S., and Lim, J.-W. (2018). A sequential treatment of intermediate tropical landfill leachate using a sequencing batch reactor (SBR) and coagulation. *Journal of Environmental Management. 205*, 244-252.

You, S., Ok, Y. S., Chen, S. S., Tsang, D. C., Kwon, E. E., Lee, J., and Wang, C.-H. (2017). A critical review on sustainable biochar system through gasification: Energy and environmental applications. *Bioresource Technology. 246*, 242-253.

Yu, Y., Long, Y., and Wu, H. (2016). Near-complete recovery of sugar monomers from cellulose and lignocellulosic biomass via a two-step process combining mechanochemical hydrolysis and dilute acid hydrolysis. *Energy & Fuels. 30*(3), 1571-1578.

Yu, Z., Dai, M., Huang, M., Fang, S., Xu, J., Lin, Y., and Ma, X. (2018a). Catalytic characteristics of the fast pyrolysis of microalgae over oil shale: analytical Py-GC/MS study. *Renewable Energy. 125*, 465-471.

Yu, Z., Dai, M., Huang, M., Fang, S., Xu, J., Lin, Y., and Ma, X. (2018b). Catalytic characteristics of the fast pyrolysis of microalgae over oil shale: Analytical Py-GC/MS study. *Renew. Energy. 125*, 465-471.

Yunpu, W., Leilei, D., Liangliang, F., Shaoqi, S., Yuhuan, L., and Roger, R. (2016). Review of microwave-assisted lignin conversion for renewable fuels and chemicals. *Journal of Analytical and Applied Pyrolysis. 119*, 104-113.

Zamri, M. F. M. A., Kamaruddin, M. A., Yusoff, M. S., Aziz, H. A., and Foo, K. Y. (2017). Semi-aerobic stabilized landfill leachate treatment by ion exchange resin: isotherm and kinetic study. *Applied Water Science. 7*, 581-590.

Zhan, H., Zhuang, X., Song, Y., Liu, J., Li, S., Chang, G., . . . Wang, X. (2019). A review on evolution of nitrogen-containing species during selective pyrolysis of waste wood-based panels. *Fuel. 253*, 1214-1228.

Zhang, H., Hu, J., Zheng, J., and Xiao, R. (2017). Fast pyrolysis of cellulosic ethanol solid residues with high ash and lignin contents in a fluidized bed. *Journal of Analytical and Applied Pyrolysis. 128*, 217-223.

Zhang, J., Jin, J., Wang, M., Naidu, R., Liu, Y., Man, Y. B., . . . Zhang, Y. (2020). Co-pyrolysis of sewage sludge and rice husk/bamboo sawdust for biochar with high aromaticity and low metal mobility. *Environmental Research. 191*, 110034.

Zhang, J., Wu, C., Hou, W., Zhao, Q., Liang, X., Lin, S., . . . Xie, Y. (2021). Biological calcium carbonate with a unique organic–inorganic composite structure to enhance biochar stability. *Environmental Science: Processes & Impacts. 23*(11), 1747-1758.

Zhang, P., Hu, H., Tang, H., Yang, Y., Liu, H., Lu, Q., . . . Yao, H. (2019). In-depth experimental study of pyrolysis characteristics of raw and cooking treated shrimp shell samples. *Renewable Energy. 139*, 730-738.

Zhang, Y., Fan, S., Liu, T., Omar, M. M., and Li, B. (2022). Perspectives into intensification for aviation oil production from microwave pyrolysis of organic wastes. *Chemical Engineering and Processing - Process Intensification. 176*, 108939.

Zhang, Y., Lei, H., Yang, Z., Qian, K., and Villota, E. (2018). Renewable high-purity mono-phenol production from catalytic microwave-induced pyrolysis of cellulose over biomass-derived activated carbon catalyst. *ACS Sustainable Chemistry & Engineering. 6*(4), 5349-5357.

Zhao, X., Zhang, J., Song, Z., Liu, H., Li, L., and Ma, C. (2011). Microwave pyrolysis of straw bale and energy balance analysis. *Journal of Analytical and Applied Pyrolysis. 92*(1), 43-49.

Zouboulis, A. I., Chai, X.-L., and Katsoyiannis, I. A. (2004). The application of bioflocculant for the removal of humic acids from stabilized landfill leachates. *Journal of Environmental Management. 70*(1), 35-41.

Zouboulis, A. I., Jun, W., and Katsoyiannis, I. A. (2003). Removal of humic acids by flotation. *Colloids and Surfaces A: Physicochemical and Engineering Aspects. 231*(1-3), 181-193.

APPENDICES

Appendix A Py-GC/MS analysis of Shrimp shell waste (SSW)

Table S1. The carbon number of each component in the shrimp shell Py-GC/MS at the final pyrolysis temperature of 500°C and the heating rate of 30°C/min (by peak area percentage, %).

Compound name	**Carbon number**	**500°C 30 °C/min**
C_0-C_5		
2-Aminoethylphosphonic acid	$C_2H_8NO_3P$	0.04
Sarcosine	$C_3H_7NO_2$	8.92
3 (R)-(-)-2-Amino-1-propanol	C_3H_9NO	0.01
(R)-(-)-2-Amino-1-propanol	C_3H_9NO	0.01
Pyrollidine,2,5-bis(imino)-	$C_4H_7N_3$	2
Butanamide	C_4H_9NO	1
Ethanamine,2-chloro-N,N-dimethyl-	$C_4H_{10}ClN$	0.59
1H-Pyrrole,2,5-dihydro-1-nitroso-	$C_4H_6N_2O$	0.19
Butanenitrile,4-oxo-	C_4H_5NO	0.05
Propanal,2-methyl-,oxime	C_4H_9NO	0.05
2-Butanamine,(S)-	$C_4H_{11}N$	0.01
4-Amino-1-butanol	$C_4H_{11}NO$	0
Pentanoic acid	$C_5H_{10}O_2$	0.02
Pentane	C_5H_{12}	0.09
Butanenitrile,3-methyl-	C_5H_9N	0.26
Thymine	$C_5H_6N_2O_2$	0.64
Propenaldimethylhydrazone	$C_5H_{10}N_2$	0.26
4-Cyclopentene-1,3-diol, trans-	$C_5H_8O_2$	0.17

Butanal,2-methyl-	$C_5H_{10}O$	0.28
Total		**14.59**
C_6-C_{10}		
Imidazole,2-amino-5-[(2-carboxy)vinyl]-	$C_6H_7N_3O_2$	1.29
Cystine	$C_6H_{12}N_2O_4S_2$	0.07
Dimethylaminomethyl-isopropyl-sulfide	$C_6H_{15}NS$	1.92
1H-Pyrrolo[1,2-c]imidazole-1,3(2H)-dione,tetrahydro-	$C_6H_8N_2O_2$	0.51
Phenol	C_6H_6O	4.07
Propyleneglycol propylether	$C_6H_{14}O_2$	0.63
2,4-Hexadien-1-ol	$C_6H_{10}O$	0.1
Toluene	C_7H_8	4.16
1H-Pyrazole,4-ethyl-3,5-dimethyl-	$C_7H_{12}N_2$	1.99
threo-4-Hydroxy-l-homoarginine lactone	$C_7H_{14}N_4O_2$	0.1
3,7-Diacetamido-7H-s-triazolo[5,1-c]-s-triazole	$C_7H_9N_7O_2$	0.02
Pyrrolo[1,2-a]pyrazine-1,4-dione, hexahydro-	$C_7H_{10}N_2O_2$	2.81
Phenol,4-methyl-	C_7H_8O	0.91
Phenol,3-methyl-	C_7H_8O	0.43
Heptanal	$C_7H_{14}O$	0.09
Bicyclo[2.2.1]hept-2-en-7-ol	$C_7H_{10}O$	0.26
1-Methyl-4-[nitromethyl]-4-piperidinol	$C_7H_{14}N_2O_3$	0.1
4-Fluorophenylacetic acid	$C_8H_7FO_2$	1.78
3-Oxocyclohexanecarboxylicacid, methylester	$C_8H_{12}O_3$	2.26
Styrene	C_8H_8	0.93
Indole	C_8H_7N	3.17
Benzene,1-isocyano-2-methyl-	C_8H_7N	0.39
1,4-diazabicyclo[4.3.0]nonan-2,5-dione,3-methyl	$C_8H_{12}N_2O_2$	0.93
3-Azonia-5-hexene-1-ol,N,N-dimethyl-,carbamateester, bromide	$C_8H_{17}N_2O_2$	0.15

Butanoic acid,4-(2-oxocyclopentyl)-	$C_9H_{14}O_3$	1.39
Pyrrolizin-1,7-dione-6-carboxylic acid,methyl(ester)	$C_9H_{11}NO_4$	1.64
Benzenepropanoic acid,?(hydroxyimino)-	$C_9H_9NO_3$	0.09
1-(5-Bicyclo[2.2.1]heptyl)ethylamine	$C_9H_{17}N$	0.02
Benzenepropanenitrile	C_9H_9N	1.96
8-Methylenecyclooctene-3,4-diol	$C_9H_{14}O_2$	0.43
Bicyclo[3.3.1]non-6-en-3-ol	$C_9H_{14}O$	0.04
3-Amino-2-(4-chlorophenyl)-2-hydroxypropanesulfonic acid	$C_9H_{12}ClNO_4S$	0.06
Pyrrolizidine-3-one,5-acetylmethyl-	$C_{10}H_{15}NO_2$	0.89
1-Decene	$C_{10}H_{20}$	0.17
2-(1,4-Diazepan-1-yl)-N-isopropylacetamide	$C_{10}H_{21}N_3O$	1.17
2,6,6-Trimethyl-bicyclo[3.1.1]hept-3-ylamine	$C_{10}H_{19}N$	0.13
2,6-Diethylaniline	$C_{10}H_{15}N$	0.01
1-(1,2,3-Trimethyl-cyclopent-2-enyl)-ethanone	$C_{10}H_{16}O$	0.43
Clasto-lactacystin ?lactone	$C_{10}H_{15}NO_4$	0.15
2-Methyl-4,5-tetramethylene-5-ethyl-2-oxazoline	$C_{10}H_{17}NO$	0.64
Tricyclo[4.4.0.0(2,8)]dec-3-en-5-ol	$C_{10}H_{14}O$	0.18
Total		**38.47**
C_{11}-C_{15}		
N,N'-Pentamethylenebis[s-3-aminopropylthiosulfuricacid]	$C_{11}H_{26}N_2O_6S_4$	2.61
Undecanedioicacid	$C_{11}H_{20}O_4$	1.36
Bicyclo[2.2.1]heptan-2-ol,7,7-dimethyl-,acetate	$C_{11}H_{18}O_2$	0.2
2,2-Dimethyl-3-vinyl-bicyclo[2.2.1]heptane	$C_{11}H_{18}$	0.03
2-Cyclohexylpiperidine	$C_{11}H_{21}N$	3.59
Acetamide,N-methyl-N-[4-(3-hydroxypyrrolidinyl)-2-butynyl]-	$C_{11}H_{18}N_2O_2$	3.03
Tricyclo[4.3.1.1(3,8)]undecan-1-amine	$C_{11}H_{19}N$	0.7

N-[3-[N-Aziridyl]propylidene]hexylamine	$C_{11}H_{22}N_2$	0.12
Pyrrolo[1,2-a]pyrazine-1,4-dione,hexahydro-3-(2-methylpropyl)-	$C_{11}H_{18}N_2O_2$	2.07
4-Chloro-3-n-hexyltetrahydropyran	$C_{11}H_{21}ClO$	0.28
1H-Azepine,hexahydro-1-(3-piperidinylcarbonyl)-	$C_{12}H_{22}N_2O$	2.3
3'-Hydroxyquinalbarbitone	$C_{12}H_{18}N_2O_4$	0.72
1-Oxaspiro[4.5]decan-3-carboxylic acid,2-oxo-4-cyano-, ethyl ester	$C_{13}H_{17}NO_4$	0.26
Tridecane	$C_{13}H_{28}$	0.44
1-Hydroxycyclododecanecarbonitrile	$C_{13}H_{23}NO$	1.89
3-(Piperidinomethyl)-2-benzothiazolinethione	$C_{13}H_{16}N_2S_2$	0.3
9-Chloro-9-methyl-9-silafluorene	$C_{13}H_{11}ClSi$	0.56
Piperazine,1-[(4-bromo-2,5-dimethoxyphenyl)methyl]-	$C_{13}H_{19}BrN_2O_2$	0.04
Benzo[h]quinoline-3-carboxylic acid,1,4-dihydro-4-oxo-	$C_{14}H_9NO_3$	0.93
2-Trifluoroacetoxydodecane	$C_{14}H_{25}F_3O_2$	0.08
Tetradecane	$C_{14}H_{30}$	0.51
1-Tetradecene	$C_{14}H_{28}$	0.96
Tertbutyloxyformamide,N-methyl-N-[4-(1-pyrrolidinyl)-2-butynyl]-	$C_{14}H_{24}N_2O_2$	5.9
5,10-Diethoxy-2,3,7,8-tetrahydro-1H,6H-dipyrrolo[1,2-a:1',2'-d]pyrazine	$C_{14}H_{22}N_2O_2$	0.87
Agomelatine	$C_{15}H_{17}NO_2$	0.24
6 Cyclopentadecanone,2-hydroxy-	$C_{15}H_{28}O_2$	3.99
Cyclopentane,(1-phenyl-1-trimethylsilylmethylene,-	$C_{15}H_{22}Si$	0.2
N,N'-Pentamethylenebis[s-3-aminopropylthiosulfuricacid]	$C_{11}H_{26}N_2O_6S_4$	2.61
Total		**34.18**
C_{16}-C_{20}		
Norcocaine	$C_{16}H_{19}NO_4$	0.95
8S-Hydroxy-4Z,6E,10Z-hexadecatrienoic acid	$C_{16}H_{26}O_3$	0.24

1,2-Ethanediamine,N,N'-bis(phenylmethyl)-	$C_{16}H_{20}N_2$	0.47
Decanoylm-nitroaniline	$C_{16}H_{24}N_2O_3$	0.17
Acetohydrazide,2-hydroxy-2-phenyl-N2-(1-methylcyclohexen-4-ylmethylene)-	$C_{16}H_{20}N_2O_2$	0
Morphinan-3,14-diol,4,5-epoxy-, (5?-	$C_{16}H_{19}NO_3$	0.15
2-(4-Hydroxy-4-methyl-tetrahydro-pyran-3-ylamino)-3-(1H-indol-2-yl)-propionic acid	$C_{17}H_{22}N_2O_4$	1.31
3-(Prop-2-enoyloxy)tetradecane	$C_{17}H_{32}O_2$	0.27
Heptadecane	$C_{17}H_{36}$	0.41
9-Octadecenenitrile, (Z)-	$C_{18}H_{33}N$	0.38
Octadecanenitrile	$C_{18}H_{35}N$	0.3
6-Octadecynenitrile	$C_{18}H_{31}N$	0.33
Phenylalanine,4-amino-N-t-butyloxycarbonyl-, t-butyl ester	$C_{18}H_{28}N_2O_4$	0.26
Gentamicin a	$C_{18}H_{36}N_4O_{10}$	0.2
8,11-Octadecadienoic acid,methyl ester	$C_{19}H_{34}O_2$	0.22
Z,Z,Z-1,4,6,9-Nonadecatetraene	$C_{19}H_{32}$	0.01
cis-11-Eicosenamide	$C_{20}H_{39}NO$	0.35
N-Desethylsunitinib	$C_{20}H_{23}FN_4O_2$	0.36
Total		**6.38**
>C₂₀		
Rauwolscine	$C_{21}H_{26}N_2O_3$	0.32
Acetic acid,2-[4-[[[2-[3-fluoro-4-(trifluoromethyl)phenyl]-4-methyl-5-thiazolyl]methyl]thio]-2-methylphenoxy]-	$C_{21}H_{17}F_4NO_3S_2$	0.72
2-[4-methyl-6-(2,6,6-trimethylcyclohex-1-enyl)hexa-1,3,5-trienyl]cyclohex-1-en-1-carboxaldehyde	$C_{23}H_{32}O$	1.04
N,N'-Bis(Carbobenzyloxy)-lysine methyl(ester)	$C_{23}H_{28}N_2O_6$	0.06
Pregn-4-ene-3,20-dione,17,21-dihydroxy-,bis(O-methyloxime)	$C_{23}H_{36}N_2O_4$	1.22
Paromomycin	$C_{23}H_{45}N_5O_{14}$	1.55

D-Glucosyl-?-1'-D-erythro-sphingosine	$C_{24}H_{47}NO_7$	0.14
Ethyliso-allocholate	$C_{26}H_{44}O_5$	0.33
Benzoic acid,4-[[(1R,2E,4E,6Z,9Z)-1-[(1S)-4-carboxy-1-hydroxybutyl]-2,4,6,9-pentadecatetraen-1-yl]thio]-	$C_{27}H_{36}O_5S$	0.92
Total		**6.3**

Table S2. The carbon number of each component in the shrimp shell Py-GC/MS at the final pyrolysis temperature of 700°C and the heating rate of 30°C/min (by peak area percentage, %).

Compound name	**Carbon number**	**700°C 30 °C/min**
C_0-C_5		
Methanethiol	CH_4S	6.01
Carbon dioxide	CO_2	15.11
Acetamide	C_2H_5NO	0.02
(R)-(-)-2-Amino-1-propanol	C_3H_9NO	0.04
Malonamic acid	$C_3H_5NO_3$	0.23
N-Methyltaurine	$C_3H_9NO_3S$	0.04
Cyclopropylcarbinol	C_4H_8O	0.47
1H-Pyrrole,2,5-dihydro-1-nitroso-	$C_4H_6N_2O$	0.31
Propanenitrile,3-(methylamino)-	$C_4H_8N_2$	0.42
Pentanal	$C_5H_{10}O$	2.65
1,3,2-Dioxaborolan-4-one,2-ethyl-5-methyl-	$C_5H_9BO_3$	1.75
Propanenitrile,2-(dimethylamino)-	$C_5H_{10}N_2$	1.21
Butanenitrile,3-methyl-	C_5H_9N	0.62
Butanenitrile,2-methyl-	C_5H_9N	0.32
1H-Pyrrole,2-methyl-	C_5H_7N	0.27
2-Cyanoamino-4,6-dihydroxypyrimidine	$C_5H_4N_4O_2$	0.31
5-Aminovalericacid	$C_5H_{11}NO_2$	0.47
Imidazole-2-carboxylic acid,4-methyl-	$C_5H_6N_2O_2$	0.06
Total		**30.31**
C_6-C_{10}		
1,3-Cyclohexadiene	C_6H_8	0.51
1-Pyrrolidinylacetonitrile	$C_6H_{10}N_2$	0.43
3-Acetyl-1H-pyrroline	C_6H_7NO	0.02
3-Pyridinecarboxylic acid,6-amino	$C_6H_6N_2O_2$	1.08
Arginine	$C_6H_{14}N_4O_2$	0.19
Imidazole,2-amino-5-[(2-carboxy)vinyl]-	$C_6H_7N_3O_2$	0.81

Phenol	C_6H_6O	0.99
Toluene	C_7H_8	5.95
1-Methyl-4-[nitromethyl]-4-piperidinol	$C_7H_{14}N_2O_3$	0.36
Pterin-6-carboxylic acid	$C_7H_5N_5O_3$	0.23
p-Cresol	C_7H_8O	1.91
Oxirane,(3-methylbutyl)-	$C_7H_{14}O$	0.17
Ethylbenzene	C_8H_{10}	1.68
Cyclopropane,pentyl-	C_8H_{16}	0.41
1-Octene	C_8H_{16}	0.38
Styrene	C_8H_8	0.83
Heptane,3-methylene-	C_8H_{16}	0.24
Hexane,2,4-dimethyl-	C_8H_{18}	0.2
3-Azonia-5-hexene-1-ol,N,N-dimethyl-,carbamateester, bromide	$C_8H_{17}N_2O_2$	0.16
1,4-diazabicyclo[4.3.0]nonan-2,5-dione,3-methyl	$C_8H_{12}N_2O_2$	0.68
Indole	C_8H_7N	2.36
Piperidine,1-(cyanoacetyl)-	$C_8H_{12}N_2O$	0.43
3,8-Dioxatricyclo[5.1.0.0(2,4)]octane,4-ethenyl-]	$C_8H_{10}O_2$	0.03
4-(2-Aminoethyl)benzenesulfonyl fluoride	$C_8H_{10}FNO_2$	0.48
Benzene,propyl-	C_9H_{12}	0.73
1,8-Nonadiyne	C_9H_{12}	0.01
Cyclopentanol,1-(methylenecyclopropyl)-	$C_9H_{14}O$	1.23
2-Oxatricyclo[4.3.1.0(3,8)]decan-10-one	$C_9H_{12}O_2$	0.68
Bicyclo[2.2.1]hept-2-en-2-amine,N,N-dimethyl-	$C_9H_{15}N$	0.39
Amphetamine	$C_9H_{13}N$	0.32
Dextroamphetamine	$C_9H_{13}N$	0.01
Benzenepropanenitrile	C_9H_9N	2.9
Pyrrolizin-1,7-dione-6-carboxylic acid,methyl(ester)	$C_9H_{11}NO_4$	1.07
1-Decene	$C_{10}H_{20}$	1.23
Bicyclo[3.1.0]hex-3-en-2-one,4-methyl-1-(1-methylethyl)-	$C_{10}H_{14}O$	0.04
2,6,6-Trimethyl-bicyclo[3.1.1]hept-3-ylamine	$C_{10}H_{19}N$	0.31
Cyclohexanepropanoic acid,2-oxo-, methylester	$C_{10}H_{16}O_3$	0.42
Total		**29.87**
C_{11}-C_{15}		
Pyrrolo[1,2-a]pyrazine-1,4-dione,hexahydro-3-(2-methylpropyl)-	$C_{11}H_{18}N_2O_2$	2.49
Acetamide,N-methyl-N-[4-(3-hydroxypyrrolidinyl)-2-butynyl]-	$C_{11}H_{18}N_2O_2$	3.00
Tricyclo[4.3.1.1(3,8)]undecan-1-amine	$C_{11}H_{19}N$	0.86
N,N'-Pentamethylenebis[s-3-aminopropylthiosulfuricacid]	$C_{11}H_{26}N_2O_6S_4$	0.65

2-Bromo-4,5-methylenedioxymethamphetamine	$C_{11}H_{14}BrNO_2$	0.58
1-Dodecene	$C_{12}H_{24}$	0.82
Cyclododecene,(E)-	$C_{12}H_{22}$	0.8
Cymiazole	$C_{12}H_{14}N_2S$	0
(E,Z,Z)-2,4,7-Tridecatrienal	$C_{13}H_{20}O$	0.5
Piperazine,1-[(4-bromo-2,5-dimethoxyphenyl)methyl]-	$C_{13}H_{19}BrN_2O_2$	0
Fenamiphossulfone	$C_{13}H_{22}NO_5PS$	0.14
Bibenzyl	$C_{14}H_{14}$	3.9
1-Tetradecene	$C_{14}H_{28}$	1.91
Tertbutyloxyformamide,N-methyl-N-[4-(1-pyrrolidinyl)-2-butynyl]-	$C_{14}H_{24}N_2O_2$	5.86
Diazene,bis(3-methylcyclohexyl)-,1,2-dioxide	$C_{14}H_{26}N_2O_2$	0.11
1-Dodecanol,3,7,11-trimethyl-	$C_{15}H_{32}O$	1.2
Z,Z-2,5-Pentadecadien-1-ol	$C_{15}H_{28}O$	0.59
5,8-Dihydroxy-4a-methyl-4,4a,4b,5,6,7,8,8a,9,10-decahydro-2(3H)-phenanthrenone	$C_{15}H_{22}O_3$	0.31
Total		**23.27**
C_{16}-C_{20}		
Cetene	$C_{16}H_{32}$	0.76
Morphinan-3,14-diol,4,5-epoxy-, (5?-	$C_{16}H_{19}NO_3$	1.57
Pyrovalerone	$C_{16}H_{23}NO$	0.35
Norcocaine	$C_{16}H_{19}NO_4$	0.87
2-Tridecyl-2-oxazoline	$C_{16}H_{31}NO$	0.16
1-Heptadecene	$C_{17}H_{34}$	0.75
1-Hexadecanol,2-methyl-	$C_{17}H_{36}O$	1.38
Heptadecasphing-4-enine	$C_{17}H_{35}NO_2$	0.12
?d-Glucofuranose,3-O-?d-lyxofuranosyl-1,2:5,6-bis-O-(1-methylethylidene)-	$C_{17}H_{28}O_{10}$	0.03
Alloxydim	$C_{17}H_{25}NO_5$	0.1
3-Trifluoroacetoxypentadecane	$C_{17}H_{31}F_3O_2$	0.7
Gentamicin a	$C_{18}H_{36}N_4O_{10}$	0.12
9-Octadecenenitrile, (Z)-	$C_{18}H_{33}N$	0.62
Octadecanenitrile	$C_{18}H_{35}N$	0.44
9-Octadecynenitrile	$C_{18}H_{31}N$	0.18
Senecionine	$C_{18}H_{25}NO_5$	0.08
Octadecane,1-chloro-	$C_{18}H_{37}Cl$	0.28
Z,Z,Z-1,4,6,9-Nonadecatetraene	$C_{19}H_{32}$	0.37
Nonadecanamide	$C_{19}H_{39}NO$	0.04
2 12,15-Octadecadiynoic acid,methyl ester	$C_{19}H_{30}O_2$	0.06

12,15-Octadecadienoic acid,methyl ester	$C_{19}H_{34}O_2$	0.32
16-Octadecenoic acid, methylester	$C_{19}H_{36}O_2$	0.15
Total		**9.45**
>C₂₀		
11-Heneicosanone	$C_{21}H_{42}O$	0.21
Octadecanoicacid, 2-propenylester	$C_{21}H_{40}O_2$	0.25
Paromomycin	$C_{23}H_{45}N_5O_{14}$	3.29
Pregn-4-ene-3,20-dione,17,21-dihydroxy-,bis(O-methyloxime)	$C_{23}H_{36}N_2O_4$	0.46
Aspidospermidin-17-ol,1-acetyl-19,21-epoxy-15,16-dimethoxy-	$C_{23}H_{30}N_2O_5$	0.34
2-[4-methyl-6-(2,6,6-trimethylcyclohex-1-enyl)hexa-1,3,5-trienyl]cyclohex-1-en-1-carboxaldehyde	$C_{23}H_{32}O$	0.43
N,N'-Bis(Carbobenzyloxy)-lysine methyl(ester)	$C_{23}H_{28}N_2O_6$	0.24
1-Tetracosene	$C_{24}H_{48}$	0.19
D-Glucosyl-?-1'-D-erythro-sphingosine	$C_{24}H_{47}NO_7$	0.04
5H-Cyclopropa(3,4)benz(1,2-e)azulen-5-one,1,1a-?1b-?4,4a,7a-?7b,8,9,9a-decahydro-4a-?7b-?9a-?trihydroxy-3(hydroxymethyl)-1,1,6,8-?tetramethyl-,9a-isobutyrate	$C_{24}H_{34}O_6$	0.01
Cyclopropanebutanoic acid,2-[[2-[[2-[(2-pentylcyclopropyl)methyl]cyclopropyl]methyl]cyclopropyl]methyl]-, methylester	$C_{25}H_{42}O_2$	0.26
Ethyliso-allocholate	$C_{26}H_{44}O_5$	0.85
cis-Moxifloxacinacyl-?D-glucuronide	$C_{27}H_{32}FN_3O_{10}$	0.03
1,8,9,10,11-Pentaphenyl-11-silatricyclo[6.2.1.0-2,7]undeca-2(7),3,5,9-tetraen	$C_{40}H_{30}Si$	0.06
Total		**6.66**

Table S3. The carbon number of each component in the shrimp shell Py-GC/MS at the final pyrolysis temperature of 900°C and the heating rate of 30°C/min (by peak area percentage, %).

Compound name	**Carbon number**	**900°C 30 °C/min**
C₀-C₅		
Methylisocyanide	C_2H_3N	8.08
Propanenitrile	C_3H_5N	1.79
2-Butene	C_4H_8	7.94
Isobutyronitrile	C_4H_7N	0.19
Imidazole-2-carboxylic acid,4-methyl-	$C_5H_6N_2O_2$	0.08

Cyclopropylacetylene	C_5H_6	5.95
Cyclopropane,1,1-dimethyl-	C_5H_{10}	0.05
1H-Pyrazole,4,5-dihydro-4,5 -dimethyl	$C_5H_{10}N_2$	0.61
Butanenitrile,3-methyl-	C_5H_9N	0.41
Total		**25.1**
C_6-C_{10}		
Imidazole,2-amino-5-[(2-carboxy)vinyl]-	$C_6H_7N_3O_2$	0.15
Cystine	$C_6H_{12}N_2O_4S_2$	0.05
Benzene	C_6H_6	6.08
1,3-Cyclopentadiene,1-methyl	C_6H_8	0.91
1,4-Cyclohexadiene	C_6H_8	1.09
trans-1,4-Hexadiene	C_6H_{10}	0.93
Cyclohexene	C_6H_{10}	0.02
3-Vinyl-1-cyclobutene	C_6H_8	0
3-Pyridinecarbonitrile, 2-nitro-	$C_6H_3N_3O_2$	0.01
2,4-Hexadien-1-ol	$C_6H_{10}O$	0.09
Toluene	C_7H_8	13.48
Cyclopentane,1,2-dimethyl-,trans-	C_7H_{14}	0.24
Benzonitrile	C_7H_5N	0.08
Tricyclo[3.1.0.0(2,4)]hex-3-ene-3-carbonitrile	C_7H_5N	0.04
Bicyclo[2.2.1]hept-2-en-7-ol	$C_7H_{10}O$	0.19
Phenol,3-methyl-	C_7H_8O	1.94
Dimethylmuconic acid	$C_8H_{10}O_4$	0.02
3,8-Dioxatricyclo[5.1.0.0(2,4)]octane,4-ethenyl-	$C_8H_{10}O_2$	0.21
Styrene	C_8H_8	3.4
Ethylbenzene	C_8H_{10}	6.16
o-Xylene	C_8H_{10}	1.09
Indole	C_8H_7N	2.91
3,8-Dioxatricyclo[5.1.0.0(2,4)]octane,4-ethenyl-	$C_8H_{10}O_2$	0.01
2-Octyn-1-ol	$C_8H_{14}O$	0.19
2-(Bromomethyl)benzylalcohol	C_8H_9BrO	0
(1-Cyanocyclohexyl) carbamate	$C_8H_{12}N_2O_2$	0.08
3-Pyridinecarboxaldehyde,O-acetyloxime,(E)-	$C_8H_8N_2O_2$	0.09
3,8-Dioxatricyclo[5.1.0.0(2,4)]octane,4-ethenyl-	$C_8H_{10}O_2$	0.21
4-(2-Aminoethyl)benzenesulfonyl fluoride	$C_8H_{10}FNO_2S$	0
Ala-Ala-Ala	$C_9H_{17}N_3O_4$	13.27
Benzene,propyl-	C_9H_{12}	0.89
Benzene,1-ethyl-2-methyl-	C_9H_{12}	0.19
Benzene,(1-methylethyl)-	C_9H_{12}	0.15
Benzene,(2-nitropropen-1-yl)-	$C_9H_9NO_2$	0.01
Bicyclo[3.3.1]non-6-en-3-ol	$C_9H_{14}O$	0.41
7,8-Dihydroneopterin	$C_9H_{13}N_5O_4$	0.5

Benzeneethanamine,2,5-difluoro-?3,4-trihydroxy-N-methyl-	$C_9H_{11}F_2NO_3$	0.02
(1R)-(-)-Myrtenal	$C_{10}H_{14}O$	0.39
Biotin	$C_{10}H_{16}N_2O_3S$	0.02
3-(3-Methoxyphenyl)propionic acid	$C_{10}H_{12}O_3$	0.01
2-Methylindene	$C_{10}H_{10}$	0.36
1H-Indole,2,3-dimethyl-	$C_{10}H_{11}N$	0.37
2-Methyl-6(S)-(3-pyridyl)tetrahydro-1,2-oxazine	$C_{10}H_{14}N_2O$	0.23
Phenprobamate	$C_{10}H_{13}NO_2$	0.03
Total		**56.52**
C_{11}-C_{15}		
Naphthalene,1-methyl-	$C_{11}H_{10}$	0.58
Benzocycloheptatriene	$C_{11}H_{10}$	0.49
Naphthalene,1,2-dihydro-3-methyl-	$C_{11}H_{12}$	0.63
Acetamide,N-methyl-N-[4-(3-hydroxypyrrolidinyl)-2-butynyl]-	$C_{11}H_{18}N_2O_2$	0.37
1-(2,8-Dihydro xyquinolin-5-yl)ethan-1-one	$C_{11}H_9NO_3$	0.67
1-Undecanol	$C_{11}H_{24}O$	0.28
Bicyclo[2.2.1]heptan-2-ol,7,7-dimethyl-,acetate	$C_{11}H_{18}O_2$	1.22
5-Methyl-6-phenyltetrahydro-1,3-oxazine-2-thione	$C_{11}H_{13}NOS$	0.01
Acetamide,N-methyl-N-[4-[4-fluoro-1-hexahydropyridyl]-2-butynyl]-	$C_{12}H_{19}FN_2O$	0.03
1,1-Cyclopropanedimethanol,2-methyl-?phenyl-	$C_{12}H_{16}O_2$	0.2
Galactonicphenylhydrazide	$C_{12}H_{18}N_2O_6$	0.06
4-Quinolinol,4-ethenyldecahydro-1,2-dimethyl-,(2?4?4a?8a?-	$C_{13}H_{23}NO$	0.02
?D-Glucopyranoside, methyl2-(acetylamino)-2-deoxy-3-O-(trimethylsilyl)-,cyclicmethylboronate	$C_{13}H_{26}BNO_6Si$	0.02
3-Trifluoroacetoxydodecane	$C_{14}H_{25}F_3O_2$	0.5
5,10-Diethoxy-2,3,7,8-tetrahydro-1H,6H-dipyrrolo[1,2-a:1',2'-d]pyrazine	$C_{14}H_{22}N_2O_2$	0
9H-Fluorene,9-methylene-	$C_{14}H_{10}$	0.22
2,4,7,9-Tetramethyl-5-decyne-4,7-diol	$C_{14}H_{26}O_2$	0.01
5,10-Diethoxy-2,3,7,8-tetrahydro-1H,6H-dipyrrolo[1,2-a:1',2'-d]pyrazine	$C_{14}H_{22}N_2O_2$	0
2(1H)-Pyridinone,3-[(2S,4S,5R)-5,6-dichloro-2,4-dimethyl-1-oxohexyl]-4-hydroxy-5,6-dimethoxy-	$C_{15}H_{21}Cl_2NO_5$	0.55
Pentadecane	$C_{15}H_{32}$	0.35
Polygodial	$C_{15}H_{22}O_2$	0

Z,Z-2,5-Pentadecadien-1-ol	$C_{15}H_{28}O$	0.02
Methyl4,6-tetradecadiynoate	$C_{15}H_{22}O_2$	0.01
2(1H)-Pyridinone,3-[(2S,4S,5R)-5,6-dichloro-2,4-dimethyl-1-oxohexyl]-4-hydroxy-5,6-dimethoxy-	$C_{15}H_{21}Cl_2NO_5$	0.55
Total		**6.79**
C_{16}-C_{20}		
Mecoprop-m-butoxyethylester	$C_{16}H_{23}ClO_4$	1.18
9-Hexadecenoicacid	$C_{16}H_{30}O_2$	0.52
3,10B-Dihydrofluoranthene	$C_{16}H_{12}$	0.01
Flunitrazepam	$C_{16}H_{12}FN_3O_3$	0
Isoquinoline-1-carbonitrile,2-hex-4-ynoyl-1,2-dihydro-	$C_{16}H_{14}N_2O$	0.1
Morphinan-3,14-diol,4,5-epoxy-, (5?-	$C_{16}H_{19}NO_3$	0.61
Mecoprop-m-butoxyethyl ester	$C_{16}H_{23}ClO_4$	0.14
2-(Ethylamino)-7-(4-hydroxy-3,5-dimethoxyphenyl)-4H,6H,7H-[1,3]thiazolo[4,5-b]pyridin-5-one	$C_{16}H_{19}N_3O_4S$	0.02
Bromosporine	$C_{17}H_{20}N_6O_4S$	0.06
Heptadecane	$C_{17}H_{36}$	0.17
1-Heptadecene	$C_{17}H_{34}$	0.13
Bromodiphenh ydramine	$C_{17}H_{20}BrNO$	0.44
Panaxydol	$C_{17}H_{24}O_2$	0.92
Panaxjapyne A	$C_{17}H_{26}O$	0.3
Gentamicin a	$C_{18}H_{36}N_4O_{10}$	0.15
[2-(4-Bromophenyl)-5-pentylcyclohex-1-en-1-yl]methanol	$C_{18}H_{25}BrO$	0.01
Methyl9,10-octadecadienoate	$C_{19}H_{34}O_2$	0.07
Carbamic acid,(1-phenylethyl)-,6-(1-hydroxy-1-methylethyl)-3-methyl-2-cyclohexen-1-yl ester,[1S-[1?S*),6	$C_{19}H_{27}NO_3$	0.03
Z,Z,Z-4,6,9-Nonadecatriene	$C_{19}H_{34}$	0.26
Boldione	$C_{19}H_{24}O_2$	1.86
Aspidofractinine, 3-oxo-	$C_{19}H_{22}N_2O$	0.02
8-Gingerol	$C_{19}H_{30}O_4$	0
8,11-Octadecadiynoic acid,methyl ester	$C_{19}H_{30}O_2$	0.13
2,5-Octadecadiynoic acid,methyl ester	$C_{19}H_{30}O_2$	0.02
Hydrocinnamic acid,o-[(1,2,3,4-tetrahydro-2-naphthyl)methyl]-	$C_{20}H_{22}O_2$	0.49
5,8,11,14-Eicosatetraynoic acid	$C_{20}H_{24}O_2$	0.03
10-Formyl-7,8-dihydrofolic acid	$C_{20}H_{21}N_7O_7$	0.04
Hydrocinnamicacid,o-[(1,2,3,4-tetrahydro-2-naphthyl)methyl]-	$C_{20}H_{22}O_2$	0.06

10-Formyl-7,8-dihydrofolic acid	$C_{20}H_{21}N_7O_7$	0
6?Hydroxy-oralturinabol	$C_{20}H_{27}ClO_3$	0.02
Quinidine1'-oxide	$C_{20}H_{24}N_2O_3$	0
Aspidofractinine-1-carboxaldehyde, 3-oxo-,(2?5?-	$C_{20}H_{22}N_2O_2$	0.01
Curan-17-oicacid,2,16-didehydro-19-hydroxy-,methyl ester,(20.xi.)-	$C_{20}H_{24}N_2O_3$	0.01
Total		**7.81**
>C₂₀		
Pregn-4-ene-3,20-dione,16,17-epoxy-,(16?-	$C_{21}H_{28}O_3$	0.03
1-Aminononadecane,N-trifluoroacetyl-	$C_{21}H_{40}F_3NO$	0
Dinaciclib	$C_{21}H_{28}N_6O_2$	0.07
5,8,11-Eicosatriynoic acid,methyl ester	$C_{21}H_{30}O_2$	0.22
4-Hydroxy-3,5-dimethyl-6-(4-(2-methyl-3-(p_x005f_x005f_x005f_x0002_nitrophenyl)-2-propenylidene)tetrahydro-2-furyl)-2-pyranone	$C_{21}H_{21}NO_6$	0.06
Hexanoic acid,hexadecylester	$C_{22}H_{44}O_2$	0.32
N-(1,3-Benzodioxol-5-ylmethyl)-3-(2-chlorophenyl)-5-methyl-4-isoxazolecarboxamide, TMSderivative	$C_{22}H_{23}ClN_2O_4Si$	0.05
Paromomycin	$C_{23}H_{45}N_5O_{14}$	0.81
N,N'-Bis(Carbobenzyloxy)-lysine methyl(ester)	$C_{23}H_{28}N_2O_6$	0.89
1-Tetracosene	$C_{24}H_{48}$	0.09
2-Propenamide,N-[4-(1-benzoyl-4-piperidinyl)butyl]-3-(3-pyridinyl)-, (2E)-	$C_{24}H_{29}N_3O_2$	0.01
D-Glucosyl-?-1'-D-erythro-sphingosine	$C_{24}H_{47}NO_7$	0.03
Luminespib	$C_{26}H_{31}N_3O_5$	0.67
Ethyl iso-allocholate	$C_{26}H_{44}O_5$	0.21
Leukotriene D4methyl ester	$C_{26}H_{42}N_2O_6S$	0.01
1(5?-Androsten-1?methyl-17?ol-3-one,di-trimethylsilyl	$C_{26}H_{46}O_2Si_2$	0.03
9,10-Secocholesta-5,7,10(19)-triene-3,24,25-triol, (3?5Z,7E)-	$C_{27}H_{44}O_3$	0.01
[5,9-Dimethyl-1-(3-phenyl-oxiran-2-yl)-deca-4,8-dienylidene]-(2-phenyl-aziridin-1-yl)-amine	$C_{28}H_{34}N_2O$	0.11
Dipyridamolemono-O-?D-glucuronide	$C_{30}H_{48}N_8O_{10}$	0.07
Asiatic acid	$C_{30}H_{48}O_5$	0.02
9-Hexadecenoicacid,9-octadecenylester, (Z,Z)-	$C_{34}H_{64}O_2$	0.01
Pregna-1,4-diene-3,20-dione,21-hydroxy-11?17-bis(trimethylsiloxy)-,bis(O-methyloxime)bis(trimethylsilyl) phosphate(ester)	$C_{35}H_{67}N_2O_8PSi_4$	0.03
9-Octadecenoicacid (Z)-,octadecyl ester	$C_{36}H_{70}O_2$	0.04

2,4,6,8,10-Tetradecapentaenoicacid,9a-(acetyloxy)-1a,1b,4,4a,5,7a,7b,8,9,9a-decahydro-4a,7b-dihydroxy-3-(hydroxymethyl)-1,1,6,8-tetramethyl-5-oxo-1H-cyclopropa[3,4]benz[1,2-e]azulen-9-yl ester,[1aR-(1a?1b?4a?7a?7b?8?9?9a?]-	$C_{36}H_{46}O_8$	0.41
Cepharanthine	$C_{37}H_{38}N_2O_6$	0.02
Osmium,(?-2,4-cyclopentadien-1-yl)methylbis(triphenylphosphine)-	$C_{42}H_{38}OSP_2$	0.01
Calcitonin, rat	$C_{148}H_{228}N_{40}O_{46}S_3$	0.02
Total		**4.25**

CURICULUM VITAE

Meng LingBo

Nationality: China

Master of Science (Chemical Technology), UMT

Email: mlingbo7@gmail.com

Date of Birth: 12 March 1998

List of Publications (directly derived from the thesis):

1. **Meng, L.**, Foong, S. Y., Yek, P. N. Y., Liew, R. K., Karami, A. M., Verma, M., Ma, N. L., Sonne, C., Lan, J. C.-W., & Lam, S. S. (2023). Pyrolysis recovery and product distribution of shrimp shell waste: Insights from thermogravimetric-Fourier transform infrared spectroscopy and pyrolysis–gas chromatography/mass spectrometry characterization. Energy & Environment, 0(0). https://doi.org/10.1177/0958305X231215317

Awards:

1. **Silver Medal, MPI 2022**. Project title: Microwave Pyrolysis of Waste Furniture to Produce Value-added Products.
2. **Bronze Prize, The 8th China International 'Internet+' 202**3. Project title: Curing Formaldehyde-free Board.

Conferences:

Oral presentation, The 6th ostgraduate Colloquium in Environmental Research (POCER), 9 – 11 June 2022. Title: Microwave Pyrolysis of Shellfish Waste for Biochar Production.